

# Reduced Widths of Individual Nuclear Energy Levels

A. M. LANE

*Atomic Energy Research Establishment, Harwell, Berkshire, England*

## CONTENTS

- I. Introduction
- II. Theoretical Prediction of Reduced Widths
  - 1. Reduced Width Amplitudes in Terms of Expansion Coefficients
    - (a) Particle Channels
    - (b) Photon Channels
  - 2. Interpretation of the Expansion Coefficients with the Shell Model
    - (a) States of Normal Parity
    - (b) States of Nonnormal Parity
    - (c) Collected Formulas for Applications in Sec. III
  - 3. Interpretation of the Expansion Coefficients with the Rotational Model
    - (a) Nucleon Channels
    - (b) Photon Channels
- III. Experimental Values of Reduced Widths of Resonance Levels in Light Nuclei
  - 1. Normal Parity States of the Mass Range  $4 < A \leq 16$ 
    - (a) Nucleon Channels
    - (b) Alpha-Particle Channels
    - (c) Deuteron Channels
    - (d) Photon Channels
    - (e) Concluding Remarks
  - 2. Nonnormal Parity States of the Mass Range  $4 < A \leq 16$ 
    - (a) Nucleon Channels
    - (b) Alpha-Particle and Deuteron Channels
    - (c) Photon Channels
    - (d) Concluding Remarks
  - 3. Nuclei in the Mass Range  $16 < A \leq 40$ 
    - (a) Normal parity States
    - (b) Nonnormal Parity States
    - (c) Nucleon Channels
    - (d) Alpha-Particle Channels
    - (e) Photon Channels

## I. Introduction

MANY hundreds of reduced widths of nuclear energy levels have been measured during the last 10 years. The theoretical interpretation of these widths has been largely statistical in nature, the reason being that most observed levels cannot possibly be identified individually. For instance, the widths for neutron and photon channels that are obtained from slow-neutron resonance reactions belong mostly to levels in regions where there are thousands of levels per Mev of excitation (Hu58).<sup>1</sup> The widths of these levels have been interpreted *statistically* in terms of "strength functions," but it is unreasonable to expect

<sup>1</sup> References are given in alphabetical order in Bibliography at the end of the paper.

that the widths of such levels should be interpreted *individually*.

However, not all of the observed widths come into this category. There are quite a number of widths about which some individual prediction may be made. These widths are those of most levels of light nuclei, and of low-lying levels of heavier nuclei. For a heavier nucleus, the excitation energy above which individual interpretation becomes impossible depends upon the proximity of closed shells. For nuclei not near closed shells this energy is  $\sim 2$  Mev; for  $\text{Pb}^{209}$ , however, unbound levels at  $\sim 5$ -Mev excitation may be identified.

Experimentally, one obtains widths of unbound levels by measuring excitation curves of resonance reactions. Widths for bound levels are obtained from measurement of yields in stripping reactions or, in the case of photon channels, from Coulomb excitation.

The present article is composed of two parts: the first part deals with the theoretical prediction of widths, and presents expressions for widths derived from the shell model (El57a) and the strong coupling version of the Bohr-Mottelson model (Bo53); the second part consists of a compilation of the observed widths of nuclei of mass number  $< 40$  together with theoretical discussion. Apart from a few photon widths, all values quoted refer to resonance levels, i.e., the values are obtained from resonance reactions, not stripping reactions. The reason for this restriction is that values from stripping reactions are not reliably determined in general. It appears that the *relative* values of widths determined in any given reaction are much more reliable than absolute values, which are sensitive to details of the particular stripping theory that is used. Bowcock (Bo55), has made an interesting attempt to remove this sensitivity and to extract reliable values, but his method has not been extensively applied.

## II. Theoretical Prediction of Reduced Widths

Following Lane and Thomas (La57), the basic notation used here is as follows:

$A$ :	the total number of nucleons
$\alpha_1$ and $\alpha_2$ :	any pair of bound fragments into which the total system may be separated
$A_1$ and $A_2$ :	the mass numbers of $\alpha_1$ and $\alpha_2$ : $A_1 + A_2 = A$

$q_1$ and $q_2$ :	the internal coordinates of $\alpha_1$ and $\alpha_2$
$I_1$ and $I_2$ :	the spins of $\alpha_1$ and $\alpha_2$
$i_1$ and $i_2$ :	the components of $I_1$ and $I_2$ in a fixed direction
$\psi_{\alpha_1 I_1 i_1}$ and $\psi_{\alpha_2 I_2 i_2}$ :	the wave functions of $\alpha_1$ and $\alpha_2$
$\mathbf{r}_c \equiv \mathbf{r}_\alpha$ :	the vector between the positions of $\alpha_1$ and $\alpha_2$
$r_c \equiv r_\alpha$ :	the radial distance between $\alpha_1$ and $\alpha_2$
$\Omega_c \equiv \Omega_\alpha$ :	the angle of $\mathbf{r}_c$ referred to the fixed direction
$a_c \equiv a_\alpha$ :	the interaction radius for $\alpha_1$ and $\alpha_2$
$dS_c$ :	the element of the channel surface in configuration space: $dS_c = a_c^2 d\Omega_c dq_1 dq_2$
$M_c \equiv M_\alpha$ :	$M_{\alpha_1} M_{\alpha_2} / M_{\alpha_1} + M_{\alpha_2}$ the reduced mass of $\alpha_1$ and $\alpha_2$
$l_c$ :	the relative angular momentum of $\alpha_1$ and $\alpha_2$
$m_c$ :	the component of $l_c$
$s$ :	the channel spin of $\alpha_1$ and $\alpha_2$ : $\mathbf{s} = \mathbf{I}_1 + \mathbf{I}_2$
$\nu$ :	the component of $s$
$J$ :	the total spin $\mathbf{J} = \mathbf{l}_c + \mathbf{s}$
$M$ :	the component of $J$
$c$ :	channel $\equiv \{\alpha_1 \alpha_2 s l_c J\}$
$X_{\lambda JM}$ :	wave function of the compound state $\lambda$ of spin $J$ with component $M$
$\gamma_{\lambda c}$ :	reduced width amplitude for the channel $c$ of the compound state $\lambda$ ; this is defined as:

$$\gamma_{\lambda c} = (\hbar^2 / 2M_c a_c)^{\frac{1}{2}} \int \varphi_{cM}^* X_{\lambda JM} dS_c, \quad (1)$$

where  $\varphi_{cM}$  is the "channel wave function"

$$\varphi_{cM} = r_c^{-1} \sum_{\substack{i_1, i_2 \\ \nu, m_c}} (I_1 I_2 i_1 i_2 | s \nu) (s l_c \nu m_c | J M) \\ \times \psi_{\alpha_1 I_1 i_1}(q_1) \psi_{\alpha_2 I_2 i_2}(q_2) (i^{l_c} Y_{m_c}^{(l_c)}(\Omega_c)), \quad (2)$$

where  $s, \nu$  are taken to denote channel spin and its magnetic quantum number. Let us define a dimensionless reduced width amplitude  $\theta_{\lambda c}$  by

$$\theta_{\lambda c} = \gamma_{\lambda c} (\hbar^2 / M_c a_c^2)^{-\frac{1}{2}}, \quad (3)$$

thus,

$$\theta_{\lambda c} = (a_c / 2)^{\frac{1}{2}} \int \varphi_{cM}^* X_{\lambda JM} dS_c. \quad (4)$$

The surface  $S_c$  is really a sum over many surfaces, one for each permutation of all  $A$  nucleons into groups of  $A_1$  and  $A_2$  individual nucleons. Let us make use of the isotopic spin formalism, then all particles are equivalent, and neutrons and protons are not distinguished separately. The number of surfaces is then  $(A! / A_1! A_2!)$ , irrespective of the numbers of neutrons and protons in  $\alpha_1$  and  $\alpha_2$ . Correspondingly, in the definition of  $\varphi_{cM}$

there should be a summation over  $(A! / A_1! A_2!)$  terms along with a normalizing factor  $(A! / A_1! A_2!)^{-\frac{1}{2}}$ . Since  $X_{\lambda JM}$  is antisymmetric in all particles, it follows that each individual surface makes the same contribution. Therefore, if  $\varphi_{cM}$  is now taken to contain definite particles in the groups  $\alpha_1$  and  $\alpha_2$ , the dimensionless reduced width amplitude is

$$\theta_{\lambda c} = (a_c / 2)^{\frac{1}{2}} (A! / A_1! A_2!)^{\frac{1}{2}} \int \varphi_{cM}^* X_{\lambda JM} dS_c. \quad (5)$$

## 1. REDUCED WIDTH AMPLITUDES IN TERMS OF EXPANSION COEFFICIENTS

### (a) Particle Channels

Before introducing specific models, it is convenient to develop expression (5) further. From the form of (5) it is evident that the  $\theta_{\lambda c}$  are closely related to the expansion coefficients in the expansion of the compound-state wave function  $X_{\lambda JM}$  in terms of the channel wave functions

$$X_{\lambda JM} = \sum \langle \lambda J | \alpha_1 \alpha_2 s l_c J; r_c \rangle \varphi_{cM}. \quad (6)$$

In this expansion the sum is over  $s$  and  $l_c$  and all states  $\alpha_1$  of  $A_1$  particular nucleons and all states  $\alpha_2$  of the other  $A_2$  nucleons. The sum also implies integration over unbound states. We stress again that here (and in future) we understand that  $\varphi_{cM}$  contains definite particular nucleons in the groups  $\alpha_1$  and  $\alpha_2$ . From (5) it follows immediately that

$$\theta_{\lambda c} = (A! / A_1! A_2!)^{\frac{1}{2}} (a_c / 2)^{\frac{1}{2}} \langle \lambda J | \alpha_1 \alpha_2 s l_c J; a_c \rangle. \quad (7)$$

Notice that the normalization of  $X_{\lambda JM}$  and the  $\varphi_{cM}$  implies that the expansion coefficients as defined by (6) satisfy the relation

$$\sum_{\alpha_1 \alpha_2 s l_c} \int_0^{a_c} |\langle \lambda J | \alpha_1 \alpha_2 s l_c J; r_c \rangle|^2 dr_c = 1. \quad (8)$$

Once an expansion of the form (6) has been established on the basis of some nuclear model, the reduced widths can be evaluated by using (7). The most natural expansions of  $X_{\lambda JM}$  arising from various models are not quite of the form (6). The differences arise from different modes of vector coupling. In (6), the channel spin is used merely to classify different spin combinations, and it has no special physical significance. We now consider two types of expansions in which alternative spin quantum members of physical significance are used instead of channel spin.

### Expansion Natural to Spin-Orbit Coupling

Instead of coupling  $I_1$  and  $I_2$  to give channel spin  $s$ ,  $I_2$  is coupled to  $l_c$  to give a new quantum number  $g$ . The expansion is now

$$X_{\lambda JM} = \sum_{\alpha_1 \alpha_2 I_1 g} \langle \lambda J | \alpha_1 \alpha_2 I_1 g J; r_c \rangle \\ \times \varphi(\alpha_1 \alpha_2 I_1 g J M), \quad (9)$$

where

$$\begin{aligned} \varphi(\alpha_1\alpha_2I_1gJM) &= r_c^{-1} \sum_{i_2, m_c, \mathfrak{M}, i_1} (I_2 l_c i_2 m_c | g \mathfrak{M}) \\ &\times (I_1 g i_1 \mathfrak{M} | JM) \psi_{\alpha_1 I_1 i_1} \psi_{\alpha_2 I_2 i_2} (i^{l_c} Y_{m_c}^{(l_c)}). \end{aligned} \quad (10)$$

We see later that this type of expansion follows most naturally from the nuclear shell model in  $j-j$  coupling. By comparing (9) and (10) with (6) and using a little Racah algebra, one easily derives the relation

$$\langle \lambda J | \alpha_1 \alpha_2 s l_c J ; r_c \rangle = \sum_{\mathfrak{g}} U(I_1 I_2 J l_c, s \mathfrak{g}) \langle \lambda J | \alpha_1 \alpha_2 I_1 g J ; r_c \rangle, \quad (11)$$

therefore, from (7),

$$\theta_{\lambda c} = (A! / A_1! A_2!)^{\frac{1}{2}} (a_c / 2)^{\frac{1}{2}} \sum_{\mathfrak{g}} U(I_1 I_2 J l_c, s \mathfrak{g}) \langle \lambda J | \alpha_1 \alpha_2 I_1 g J ; a_c \rangle. \quad (12)$$

#### Expansion Natural to $L-S$ Coupling

If an  $L-S$  coupling situation holds in the nucleus so that states  $\lambda$ ,  $\alpha_1$ , and  $\alpha_2$  can be assigned quantum numbers  $SL$ ,  $S_1 L_1$ , and  $S_2 L_2$ , respectively, the most natural expansion of  $X_{\lambda SLM S M_L}$  is

$$X_{\lambda SLM S M_L} = \sum_{\alpha_1 \alpha_2 l_c \mathcal{L}} \langle \lambda SL | \alpha_1 \alpha_2 \mathcal{L} SL ; r_c \rangle \times \varphi(\alpha_1 \alpha_2 \mathcal{L} SLM S M_L), \quad (13)$$

where

$$\begin{aligned} \varphi(\alpha_1 \alpha_2 \mathcal{L} SLM S M_L) &= r_c^{-1} \sum_{M_L, M_{L_2}, M_{S_1}, M_{S_2}, \mathfrak{M}} (L_2 l_c M_{L_2} m_c | \mathcal{L} \mathfrak{M}) \\ &\times (L_1 \mathcal{L} M_{L_1} \mathfrak{M} | LM_L) (S_1 S_2 M_{S_1} M_{S_2} | SM_S) \\ &\times \psi(\alpha_1 S_1 L_1 M_{S_1} M_{L_1}) \psi(\alpha_2 S_2 L_2 M_{S_2} M_{L_2}) \\ &\times i^{l_c} Y_{m_c}^{(l_c)}. \end{aligned} \quad (14)$$

The new quantum number in this case is  $\mathcal{L}$ , which is formed by coupling  $L_2$  and  $l_c$  together. By using the relation

$$X_{\lambda JM} = \sum_{M S M_L} (SLM S M_L | JM) X_{\lambda SLM S M_L}, \quad (15)$$

and similar ones for  $\psi_{\alpha_1 I_1 i_1}$  and  $\psi_{\alpha_2 I_2 i_2}$ , we can relate the expansions (13) and (6) to derive

$$\langle \lambda J | \alpha_1 \alpha_2 s l_c J ; r_c \rangle = \sum_{\mathcal{L}} (S_1 L_1 I_1, S_2 L_2 I_2, SLJ, l_c \mathcal{L} S) \times \langle \lambda SL | \alpha_1 \alpha_2 \mathcal{L} SL ; r_c \rangle, \quad (16)$$

where the new symbol represents the quantity

$$\begin{aligned} (-)^{I_1 - S - S_1 - 2s} \sum_f (-)^{-f} U(L_2 S_2 S I_1, I_2 f) \\ \times U(f L_2 J l_c, s \mathcal{L}) U(L_1 S_1 f S_2, I_1 S) U(SL_1 J \mathcal{L}, f L), \end{aligned} \quad (17)$$

which can be written as a  $12-j$  symbol (E155a). Thus, in  $L-S$  coupling, we have the formula for the reduced width amplitude

$$\begin{aligned} \theta_{\lambda c} &= (A! / A_1! A_2!)^{\frac{1}{2}} (a_c / 2)^{\frac{1}{2}} \\ &\times \sum_{\mathcal{L}} (S_1 L_1 I_1, S_2 L_2 I_2, SLJ, l_c \mathcal{L} S) \\ &\times \langle \lambda SL | \alpha_1 \alpha_2 \mathcal{L} SL ; a_c \rangle \\ &\equiv \theta(\lambda SL ; \alpha_1 S_1 L_1, \alpha_2 S_2 L_2, s l_c J) \quad (\text{say}). \end{aligned} \quad (18)$$

#### Treatment of Arbitrary Coupling

Even when an  $L-S$  coupling situation does not exist in the nucleus, it is often convenient to work in terms of an  $L-S$  representation; i.e., to expand

$$\begin{aligned} X_{\lambda JM} &= \sum_{\mu SL} \langle \lambda J | \mu SL \rangle X_{\mu J(SL)M}, \\ \psi_{\alpha_1 I_1 i_1} &= \sum_{\beta_1 S_1 L_1} \langle \alpha_1 I_1 | \beta_1 S_1 L_1 \rangle \psi_{\beta_1 I_1(S_1 L_1) i_1}, \\ \psi_{\alpha_2 I_2 i_2} &= \sum_{\beta_2 S_2 L_2} \langle \alpha_2 I_2 | \beta_2 S_2 L_2 \rangle \psi_{\beta_2 I_2(S_2 L_2) i_2}, \end{aligned} \quad (19)$$

where the wave functions on the right form complete sets of  $L-S$  wave functions. We can now express any reduced width in terms of the expansion coefficients in (19) and the reduced width of (18),

$$\theta_{\lambda c} = \sum_{\substack{\mu SL \\ \beta_1 S_1 L_1 \\ \beta_2 S_2 L_2}} \langle \lambda J | \mu SL \rangle \langle \alpha_1 I_1 | \beta_1 S_1 L_1 \rangle \langle \alpha_2 I_2 | \beta_2 S_2 L_2 \rangle \times \theta(\mu SL, \beta_1 S_1 L_1, \beta_2 S_2 L_2, s l_c J). \quad (20)$$

We now consider specializations to various particular types of channels  $c$ .

*Nucleon channels.*  $\alpha_2 \equiv$  nucleon,  $I_2 \equiv \frac{1}{2}$ ,  $(A! / A_1! A_2!) = A$ .

*Spin-orbit coupling:* The expansion (9), although appropriate to the situation of spin-orbit coupling, is perfectly general, as is the consequent formula (12) for reduced width amplitude. On specializing to the case of nucleon processes, (12) becomes

$$\theta_{\lambda c} = A^{\frac{1}{2}} (a_c / 2)^{\frac{1}{2}} \sum_j U(I_1 \frac{1}{2} J l_c, s j) \langle \lambda J | \alpha_1 \alpha_2 I_1 j J ; a_c \rangle, \quad (21)$$

where we write  $j$  instead of  $\mathfrak{g}$  as is customary for nucleons and where  $\langle \lambda J | \alpha_1 \alpha_2 I_1 j J ; r_c \rangle$  are the expansion coefficients as in Eq. (9). Notice that, on squaring and summing over channel spins, the vector coupling coefficient disappears:

$$\sum_{s=I_1 \pm \frac{1}{2}} \theta_{\lambda c}^2 = A (a_c / 2) \sum_j |\langle \lambda J | \alpha_1 \alpha_2 I_1 j J ; a_c \rangle|^2. \quad (22)$$

If we can assume that the value of an expansion coefficient at  $r_c = a_c$  is roughly equal to its average over the interior  $r_c \leq a_c$ , from (8) it follows that

$$\sum_c \theta_{\lambda c}^2 \sim A / 2, \quad (23)$$

where, as in (8), the sum includes an integration over unbound residual states  $\alpha_1$ .

*L-S coupling:* Formula (18) for reduced width amplitude in *L-S* coupling is appreciably simplified when specialization to nucleon channels is made. By putting  $L_2 \equiv 0$  in (17) and (18)

$$(S_1 L_1 J_1, \frac{1}{2} 0 \frac{1}{2}, S L J, l_c l_c S) \\ = (-)^{I_1 - S - S_1 + s} U(L_1 S_1 s \frac{1}{2}, I_1 S) U(S L_1 J l_c, S L), \quad (24)$$

$$\theta_{\lambda c} = A^{\frac{1}{2}} (a_c/2)^{\frac{1}{2}} (-)^{I_1 - S - S_1 + s} U(L_1 S_1 s \frac{1}{2}, I_1 S) \\ \times U(S L_1 J l_c, S L) \langle \lambda S L | \alpha_1 \alpha_2 l_c S L; a_c \rangle. \quad (25)$$

By summing the square of (24) over  $S$  and  $I_1$ , we get the formula corresponding to (22) in spin-orbit coupling,

$$\sum_{I_1 = |L_1 - S_1|}^{L_1 + S_1} \theta_{\lambda c}^2 = A (a_c/2) |\langle \lambda S L | \alpha_1 \alpha_2 l_c S L; a_c \rangle|^2. \quad (26)$$

Arguing as before, one can then derive the sum rule (23).

*Deuteron channels.*  $\alpha_2 \equiv$  deuteron,  $I_2 \equiv 1$ ,

$$(A! / A_1! A_2!) = A(A-1)/2.$$

*Spin-orbit coupling:* From (12),

$$\theta_{\lambda c} = (A(A-1)/2)^{\frac{1}{2}} (a_c/2)^{\frac{1}{2}} \sum_{\mathcal{J} = l_c, l_c \pm 1} U(I_1 1 J l_c, S \mathcal{J}) \\ \times \langle \lambda J | \alpha_1 \alpha_2 I_1 \mathcal{J} J; a_c \rangle. \quad (27)$$

*L-S coupling:* From (18), by putting  $L_2 \equiv 0$ ,  $S_2 \equiv 0$ ,

$$\theta_{\lambda c} = (A(A-1)/2)^{\frac{1}{2}} (a_c/2)^{\frac{1}{2}} (-)^{I_1 - S - S_1 + s} \\ \times U(L_1 S_1 s 1, I_1 S) U(S L_1 J l_c, S L) \\ \times \langle \lambda S L | \alpha_1 \alpha_2 l_c S L; a_c \rangle. \quad (28)$$

Just as for nucleon processes, we can derive a sum rule like (23), but now with  $A$  replaced by  $A(A-1)/2$ . The sum includes not only integration over unbound states of the residual nucleus but also integration over unbound states of the nucleon-nucleon system.

*Alpha channels.*  $\alpha_2 \equiv$  alpha,  $I_2 = 0$ ,

$$(A! / A_1! A_2!) = A! / (A-4)! 4!.$$

*Spin-orbit coupling:* From (12), with  $I_2 = 0$ ,  $\mathcal{J} = l_c$ ,

$$\theta_{\lambda c} = (A! / (A-4)! 4!)^{\frac{1}{2}} (a_c/2)^{\frac{1}{2}} \langle \lambda J | \alpha_1 \alpha_2 I_1 l_c J; a_c \rangle. \quad (29)$$

*L-S coupling:* From (18), with  $L_2 = S_2 = 0$ ,

$$\theta_{\lambda c} = (A! / (A-4)! 4!)^{\frac{1}{2}} (a_c/2)^{\frac{1}{2}} U(S L_1 J l_c, I_1 L) \\ (-)^{-2S_1 - I_1 - L} \langle \lambda S L | \alpha_1 \alpha_2 l_c S L; a_c \rangle. \quad (30)$$

Again a sum rule like (23) can be derived with  $A$  replaced by  $[A! / (A-4)! 4!]$ .

## (b) Photon Channels

For such channels, the reduced width amplitudes are electromagnetic matrix elements. The evaluation of these does not follow directly from the previous formulas but involves special considerations. We consider only  $E\mathcal{L}$  and  $M1$  multipole radiation as represented by the operators  $H_{\mathfrak{M}}^{(E\mathcal{L})}$  and  $H_{\mathfrak{M}}^{(M1)}$ ; each of these is a sum (over all particles) of the single-particle operators

$$h_{\mathfrak{M}}^{(E\mathcal{L})} = e[\frac{1}{2} - t_3 - (Z/A^{\mathcal{L}})] r^{\mathcal{L}} Y_{\mathfrak{M}}^{(\mathcal{L})}(\Omega), \quad (31)$$

$$h_{\mathfrak{M}}^{(M1)}(\text{space}) = (e\hbar/2mc)(\frac{1}{2} - t_3)(\nabla r Y_{\mathfrak{M}}^{(1)} \cdot \mathbf{1}), \quad (32)$$

$$h_{\mathfrak{M}}^{(M1)}(\text{spin}) = (e\hbar/2mc)[(\frac{1}{2} - t_3)g_p \\ + (\frac{1}{2} + t_3)g_n](\nabla r Y_{\mathfrak{M}}^{(1)} \cdot \mathbf{s}), \quad (33)$$

where  $m$  is the nucleon mass,  $t_3 = -\frac{1}{2}$  for protons,  $+\frac{1}{2}$  for neutrons, and  $g_p, g_n$  are the gyromagnetic ratios for protons and neutrons. In (31), the recoil effect for  $E\mathcal{L}$  radiation has been allowed for by the  $Z/A^{\mathcal{L}}$  term; also, certain small terms have been dropped. We know from the algebra of Racah (Ra42) that the matrix elements of any one component  $H_{\mathfrak{M}}^{(\mathcal{L})}$  of an operator of degree  $\mathcal{L}$  is related simply to the matrix elements of any other component  $H_{\mathfrak{M}'}^{(\mathcal{L})}$  through the relation (in Racah's notation)

$$(\lambda J M | H_{\mathfrak{M}}^{(\mathcal{L})} | \lambda' J' M') \\ = \frac{(J' \mathcal{L} M' \mathfrak{M} | J M) (\lambda J || H^{(\mathcal{L})} || \lambda' J')}{(2J+1)^{\frac{1}{2}}}, \quad (34)$$

where  $(\lambda J || H^{(\mathcal{L})} || \lambda' J')$  is a "reduced matrix element" that does not depend on any directional quantum numbers. Racah uses the phase convention

$$(\lambda J M | H_{\mathfrak{M}}^{(\mathcal{L})} | \lambda' J' M') \\ = (-)^{\mathfrak{M}} (\lambda' J' M' | H_{-\mathfrak{M}}^{(\mathcal{L})} | \lambda J M), \quad (35)$$

or, equivalently

$$(\lambda J || H^{(\mathcal{L})} || \lambda' J') = (-)^{J-J'} (\lambda' J' || H^{(\mathcal{L})} || \lambda J). \quad (36)$$

From (34), it follows that

$$\frac{(\lambda J || H^{(\mathcal{L})} || \lambda' J')}{(2J+1)^{\frac{1}{2}}} = \sum_{M'+m=M} (J' \mathcal{L} M' \mathfrak{M} | J M) \\ \times (\lambda J M | H_{\mathfrak{M}}^{(\mathcal{L})} | \lambda' J' M'), \quad (37)$$

and this is the formula we use to evaluate the reduced matrix elements. The square of (37) is precisely the quantity  $B(\mathcal{L})$  that was introduced by Bohr and Mottelson (Bo53).

## Spin-Orbit Coupling

Consider that  $\alpha_2$  is a nucleon in expansion (9), and make such an expansion for each of the states  $\lambda$  and  $\lambda'$ . These expansions enable us to develop expressions for the matrix elements of space and spin operators as follows.

*Space operator of degree  $\mathcal{E}$ .* By using formula (37) and expansion (9) with  $\alpha_2 \equiv$  nucleon, use of the Racah algebra gives

$$\frac{(\lambda J \| H^{(\mathcal{E})}(\text{space}) \| \lambda' J')}{(2J+1)^{\frac{1}{2}}} = A \sum_{\alpha_1 l_c l_c' j j'} U(\mathcal{E} l_c' j \frac{1}{2}, l_c j') U(\mathcal{E} j' J I_1, j J') \frac{(\langle \lambda J | \alpha_1 \alpha_2 I_1 j J; r_c \rangle Y^{(l_c)} \| h^{(\mathcal{E})}(\text{space}) \| \langle \lambda' J' | \alpha_1 \alpha_2 I_1 j' J'; r_c \rangle Y^{(l_c')})}{(2l_c+1)^{\frac{1}{2}}}. \quad (38)$$

*Spin operator of degree  $\mathcal{E}$ .* In this case from (37) and (9) we have

$$\frac{(\lambda J \| H^{(\mathcal{E})}(\text{spin}) \| \lambda' J')}{(2J+1)^{\frac{1}{2}}} = A \sum_{\alpha_1 l_c i i'} (-)^{i-i'} U(\mathcal{E} \frac{1}{2} j l_c, \frac{1}{2} j') U(\mathcal{E} j' J I_1, j J') \times \frac{(\langle \lambda J | \alpha_1 \alpha_2 I_1 j J; r_c \rangle \| h^{(\mathcal{E})}(\text{spin}) \| \langle \lambda' J' | \alpha_1 \alpha_2 J_1 j' J'; r_c \rangle)}{\sqrt{2}}. \quad (39)$$

*L-S Coupling*

Now we consider states  $\lambda$  and  $\lambda'$  expanded (with  $\alpha_2 \equiv$  nucleon) as in Eq. (13).

*Space operator of degree  $\mathcal{E}$ .*

$$\frac{(\lambda J \| H^{(\mathcal{E})}(\text{space}) \| \lambda' J')}{(2J+1)^{\frac{1}{2}}} = A \sum_{\alpha_1 l_c l_c' S L L'} U(\mathcal{E} l_c' L L_1, l_c L') U(\mathcal{E} L' J S, L J') \times \frac{(\langle \lambda J | \alpha_1 \alpha_2 l_c S L; r_c \rangle Y^{(l_c)} \| h^{(\mathcal{E})}(\text{space}) \| \langle \lambda' J' | \alpha_1 \alpha_2 l_c' S' L'; r_c \rangle Y^{(l_c')})}{(2l_c+1)^{\frac{1}{2}}}. \quad (40)$$

*Spin operator of degree  $\mathcal{E}$ .*

$$\frac{(\lambda J \| H^{(\mathcal{E})}(\text{spin}) \| \lambda' J')}{(2J+1)^{\frac{1}{2}}} = A \sum_{\alpha_1 l_c L S S'} (-)^{s'-s+J'-J} U(\mathcal{E} \frac{1}{2} S S_1, \frac{1}{2} S') U(\mathcal{E} S' J L, S J') \times \frac{(\langle \lambda J | \alpha_1 \alpha_2 l_c S L; r_c \rangle \| h^{(\mathcal{E})}(\text{spin}) \| \langle \lambda' J' | \alpha_1 \alpha_2 l_c' S' L'; r_c \rangle)}{\sqrt{2}}. \quad (41)$$

#### Partial Reduction of Single-Particle Matrix Elements

The single-particle space matrix element in (38) can be partially evaluated for the three types of multipole order we are considering (on replacing  $l_c, l_c'$  by  $l, l'$  as is usual for nucleons):

$$\frac{(\langle \lambda J | \alpha_1 \alpha_2 I_1 j J; r_c \rangle Y^{(l)} \| h^{(\mathcal{E})}(\text{space}) \| \langle \lambda' J' | \alpha_1 \alpha_2 I_1 j' J'; r_c \rangle Y^{(l')})}{(2l+1)^{\frac{1}{2}}} = \begin{cases} (-)^{\mathcal{E}} e(l \mathcal{E} 0 0 | l' 0) \left[ \frac{1}{2} - m_l - (Z/A)^{\mathcal{E}} \right] \int \langle \lambda J | \alpha_1 \alpha_2 I_1 j J; r_c \rangle \langle \lambda' J' | \alpha_1 \alpha_2 I_1 j' J'; r_c \rangle r_c^{\mathcal{E}} dr_c & \text{for } E\mathcal{E} \quad (42) \\ (e\hbar/2mc) \delta_{l l'} [l(l+1)]^{\frac{1}{2}} (\frac{1}{2} - m_l) \int \langle \lambda J | \alpha_1 \alpha_2 I_1 j J; r_c \rangle \langle \lambda' J' | \alpha_1 \alpha_2 I_1 j' J'; r_c \rangle dr_c & \text{for } M1(\text{space}). \quad (43) \end{cases}$$

The single-particle space matrix element in (40) can be similarly reduced. The only single-particle spin matrix element we are concerned with is that for  $M1$  (spin) radiation. The element occurring in (39) can be written

$$\frac{(\langle \lambda J | \alpha_1 \alpha_2 I_1 j J; r_c \rangle \| h^{(M1)}(\text{spin}) \| \langle \lambda' J' | \alpha_1 \alpha_2 I_1 j' J'; r_c \rangle)}{\sqrt{2}} = (e\hbar/2mc) \left( \frac{3}{2} \right)^{\frac{1}{2}} \left\{ \left( \frac{1}{2} - m_l \right) g_p + \left( \frac{1}{2} + m_l \right) g_n \right\} \times \int \langle \lambda J | \alpha_1 \alpha_2 I_1 j J; r_c \rangle \langle \lambda' J' | \alpha_1 \alpha_2 I_1 j' J'; r_c \rangle dr_c, \quad (44)$$

and that occurring in (41) can be similarly expressed. In formulas (42) and (43), there is an implicit assumption that the motion of a nucleon relative to the centroid

of the whole system (which produces radiation) is approximated by the motion relative to the centroid of the other nucleons. This is true only to  $O(1/A)$ , but

since this error is inherent in the model we use to evaluate the expansion coefficients (the shell model), we need not be concerned with it.

## 2. INTERPRETATION OF THE EXPANSION COEFFICIENTS WITH THE SHELL MODEL

Having seen how the reduced widths of nuclear energy levels can be expressed in terms of certain expansion coefficients, we now discuss the interpretation of these coefficients on the basis of the shell model. We do not interrupt the development here to introduce the concepts and assumptions of the shell model, but refer to a recent review of this subject (E157a).

At this stage we introduce a separation of the discussion which is carried through to the end of the section, namely, nuclear states are discussed according to whether they are of "normal" or "nonnormal" parity. The normal parity of a nucleus is the parity of the ground state and the nonnormal parity is simply the opposite parity. This division is natural on the shell model, where the lowest states of normal parity have the normal configuration, i.e., a number of close shells and a few "loose" particles in an unfilled orbit. Non-normal parity states, on the other hand, have a more complicated structure since they must involve the excitation of a particle to a higher orbit or the disturbance of the closed shells. In Table I we give the configurations of the lowest states of normal and non-normal parity in light nuclei.

### (a) States of Normal Parity

The known states of normal parity in light nuclei that occur above the lowest disintegration thresholds usually can be assumed to belong to the normal configuration, as can the final states that are formed in the breakup of the free states. Thus our main interest is in processes of the form

$$\left\{ \begin{array}{l} \text{Compound State} \\ \lambda \{ (\text{closed shells})^{(A-n)}(l)^n \} \end{array} \right\} \rightleftharpoons \left\{ \begin{array}{l} \text{Channel State} \\ \alpha_1 \{ (\text{closed shells})^{(A-n)}(l)^{n_1} \} + \alpha_2 \end{array} \right\}, \quad (45)$$

i.e., the compound state  $\lambda$  has  $(A-n)$  nucleons in closed shells and  $n$  in the  $l$  orbit, and the channel state consists of the residual nucleus  $\alpha_1$  with the same closed shell and  $n_1$  particles in the  $l$  orbit and the emitted nucleus  $\alpha_2$  containing  $n_2 (= n - n_1)$  nucleons. Since the closed shells play no role in this type of process, there is no need to expand the wave function of all  $A$  nucleons as we have done in the previous section but only the wave function of the  $n$  "loose" particles. It so happens that expansions of states of the loose particles that are very similar to what we require are well known in shell-model theory. These are the "fractional parentage" expansions. Tables of such expansions have been given for two types of states: (a) states of Russell-Saunders

coupling with quantum numbers  $T, S, L$ , and spatial symmetry (Ja51); (b) states of spin-orbit coupling with quantum numbers  $J, T$ , and seniority (Ed52). Thus, if we believed nuclear states to be either of these two types, we could read off the expansion coefficients from the tables and immediately predict their reduced widths. Even if states are not of these simple types in practice, we can often expand them in terms of one of the simple sets as in Eq. (19); the required reduced widths then follow immediately on use of Eq. (20).

To find expansions of type (19), we simply carry through a conventional shell-model calculation to find the expansions of what we believe to be the actual nuclear states in terms of one of the two kinds of complete sets mentioned previously, i.e., set up the total interaction matrices in one of the complete sets and diagonalize them.

We now discuss in more detail the relations between fractional parentage expansions and the expansions of Sec. II.1. Let us suppose that we have chosen a complete set of Russell-Saunders wave functions, and that we are expanding state  $\lambda(TSL)$  of  $(l^n)$  into state  $\beta_1(T_1S_1L_1)$  of  $(l^{n_1})$  and  $\beta_2(T_2S_2L_2)$  of  $(l^{n_2})$ , where  $\beta_1$  and  $\beta_2$  contain definite individual nucleons. This expansion is usually written in the form (Ja51)

$$\begin{aligned} X_{\lambda T S L M T M S M L} = & \sum_{\beta_1 \beta_2} \langle \lambda | \beta_1 \beta_2 \rangle \sum (T_1 T_2 M T_1 M T_2 | T M T) \\ & \times (L_1 \mathcal{L} M L_1 \mathcal{M} | L M L) (S_1 S_2 M S_1 M S_2 | S M S) \\ & \times \psi(\beta_1 T_1 S_1 L_1 M T_1 M S_1 M L_1) \\ & \times \psi(\beta_2 T_2 S_2 \mathcal{L} M T_2 M S_2 \mathcal{M} L) \quad (46) \end{aligned}$$

[writing  $\mathcal{L}$  for  $L_2$  in keeping with expansion (13)], where the second sum is over magnetic quantum numbers and  $\langle \lambda | \beta_1 \beta_2 \rangle$  is an abbreviation for the full coefficient of fractional parentage (c.f.p.)

$$\langle \lambda | \beta_1 \beta_2 \rangle \equiv \langle (l^n) \lambda(TSL) | (l^{n_1}) \beta_1(T_1 S_1 L_1), \times (l^{n_2}) \beta_2(T_2 S_2 L_2) \rangle.$$

By comparing expansion (46) with the previous expansion [Eqs. (13) and (14)], we can associate  $\beta_1$  with  $\alpha_1$ .  $\beta_2$  cannot be identified with  $\alpha_2$ , however, since the former consists of  $n_2$  nucleons moving in the  $l$  orbit and the latter is a composite particle of  $n_2$  nucleons moving relative to  $\alpha_1$  with angular momentum  $l_c$ . Thus the relation between the expansion coefficient of (13) and the c.f.p. of (46) is complicated by an overlap integral. The relation can easily be seen to be

$$\begin{aligned} \langle \lambda T S L | \alpha_1 \alpha_2 l T S L; r_c \rangle & = (n! / n_1! n_2!)^{1/2} (A_1! A_2! / A!)^{1/2} (T_1 T_2 M T_1 M T_2 | T M T) \\ & \times \sum_{\beta_1 \beta_2} \langle \lambda | \beta_1 \beta_2 \rangle \delta_{\alpha_1 \beta_1} \delta_{\alpha_2 \beta_2} \mathcal{O}_{\alpha_2 l_c, \beta_2}(r_c), \quad (47) \end{aligned}$$

TABLE I. Lowest and next-to-lowest configurations of nuclear states in the mass ranges  $4 < A \leq 16$  and  $16 < A \leq 40$ . The next-to-lowest configurations of normal parity lie in energy  $2\hbar\omega$  above the lowest, and the lowest configurations of nonnormal parity lie midway between the two. ( $\hbar\omega$  is the quantum of the harmonic oscillator well.)

Mass range	Configurations of normal parity		Configurations of nonnormal parity
	Lowest	Next-to-lowest	Lowest
$4 < A \leq 16$	$(1s)^4(1p)^n$	$(1s)^2(1p)^{n+2}$ $(1s)^3(1p)^n(2s,1d)$ $(1s)^4(1p)^{n-2}(2s,1d)^2$ $(1s)^4(1p)^{n-1}(2p,1f)$	$(1s)^3(1p)^{n+1}$ $(1s)^4(1p)^{n-1}(2s,1d)$
$16 < A \leq 40$	$(1s)^4(1p)^{12}(2s,1d)^n$	$(1s)^3(1p)^{12}(2s,1d)^{n+1}$ $(1s)^4(1p)^{10}(2s,1d)^{n+2}$ $(1s)^4(1p)^{11}(2s,1d)^n(1p,1f)$ $(1s)^4(1p)^{12}(2s,1d)^{n-1}(3s,2g,1g)$	$(1s)^4(1p)^{11}(2s,1d)^{n+1}$ $(1s)^4(1p)^{12}(2s,1d)^{n-1}(1p,1f)$

where the first factor merely takes account of the fact that all  $A$  nucleons are included in expansion (13), but only the  $n$  loose ones are in expansion (46). The last factor is the space overlap integral between  $n_2 (= A_2)$  nucleons moving in the  $l$  orbit about the well center, and particle  $\alpha_2$  separating from  $\alpha_1$  with relative orbital angular momentum  $l_c$ :

$$\Theta_{\alpha_2 l_c, \beta_2}(r_c) = a_c \int [\psi(\beta_2 \mathcal{E} \mathfrak{M})(l^n)]^* \left[ \sum_{M L_2, m} \langle L_2 M L_2 m | \mathcal{E} \mathfrak{M} \rangle \psi(\alpha_2 L_2 M L_2(q_2)) \times Y_{m_c}^{(l_c)}(\Omega_c) \right] dq_2 d\Omega_c. \quad (48)$$

$q_2$  represents the internal coordinates of  $\alpha_2$ , and  $\Omega_c$  is the angle of the vector  $r_c$  joining  $\alpha_1$  and  $\alpha_2$ .

For  $j-j$  coupling we can write formulas corresponding to those just given for  $L-S$  coupling. The fractional parentage expansion of state  $\lambda(JT)$  of  $(j^n)$  into states  $\alpha_1(J_1 T_1), \alpha_2(J_2 T_2)$  of  $(j^{n_1}), (j^{n_2})$ , respectively, is (Ed52)

$$\begin{aligned} & X_{\lambda T J M_T M_J} \\ &= \sum_{\beta_1 \beta_2} \langle \lambda | \beta_1 \beta_2 \rangle \sum_{\text{mag.}} \langle T_1 T_2 M_T M_T | T M_T \rangle \\ & \times \langle I_1 J_1 \mathfrak{M} | J M_J \rangle \psi(\beta_1 I_1 T_1 i_1 M_T i_1) \\ & \quad \psi(\beta_2 J_2 T_2 \mathfrak{M} M_T), \quad (49) \end{aligned}$$

where  $\langle \lambda | \beta_1 \beta_2 \rangle$  is written for the full c.f.p.,

$$\langle \lambda | \beta_1 \beta_2 \rangle \equiv \langle (j^n) \lambda T J | (j^{n_1}) \beta_1 (T_1 I_1) (j^{n_2}) \beta_2 (T_2 J) \rangle. \quad (50)$$

By comparing (49) with (9) and (10), and identifying  $\beta_1$  with  $\alpha_1$ ,

$$\begin{aligned} & \langle \lambda T J | \alpha_1 \alpha_2 I_1 J J; r_c \rangle \\ &= \left( \frac{n!}{n_1! n_2!} \frac{A_1! A_2!}{A!} \right)^{\frac{1}{2}} \langle T_1 T_2 M_T M_T | T M_T \rangle \\ & \quad \times \sum_{\beta_1 \beta_2} \langle \lambda | \beta_1 \beta_2 \rangle \delta_{\alpha_1 \beta_1} \Theta_{\alpha_2 l_c, \beta_2}(r_c), \quad (51) \end{aligned}$$

where the overlap integral is

$$\Theta_{\alpha_2 l_c, \beta_2}(r_c) = a_c \int [\psi(\beta_2 \mathcal{E} \mathfrak{M}(j^{n_2})]^* \left[ \sum_{i_2, m_c} \langle I_2 l_c i_2 m_c | \mathcal{E} \mathfrak{M} \rangle \times \psi(\alpha_2 I_2 i_2(q_2) Y_{m_c}^{(l_c)}(\Omega_c) \right] dq_2 d\Omega_c. \quad (52)$$

#### Evaluation of the c.f.p. in Special Cases

For nucleon, deuteron, and alpha channels, the appropriate fractional parentage expansions (46) and (49) are those in which  $n_2 = 1, 2$ , and  $4$ , respectively. Those for  $n_2 = 1$  are tabulated, and so are some for  $n_2 = 2$  (El53). The rest of those for  $n_2 = 2$  and those for  $n_2 = 4$  can be obtained by "iterating" those for  $n_2 = 1$ .

#### Evaluation of the Overlap in Special Cases

For nucleon channels ( $\alpha_2 \equiv$  nucleon), the overlap of both formulas (48) and (52) simply reduces to the single-particle radial wave function of the  $l$  orbit,  $\phi_l(r)$ , say. By the normalization of  $X_\lambda$ , the normalization of  $\phi_l$  must be

$$\int_0^{a_c} |\phi_l(r)|^2 dr = 1, \quad (53)$$

instead of the usual normalization of shell-model theory in which the upper limit is infinity. However, the differences in the two normalizations is small. In Table II expressions are given for some single-particle radial wave functions of a harmonic oscillator well.

For deuteron channels formula (50) becomes

$$\Theta_{\alpha_2 l_c, \beta_2}(L-S) = a_c \delta_{l_c, \mathcal{E}} \int [\psi(\beta_2 \mathcal{E} \mathfrak{M})(l^2)]^* \times [\psi_d(q_2) Y_{m_c}^{(l_c)}(\Omega_c)] dq_2 d\Omega_c, \quad (54)$$

if we assume the deuteron to be in an  $S$  state. Formula (52) giving the  $j-j$  coupling overlap becomes

$$\Theta_{\alpha_2 l_c, \beta_2}(j-j) = a_c \int [\psi(\beta_2 \mathcal{E} \mathfrak{M})(j^2)]^* \times \left[ \sum (1 l_c i_1 m | \mathcal{E} \mathfrak{M}) \psi_d(q_2) Y_{m_c}^{(l_c)}(\Omega_c) \right] dq_2 d\Omega_c. \quad (55)$$

By recoupling vectors, it can be seen that this is related to the overlap of (54) by

$$\Theta_{\alpha_2 l_c, \beta_2}(j-j) = \Theta_{\alpha_2 l_c, \beta_2}(L-S) \left[ \sum_j (-)^{j+l-l_c-f} \times U\left(\frac{1}{2} l j j, j f\right) U\left(\frac{1}{2} l f l, j l_c\right) U\left(\frac{1}{2} \frac{1}{2} j l_c, S f\right) \right], \quad (56)$$

with  $S$ , the intrinsic spin of the deuteron, equal to one.

TABLE II. Radial oscillator wave functions  $\phi_l(r)$  for the four lowest orbits, normalized according to (53). The oscillator potential may be written in terms of the "size parameter"  $b$  as  $V(r) = (m/2)(\hbar/m\omega)^2 r^2$ . The oscillator quantum  $\hbar\omega$  is related to  $b$  by  $\hbar\omega = \hbar^2/m\omega^2$ . The quantities  $z$ ,  $z_0$ , and  $I$  are defined by  $z = r/b$ ,  $z_0 = a_c/b$ , and  $I = \exp(z_0^2 \int_0^{z_0} \exp(-z^2) dz)$ . The third column is related to the dimensionless single-particle reduced widths  $\theta_p^2$  by  $\theta_p^2 = \frac{1}{2}[r\phi^2(r)]_{a_c}$ . The last column gives the logarithmic derivatives of the radial wave functions.

Orbit	Eigenvalue	$r\phi^2(r)$	$f = (r/\phi) (d\phi/dr)$
1s	$3\hbar\omega/2$	$2z^3 \exp(z_0^2 - z^2) (I - z_0)^{-1}$	$1 - z^2$
1p	$5\hbar\omega/2$	$4z^5 \exp(z_0^2 - z^2) (3I - 2z_0^3 - 3z_0)^{-1}$	$2 - z^2$
1d	$7\hbar\omega/2$	$8z^7 \exp(z_0^2 - z^2) (15I - 4z_0^5 - 10z_0^3 - 15z_0)^{-1}$	$3 - z^2$
2s	$7\hbar\omega/2$	$4z(z^2 - \frac{3}{2}z_0^2) \exp(z_0^2 - z^2) (3I - 2z_0^3 + z_0^3 - 3z_0)^{-1}$	$3 - z^2 + 3/z^2 - \frac{3}{2}$

Overlap (54) can be evaluated by using the convenient transformation methods of Talmi (Ta51). As an example, consider two 1p nucleons coupled up to give  $\mathfrak{L}=2$ , i.e., orbital angular momenta parallel. The evaluation of (54) is independent of the value of  $\mathfrak{M}$ , but it is convenient to take  $\mathfrak{M}=+2$ . By taking the oscillator wave functions normalized over all space (which can incur only a small error),

$$\begin{aligned} \psi(\beta_2 \mathfrak{L} \mathfrak{M} (l^2)) &= \left[ \frac{\phi_{1p}(r_n)}{r_n} Y_{1(1)}(\Omega_n) \right] \left[ \frac{\phi_{1p}(r_p)}{r_p} Y_{1(1)}(\Omega_p) \right] \\ &= (\pi)^{-3} b^{-6} (x_n + iy_n)(x_p + iy_p) \exp\left[-\frac{r_n^2 + r_p^2}{2b^2}\right] \\ &= \left(\frac{32}{15\pi^2 b^{10}}\right)^{\frac{1}{2}} \left[ r_c^2 Y_{2(2)}(\Omega_c) - \frac{1}{4} q^2 Y_{2(2)}(\Omega) \right] \\ &\quad \times \exp\left[-\frac{2r_c^2 + (q^2/2)}{2b^2}\right], \quad (57) \end{aligned}$$

where we have made the transformation

$$\mathbf{r}_n = \mathbf{r}_c + \frac{1}{2}\mathbf{q}, \quad \mathbf{r}_p = \mathbf{r}_c - \frac{1}{2}\mathbf{q}. \quad (58)$$

The center-of-mass coordinate is  $\mathbf{r}_c$  and  $\mathbf{q} \equiv (q, \Omega)$  is the internal coordinate of the neutron-proton system, and  $b$  is the oscillator-well size parameter (see caption to Table II for precise definition).

On using (55), we have the overlap

$$\mathcal{O}_{dL_c, \beta_2} = \left[ \frac{64a_c^2}{75b^7} \left(\frac{2}{\pi}\right)^{\frac{1}{2}} \right]^{\frac{1}{2}} o_d r_c^2 \exp(-r_c^2/2b^2), \quad (59)$$

where we have defined a new overlap (dimensionless) for the integral over the internal coordinate,

$$o_d = \int \left[ \frac{\phi_{1s}(q/\sqrt{2})}{q(4\pi)^{\frac{1}{2}}} \right] \psi_d(q) dq. \quad (60)$$

The dimensionless reduced width  $\theta^2$ , which is equal to  $a_c/2$  times the square of the overlap evaluated at  $r_c = a_c$  is, from (59),

$$\theta^2 = \frac{32}{15} \left(\frac{2}{\pi}\right)^{\frac{1}{2}} z_0^7 \exp(-2z_0^2) (o_d)^2, \quad (61)$$

where  $z_0 = a_c/b$ .

### Evaluation of Overlap at the Nuclear Surface

The nuclear shell model gives only an approximation to the actual nuclear wave function. This approximation in most practical applications appears to be a surprisingly good one. However, one has to be careful in each application to make sure that the model is not taken so literally that certain inherent errors in the shell model are magnified to a point where spurious results can arise. As an example, one can recall the fact that the normal version of the shell model does not explicitly separate the center-of-mass motion. In most applications this limitation of the model can be forgotten because the errors incurred are at most  $O(1/A)$ . When used for computing  $E1$  matrix elements, however, the model, when used naively, does not give the well-known isotopic-spin selection rule and, therefore, can give large errors. This does not mean that the model is useless in such applications, but merely that one must make special allowance for its limitations. This is done simply by changing the  $E1$  operator into an effective operator which includes a recoil term as in (31). The model can then be used to the same degree of accuracy as in other applications.

A second example of where we have to be careful in applying the model too literally arises in the present work when we evaluate the overlaps at the interaction radii,  $r_c = a_c$ , for the purpose of estimating reduced widths.

Let us consider the special case of *nucleon* processes. The overlap for such processes is just the single-particle radial wave function, and the estimation of reduced widths involves the evaluation of this wave function at the interaction radius for a nucleon and the residual nucleus. An evaluation using the oscillator shell model is subject to two errors, one from the oscillator shape, one from the nature of the shell model:

(i) the first error arises because the interaction radius  $r = a_c$  usually comes well outside the turning point of the orbit in the oscillator well, and this means (cf. the third column in Table II) that the value of the single-particle width

$$\theta_p^2 = [r/2\phi^2(r)]_{r=a_c}$$

is very small with the precise value depending hypersensitively on the point of evaluation. As an example, consider  $N^{13}$  as the compound nucleus. A normal parity state belongs to  $(1s)^4(1p)^9$ , and we are interested in the value of  $\theta_p^2$  for a channel with a  $p$  wave nucleon. The



usual formula,  $a_c = 1.45(A_1^{1/3} + A_2^{1/3}) \times 10^{-13}$  cm, gives for the interaction radius in this case the value  $4.77 \times 10^{-13}$  cm. The turning point of the  $1p$  orbit occurs at the point  $r^2 = [5 + (17)^{1/2}]b^2/2$ . Now, from a study of Coulomb energies of mirror nuclei (Ca54b), we know that the value of  $b$  for nuclei in the  $1p$  shell is  $\sim 1.67 \times 10^{-13}$  cm. By taking this value, the turning point of the  $1p$  orbit is at  $3.60 \times 10^{-13}$  cm which is  $1.17 \times 10^{-13}$  cm inside the interaction radius. The value of  $\theta_p^2$ , using the second column of Table II, is found to be 0.036, which is much less than the single-particle reduced width ( $\theta_p^2 \sim 0.5$ ).

The reason for this anomaly is clearly that the infinite oscillator well, although providing wave functions that are suitable for most calculations, nevertheless has certain deficiencies and occasionally gives spurious results as in the present case. We now discuss how the most reasonable nuclear well differs from the infinite oscillator well. Clearly, the main difference is that the actual nuclear well has a finite depth. The most consistent depth for a given light nucleus seems to be that for which the last orbit fills near the top of the well (to within a few Mev). This choice would represent the observed fact that the states in single-particle nuclei ( $\text{He}^5$ ,  $\text{O}^{17}$ ) occur near the dissociation energy for nuclear emission. If we remove the infinite walls of the oscillator well, the various orbits fall somewhat in energy because they are less confined. They also spread out considerably (except for those orbits still tightly bound) and the value of  $\theta_p^2$  will rise to  $\sim 0.5$ . It might be thought that the reasonable well for a given nucleus can be achieved by simply rounding off the edge of the usual oscillator well at the orbit that is filling [Fig. 1(a)]. However, this is not so. For instance, in the  $1p$  shell, rounding off the oscillator well with  $b = 1.67 \times 10^{-13}$  cm causes the bulk of the  $1p$  wave function to move outwards. This means that particles are further apart and that the Coulomb mirror energies are underestimated. What we really want is that the wave functions spread out in both directions instead of only outwards. This is quali-

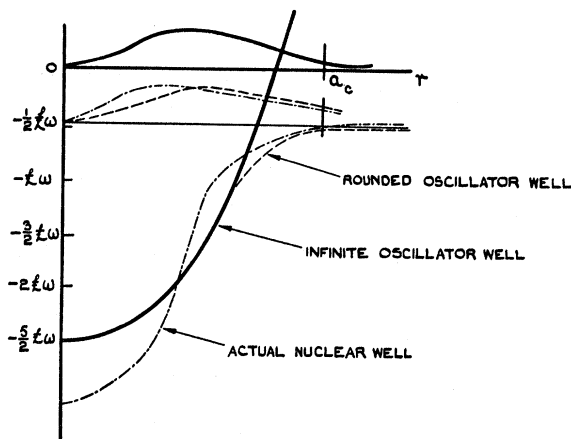
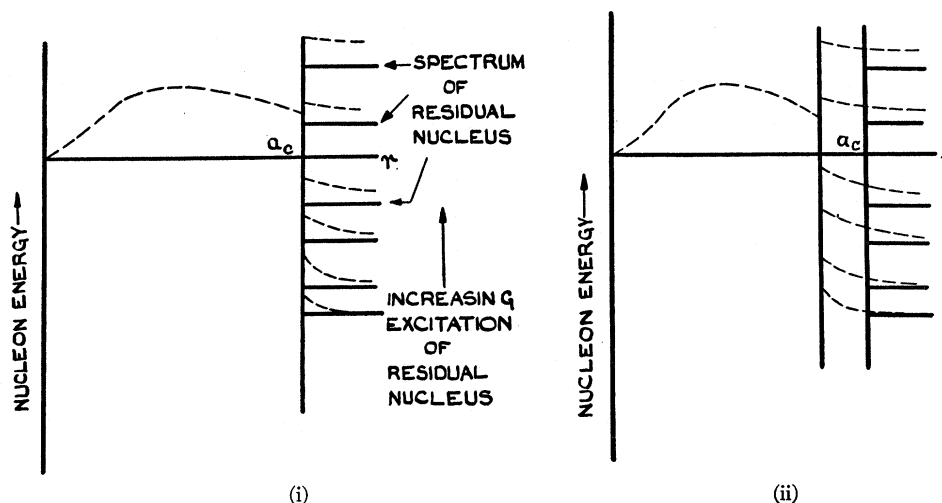


FIG. 1(a). Various well shapes and the corresponding radial  $1p$  wave functions (qualitative only).

tatively achieved with a bell-shaped well [Fig. 1(a)] that is narrower and deeper than the oscillator well, and also is finite with a tail on it. This would thus seem to be the most "reasonable" nuclear well. It would give wave functions that have reasonable values of  $\theta_p^2$  at the interaction radius, yet, at the same time, it should, in other respects, behave like the infinite oscillator well. Unfortunately, it is not possible to perform analytical calculations with the bell-shaped well and so one cannot be very precise about the values of  $\theta_p^2$  that it predicts. Since, however, there are often uncertainties in the experimental reduced widths of the order of 30%, this is not a serious fault. We try the value  $\sim 0.60$  for  $\theta_p^2$  for all orbits with an understood possible uncertainty of the order of 30%. This choice is seen in the next section to be corroborated by the experimental data.

(ii) The second kind of error that arises when the oscillator shell model is used naively does not arise from the shape of the well but from the structure of the shell model itself. This trouble is that the shell-model

FIG. 1(b). Illustrating the transition from the shell-model wave function of a single particle inside the nucleus ( $r < a_c$ ) to the actual external wave function in the external region ( $r > a_c$ ). Figure (i) shows the situation when the transition region is very sharp, i.e., when the sharing of energy take place in a very small radial distance at  $r = a_c$ . Figure (ii) illustrates the more realistic situation of a finite transition region. In this latter case, the wave functions (shown by broken lines) are smooth across the transition region.



wave function does not obviously satisfy the set of boundary conditions  $B_c=S_c$  that we normally impose upon a compound state  $\lambda$  in resonance reaction theory (La57). This is obviously true because, even when the shape of the well is adjusted in the way we have just discussed, the usual shell-model wave functions *cannot* represent the correct radial wave function *outside* the point  $r=a_c$ . The reason is that, in the shell model, it is assumed that all particles in the same orbit always have the same energy whereas, actually, when a nucleon separates from the rest of the system beyond the point where it has no polarizing interaction, it has a special energy of its own depending on the energy of the residual configuration. It is the fact that states of the residual nucleus are split up in energy that gives rise to this situation. If there were no splitting, the energy of a nucleon outside  $a_c$  would always be the same so the shell-model wave function would be accurate there. Another way of saying the same thing is that, when a particle is brought into the nucleus from outside, the interactions with other nucleons cause it to change its energy from its special energy outside to the mean orbit energy inside, if however, there were no interactions, there could be no sharing of energy and hence the energy of the nucleon is the same wherever it is. Notice that it is the fact that the shell model (with energy splittings) *can* describe the shaping of energy brought into the nucleus that enables it to be used to describe compound-nucleus processes in nuclear reactions in the way we are doing.

For simplicity, let us assume that the energy sharing takes place in an infinitely small region at the interaction radius  $a_c$  assumed the same for all nucleon processes. This situation is depicted in Fig. 1(b). Inside  $a_c$ , all nucleons have the same mean energy and the same wave function. Outside  $a_c$ , a nucleon has an energy depending on the energy of the residual nucleus, and its wave function is the solution at this energy of the Schrödinger equation with the normal external barrier. Thus, there are discontinuities in slopes of the radial wave functions at  $a_c$ . On this simple picture, since the single-particle wave functions inside  $r=a_c$  do not depend on external energy, the single-particle reduced widths  $\theta_p^2 = \frac{1}{2}a_c\phi^2(a_c)$  are the same for all processes, i.e., there is no dependence on the energy of the residual nucleus. When this extreme picture is relaxed and the region of energy sharing is considered to be finite, the value of  $\theta_p^2$  depends on the state of the residual nucleus. The main change is in the values of  $\theta_p^2$  for those processes in which the nucleon energy is very negative outside  $r=a_c$ . If energy sharing does not take place precisely at  $r=a_c$ , the negative energy persists inside this point, and the exponential increase of the wave function for decreasing  $r$  continues. This means that, for such processes,  $\theta_p^2$  may be much smaller than when the sharing is immediate at  $r=a_c$ . However, this seriously affects only the prediction of

reduced widths for negative energy processes such as those relevant to stripping reactions in which the final state is bound. For other processes, such as those of resonance reactions,  $\theta_p^2$  should not deviate far from the value it has when the sharing region is very small.

Finally, we make a few remarks about the evaluation of the overlap of deuteron processes at the interaction radius. This evaluation is affected even more than that for nucleon overlaps by the unreal attenuation of the radial wave functions caused by the infinite sides of the oscillator well since *two* nucleons are involved. It is difficult to see how the overlap is altered on changing to the finite bell-shaped well of Fig. 1(a) because we can no longer make the simple transformation (58), which is only correct for oscillator wave functions. However, it should be qualitatively correct to retain the integral  $o_d$  over the internal coordinate of the deuteron in formula (61) and to put the factor  $z_0^7 \exp(-2z_0^2)$  which contains the spurious attenuation equal to unity; therefore,  $\theta^2 \sim 2(o_d)^2$ .

#### Photon Channels

Equations (42) to (44) give expressions for matrix elements to be inserted in (38) and (39) to obtain total matrix elements for  $E1$  and  $M1$  radiation between states in spin-orbit coupling. There exist other equations, identical in form, for the  $L-S$  coupling matrix elements to be inserted in (40) and (41). When a nuclear shell model is used, all the expansion coefficients have the form [from Eq. (51) with  $\alpha_2 \equiv$  nucleon,  $\beta_2 \equiv j$  nucleon,  $\beta_1 \equiv \alpha_1$ ]

$$\begin{aligned} \langle \lambda J | \alpha_1 \alpha_2 I_1 j J ; r_c \rangle \\ = (n/A)^{\frac{1}{2}} (T_{\frac{1}{2}} M_{T_1 m_{\alpha_1}} | T M_T \rangle \langle \lambda | \beta_1 \beta_2 \rangle \phi_l(r), \end{aligned} \quad (62)$$

where  $\phi_l(r)$  is the single-particle radial wave function of the  $j$  orbit. The essential part of expressions (42) to (44) are the radial integrals. When we insert the shell-model expressions above for the expansion coefficients, we have for these integrals

$$\begin{aligned} \int \langle \lambda J | \alpha_1 \alpha_2 I_1 j J ; r \rangle \langle \lambda' J' | \alpha_1 \alpha_2 I_1 j' J' ; r \rangle r^2 dr \\ = (n/A) (T_{\frac{1}{2}} M_{T_1 m_{\alpha_2}} | T M_T \rangle (T_{\frac{1}{2}} M_{T_2 m_{\alpha_2}} | T M_T \rangle \\ \times \langle \lambda | \beta_1 \beta_2 \rangle \langle \lambda' | \beta_1 \beta_2 \rangle I(\mathcal{E}; l, l'), \end{aligned} \quad (63)$$

where

$$I(\mathcal{E}; l, l') = \int_0^{a_c} \phi_l(r) \phi_{l'}(r) r^2 dr. \quad (64)$$

In these integrals the upper limit should be the interaction radius for nucleons  $r=a_c$ , and the radial wave functions should be normalized inside this point. However, we take the upper limit at infinity and the normalization over all space. This should incur no serious error. With oscillator wave functions, we have the values of  $I(\mathcal{E}; l, l')$  shown in Table III. [The relevant integral for  $M1$  transitions is  $I(0; l, l')$ .]

TABLE III. Values of the radial integrals  $I(\mathcal{E}; l, l')$  when oscillator wave functions are used. The integral  $I(0; l, l')$ , which is appropriate for  $M1$  transitions, equals  $\delta_{ll'}$ .

$l, l'$ $I(1; l, l')$	$1s, 1p$ $b(\frac{3}{2})^{\frac{1}{2}}$	$2s, 1p$ $b$	$1d, 1p$ $b(\frac{5}{2})^{\frac{1}{2}}$	$2s, 2p$ $b(\frac{3}{2})^{\frac{1}{2}}$	$1d, 2p$ $b$	$1d, 1f$ $b(\frac{7}{2})^{\frac{1}{2}}$
$l, l'$ $I(2; l, l')$	$1p, 1p$ $\frac{1}{2}b^2$		$2s, 1d$ $(10)^{\frac{1}{2}}b^2$		$1d, 1d$ $\frac{1}{2}b^2$	
$l, l'$ $I(3; l, l')$					$1p, 1d$ $(245/8)^{\frac{1}{2}}b^3$	

### (b) States of Nonnormal Parity

In principle, it is possible to deal with states of nonnormal parity with just the same program that was suggested for states of normal parity, i.e., first set up complete sets of states, then evaluate reduced width amplitudes for these states, and finally express the actual states in terms of the complete set by diagonalizing interactions. The practical trouble in applying this program to nonnormal parity states is the great amount of computational labor involved in the last step arising from the largeness of the complete set.

To illustrate this remark, let us consider states of  $J=\frac{1}{2}$ ,  $T=\frac{1}{2}$  in  $C^{13}$  with negative (normal) and positive (nonnormal) parity. In the former case, as can be seen from Table I, there is one configuration that is uniquely lowest,  $(1s)^4(1p)^9$ . It can be easily checked from published lists of states that there are only five states of  $J=\frac{1}{2}$ ,  $T=\frac{1}{2}$  arising from this configuration. Consequently, the matrices involved in the last stage of the program are five-by-five, and these are easily diagonalized without much labor.

From Table I it can be seen that states of positive parity in  $C^{13}$  arise from not one, but three configurations that have about the same energy (exactly the same on an oscillator well with no spin-orbit splitting):

$$(1s)^4(1p)^8 2s, \quad (1s)^4(1p)^8 1d, \quad (1s)^3(1p)^{10}. \quad (65)$$

There is no difficulty about setting up a complete set of states. Given any complete sets of states of  $(1p)^8$  and  $(1p)^{10}$ , one can construct the complete set we need by coupling on the odd nucleon (or hole) to these states and then antisymmetrizing. This is the "genealogical" method of constructing states. By using the published lists of states, it is quickly found that there are 75 states of  $J=\frac{1}{2}$ ,  $T=\frac{1}{2}$  in the complete set, the foregoing three configurations giving 19, 50, and 6 states, respectively.

The great amount of labor involved in dealing with this complete set tempts one to make simplifying approximations, even those with no obvious justification. For instance, one can limit the number of states in the set one uses. In practice we are interested in the lowest few states of spectra, and it seems clear that for such states, the most important members of the complete set are those whose "parent" states [of  $(1p)^8$  and  $(1p)^{10}$ ] are lowest in energy. As yet we have not specified any particular sets of parent states, but let us now

choose these sets to be the actual eigenstates of the parent nuclei. In our example these are the positive parity states of  $C^{12}$ ,  $N^{14}$ . [These are known to be well represented by the configurations  $(1p)^8$ ,  $(1p)^{10}$  taken in intermediate coupling.] This choice should enable a more severe limitation of the complete set than any other.

What we propose to do, in fact, is to set up a very simplified model for the nonnormal parity states in which we carry this latter type of approximation to the extreme, i.e., we try to identify members of the last mentioned type of complete set with the actual nuclear states. [A somewhat generalized version of the same model has been examined independently by G. C. Phillips (private communication); see Re56(b).] This model implies two strong assumptions.

(i) Each state has a pure configuration (i.e., in our example one of the three configurations listed).

(ii) Each state has a unique "parent" state, which is a proper state of the parent nucleus (i.e.,  $C^{12}$  or  $N^{14}$  in our example).

Physically, the model implies that the polarizing power of an odd nucleon or hole in the presence of a group (core) of equivalent particles is very limited such that the interactions do not disturb the core, or, for that matter, the orbit of the odd nucleon. As a refinement, we regard the odd nucleon as being spin-orbit coupled having a  $j$  value besides an  $l$  value. In general, in the  $1p$  shell, the model implies that states of nonnormal parity are one of four types; for a nucleus of normal configuration  $(1s)^4(1p)^n$ ,

$$\begin{aligned}
 (A) \quad & [(1s)^4(1p)^{n-1}]_{\alpha_1} + 2s_{\frac{1}{2}}, \\
 (B) \quad & [(1s)^4(1p)^{n-1}]_{\alpha_1} + 1d_{\frac{3}{2}}, \\
 (C) \quad & [(1s)^4(1p)^{n-1}]_{\alpha_1} + 1d_{\frac{5}{2}}, \\
 (D) \quad & [(1s)^4(1p)^{n+1}]_{\alpha_1} - 1s_{\frac{1}{2}},
 \end{aligned} \quad (66)$$

where  $\alpha_1$  is taken to label the actual eigenstates of the bracketed "core" configurations.

The simplified model makes immediate predictions about certain common types of data such as spectra and nucleon reduced widths. The predicted spectrum of nonnormal parity states of a  $1p$ -shell nucleus consists of four families of types (A)(B)(C)(D), the first three of which reproduce the observed spectrum of  $(1s)^4(1p)^{n-1}$  and the last reproducing that of  $(1s)^4(1p)^{n+1}$ . The four families can be superposed once the relative energies of the four single-particle states is given.

The only reduced nucleon widths that are important in practice are those with the ground state of the nucleus with one less nucleon as the residual nucleus. The predictions about the values of these reduced widths are immediate on the present model:

Type (A): single-particle value for  $s$ -wave emission when the core state  $\alpha_1$  is the ground state; zero otherwise.

Types (B), (C): single-particle value for  $d$ -wave emission when the core state  $\alpha_1$  is the ground state; zero otherwise.

Type (D): always zero.

It follows that one can very quickly discover, on examining the experimental data, whether the model can be taken at all seriously. We see in Sec. III.2 that the model works well, in fact almost disconcertingly so. We will see evidence in the case of  $N^{13}$  that the polarizing power of the interaction between the odd nucleon and the  $C^{12}$  core is such that it is only when two core states occur within an Mev or so of each other that they begin to mix appreciably. However, it should not be assumed that the model is always successful. For instance, in the case of  $N^{15}$ , the model gives a poor account of the observed states, which involve large mixing of core states (Ha57b) of  $N^{14}$ . It is reasonable that the model should work better in  $N^{13}$  than  $N^{15}$  since the spacing of the core states is larger for  $N^{13}$  than for  $N^{15}$ .

We do not discuss deuteron and alpha processes from nonnormal parity states. There is not very much data, and the labor involved together with inherent uncertainties and the tentativeness of the model do not make the effort worth it. However, we do discuss radiation processes, which are all of the electric-dipole type leading to states of normal parity. For computing the matrix elements of such processes, we must express the structure of states on our model more explicitly. For a core state of  $(n-1)$  nucleons and an odd nucleon  $j$ ,

$$X_{\lambda T J M T M J} = \{n^{-\frac{1}{2}} \sum_i (-)^i\} \\ \times \sum (T_{1\frac{1}{2}} M_{T_1 m_i} | T M_T) (I_1 j i_1 m_j | J M_J) \\ \times \psi(\alpha_1 T_1 I_1 M_{T_1} i_1)^{(-i)} \psi(l j m_i m_j)^{(i)}, \quad (67)$$

where  $\{n^{-\frac{1}{2}} \sum_i (-)^i\}$  is the antisymmetrizing operator and the superscript  $(-i)$  means "does not contain particle  $i$ ."

### (c) Collected Formulas for Applications in Sec. III

In Sec. III we compare theoretical and experimental reduced widths. This is done quantitatively only for certain nucleon and electromagnetic processes, and we give here shell-model formulas for the reduced widths of such processes. All these formulas have been given explicitly or implicitly in the present subsection, but we collect them here for convenience.

#### Nucleon Channels

The reduced width of a normal parity compound state of configuration  $(l)^n$  for a channel state  $(l)^{n-1}$  and an  $l$ -wave nucleon is given in  $L-S$  coupling [from (25)

and (49)] by

$$\theta_{\lambda c}/\theta_p = (-)^{S_1+S_2-S-J_1} n^{\frac{1}{2}} (T_{1\frac{1}{2}} M_{T_1 m_i} | T M_T) \\ \times U(L_1 S_1 s \frac{1}{2}, J_1 S) U(S L_1 J_1 l, s L) \langle \lambda | \alpha_1 \rangle, \quad (68)$$

where  $\theta_p$  is the single-particle value,

$$\theta_p = (a_c/2)^{\frac{1}{2}} \phi_l(a_c). \quad (69)$$

In  $j-j$  coupling, for compound state  $(j)^n$  and residual state  $(j)^{n-1}$  where  $j = l \pm \frac{1}{2}$ , we have [from (21) and (52)]

$$\theta_{\lambda c}/\theta_p = n^{\frac{1}{2}} (T_{1\frac{1}{2}} M_{T_1 m_i} | T M_T) U(J_{1\frac{1}{2}} J_1 l, s j) \langle \lambda | \alpha_1 \rangle. \quad (70)$$

The c.f.p. for  $L-S$  and  $j-j$  coupling can be found in the literature (Ja51, Ed52) except for the c.f.p. in the upper halves of shells in  $j-j$  coupling. These are simply related to the "mirror" c.f.p. in the lower halves of shells by the formula (Ra43)

$$\langle j^{2i+2-n}(\lambda T J) | j^{2i+1-n}(\alpha_1 T_1 J_1) \rangle \\ = (-)^{J_1-T_1-J-T+i+\frac{1}{2}} \langle j^{n+1}(\alpha_1 T_1 J_1) | j^n(\lambda T J) \rangle \\ \times \left[ \frac{(n+1)(2T_1+1)(2J_1+1)}{(4j+2-n)(2T+1)(2J+1)} \right]^{\frac{1}{2}}. \quad (71)$$

For nucleon channels and *nonnormal* parity states, the predicted reduced widths on the simplified model have been discussed below Eq. (66).

We write the quantity  $\theta_{\lambda c}/\theta_p$  as the symbol  $\Lambda_{\lambda c}$  and we use this as the basis of our comparison of experiment and theory,

$$\Lambda_{\lambda c} = \theta_{\lambda c}/\theta_p = (\Gamma_{\lambda c}/\Gamma_p)^{\frac{1}{2}}. \quad (72)$$

#### Photon Channels

We may define a quantity similar to  $\Lambda_{\lambda c}$  for electromagnetic processes by

$$\Lambda_{\lambda c} = \left( \frac{\Gamma_{\lambda c}}{\Gamma_p} \right)^{\frac{1}{2}} \frac{(\lambda J \| H^{(\mathcal{E})} \| \lambda' J')}{(2J+1)^{\frac{1}{2}}} / \text{(single-particle value)}. \quad (73)$$

However, there is ambiguity in the evaluation of the single-particle value depending on whether the particle is a proton or neutron and upon the coupling of the orbital motion to the spin.

We conventionally adopt the following choices for the single-particle values.

*Electric multipole.* Evaluate for a proton with no orbit-spin coupling:

$$\text{(single-particle value)} \\ = \frac{(l \| h^{(\mathcal{E})}(\text{space}) \| l')}{(2l+1)^{\frac{1}{2}}} = \left( \frac{2\mathcal{E}+1}{4\pi} \right)^{\frac{1}{2}} (-)^{\mathcal{E}} \\ \times (l \mathcal{E} 0 0 | l' 0) I(\mathcal{E}; l, l') e(1-Z/A^{\mathcal{E}}). \quad (74)$$

*Magnetic dipole.* Evaluate for a proton with no orbital motion:

(single-particle value)

$$= \frac{\langle s || h^{(M1)}(\text{spin}) || s \rangle}{(2s+1)^{\frac{1}{2}}} = \frac{3}{4\pi^{\frac{1}{2}}} g_p \left( \frac{e\hbar}{2mc} \right). \quad (75)$$

The theoretical formulas for  $\Lambda_{\lambda c}$  in  $L-S$  coupling are then, from (42)-(44), and (53),

$$\begin{aligned} \Lambda_{\lambda c}(E\mathcal{E}) &= \delta_{SS'} n \sum_{\alpha_1} \langle \lambda | \alpha_1 \rangle \langle \lambda' | \alpha_1 \rangle U(\mathcal{E}' LL_1, l'l') \\ &\quad \times U(\mathcal{E}' JS, LJ') \\ &\quad \times \left\{ \frac{\frac{1}{2}(\delta_{TT'} - \tau_1) - (Z/A^{\mathcal{E}})\delta_{TT'}}{1 - (Z/A^{\mathcal{E}})} \right\}, \quad (76) \end{aligned}$$

$$\begin{aligned} \Lambda_{\lambda c}(M1) &= \delta_{l'l'} (n/\sqrt{3}g_p) \sum_{\alpha_1} \langle \lambda | \alpha_1 \rangle \langle \lambda' | \alpha_1 \rangle \\ &\quad \times \{ \delta_{SS'} U(1' LL_1, l'l') U(1' JS, LJ') \\ &\quad \times (\delta_{TT'} - \tau_1) [l(l+1)]^{\frac{1}{2}} \\ &\quad + \delta_{LL'} (-)^{J'-S'-J+S} U(1S' JL, SJ') \\ &\quad \times U(1\frac{1}{2} SS_1, \frac{1}{2} S') (\sqrt{3}/2) [(\delta_{TT'} - \tau_1)g_p \\ &\quad + (\delta_{TT'} + \tau_1)g_n] \}, \quad (77) \end{aligned}$$

where the new quantity  $\tau_1$  is defined by

$$\begin{aligned} \tau_1 &= (-)^{2T_1 - T - T'} \sqrt{3} (1T' 0 M_T | T M_T) \\ &\quad \times U(1\frac{1}{2} T T_1, \frac{1}{2} T'), \quad (78) \end{aligned}$$

and is tabulated in Table IV.

These formulas apply to transitions of the type  $\lambda(l_0^{n-1}l) \rightarrow \lambda'(l_0^{n-1}l')$  with  $\alpha_1$  labeling the states of  $l_0^{n-1}$  and where  $l$  and  $l'$  may or may not be equal to  $l_0$ . From formula (67) it follows that, if  $l \neq l_0$ , our simple model for states of the type  $(l_0^{n-1}l)$  gives for the c.f.p.,

$$\langle \lambda(l_0^{n-1}l) | \alpha_1(l_0^{n-1}) \rangle = n^{-\frac{1}{2}}. \quad (79)$$

For states of configurations  $l_0^{n-1}l$  ( $l \neq l_0$ ) it is of interest to consider a possible structure in which the core  $(l_0^{n-1})_{\alpha_1}$  is in  $L-S$  coupling with a total spin  $\mathbf{J}_1 = \mathbf{L}_1 + \mathbf{S}_1$  and where the odd particle is spin-orbit coupled,  $j = l \pm \frac{1}{2}$ , before being coupled on to  $J_1$  in the total state. For  $E\mathcal{E}$

$$\Lambda_{\lambda c}^2(E\mathcal{E}) = \left\{ \frac{\mathcal{E}[(2\mathcal{E}+1)!!]^2 \times 0.694 \times 10^{-6} (197.3)^{2\mathcal{E}+1}}{2(2\mathcal{E}+1)(\mathcal{E}+1)} \right\} \frac{\Gamma_{\text{obs}}}{E_{\gamma}^{2\mathcal{E}+1} [1 - (Z/A^{\mathcal{E}})]^2 [(\mathcal{E} 00 | l' 0) I(\mathcal{E}; l, l')]^2}, \quad (83)$$

where  $I(\mathcal{E}, l, l')$  is in units of  $(10^{-18} \text{ cm})^{\mathcal{E}}$ ,  $E_{\gamma}$  in Mev,  $\Gamma_{\text{obs}}$  in ev. The values of the first factor for dipole ( $\mathcal{E}=1$ ) and quadrupole ( $\mathcal{E}=2$ ) radiation are

$$\begin{aligned} \mathcal{E}=1: \quad \{ \} &= 3.977, \\ \mathcal{E}=2: \quad \{ \} &= 3.11 \times 10^6. \quad (84) \end{aligned}$$

For magnetic-dipole radiation, the corresponding for-

TABLE IV. Values of the isotopic spin factor  $\tau_1$  defined in (78), along with other relevant quantities.  $g_n$  and  $g_p$  are the gyromagnetic ratios for the neutron and proton.

$T$	$T'$	$M_T$	$T_1$	$\tau_1$	$\delta_{TT'} - \tau_1$	$\delta_{TT'} + \tau_1$	$(\delta_{TT'} - \tau_1)g_p$ $+ (\delta_{TT'} + \tau_1)g_n$
$\frac{1}{2}$	$\frac{1}{2}$	$\frac{1}{2}$	0	1	0	2	$2g_n = -7.652$
$\frac{1}{2}$	$\frac{1}{2}$	$\frac{1}{2}$	1	$-\frac{1}{2}$	$\frac{3}{2}$	2	$\frac{2}{3}(g_n + 2g_p) = 4.898$
$\frac{1}{2}$	$\frac{1}{2}$	$-\frac{1}{2}$	0	-1	1	0	$2g_p = 11.172$
$\frac{1}{2}$	$\frac{1}{2}$	$-\frac{1}{2}$	1	$\frac{1}{2}$	$\frac{3}{2}$	$\frac{3}{2}$	$\frac{2}{3}(2g_n + g_p) = -1.384$
0	0	0	$\frac{1}{2}$	0	1	1	$g_n + g_p = 1.760$
0	1	0	$\frac{1}{2}$	1	-1	1	$g_n - g_p = -9.412$
1	1	0	$\frac{1}{2}$	0	1	1	$g_n + g_p = 1.760$
1	1	0	$\frac{3}{2}$	0	1	1	$g_n + g_p = 1.760$
1	1	1	$\frac{1}{2}$	1	0	2	$2g_n = -7.652$
1	1	1	$\frac{3}{2}$	$-\frac{1}{2}$	$\frac{3}{2}$	$\frac{1}{2}$	$\frac{1}{2}(3g_p + g_n) = 6.466$
1	1	-1	$\frac{1}{2}$	-1	2	0	$2g_p = 11.172$
1	1	-1	$\frac{3}{2}$	$\frac{1}{2}$	$\frac{3}{2}$	$\frac{3}{2}$	$\frac{1}{2}(g_p + 3g_n) = -2.946$

transitions with the final state in pure  $L-S$  coupling and the initial state of this type,

$$\begin{aligned} \Lambda_{\lambda c}(E\mathcal{E}) &= (-)^{J_1 - J + S_1 - S' - J'} n^{\frac{1}{2}} \sum_j (-)^j \\ &\quad \times U(l' L_1 J' S', L' f) U(\frac{1}{2} S_1 f L_1, S' J_1) \\ &\quad \times U(l\frac{1}{2} J J_1, j f) U(\mathcal{E}' J f, l' J') \langle \lambda' | \alpha_1 \rangle \\ &\quad \times \left\{ \left[ \frac{1}{2}(\delta_{TT'} - \tau_1) - (Z/A^{\mathcal{E}})\delta_{TT'} \right] / 1 - (Z/A^{\mathcal{E}}) \right\}. \quad (80) \end{aligned}$$

In  $j-j$  coupling the corresponding formulas are [from (38), (39), (42)-(44), and (63)],

$$\begin{aligned} \Lambda_{\lambda c}(E\mathcal{E}) &= n \sum_{\alpha_1} \langle \lambda | \alpha_1 \rangle \langle \lambda' | \alpha_1 \rangle U(\mathcal{E}' j\frac{1}{2}, l' j') \\ &\quad \times U(\mathcal{E}' j' J J_1, j' J') \left\{ \left[ \frac{1}{2}(\delta_{TT'} - \tau_1) \right. \right. \\ &\quad \left. \left. - (Z/A^{\mathcal{E}})\delta_{TT'} \right] / 1 - (Z/A^{\mathcal{E}}) \right\}, \quad (81) \end{aligned}$$

$$\begin{aligned} \Lambda_{\lambda c}(M1) &= (n\delta_{l'l'}/\sqrt{3}g_p) \sum_{\alpha_1} \langle \lambda | \alpha_1 \rangle \langle \lambda' | \alpha_1 \rangle U(1' j' J J_1, j' J') \\ &\quad \times \{ U(1' j\frac{1}{2}, l' j') (\delta_{TT'} - \tau_1) [l(l+1)]^{\frac{1}{2}} \\ &\quad + (-)^{i-i'} U(1\frac{1}{2} j l, \frac{1}{2} j') (\sqrt{3}/2) \\ &\quad \times [(\delta_{TT'} - \tau_1)g_p + (\delta_{TT'} + \tau_1)g_n] \}. \quad (82) \end{aligned}$$

The formula for extracting the experimental value of  $\Lambda^2$  from an observed width  $\Gamma_{\text{obs}}$  for electric-multipole radiation is

$$\Lambda_{\lambda c}^2(M1) = 15.45 \Gamma_{\text{obs}} / E_{\gamma}^3. \quad (85)$$

### 3. INTERPRETATION OF THE EXPANSION COEFFICIENTS WITH THE ROTATIONAL MODEL

Recently it has been shown that a number of the light nuclei in the mass region  $A=19$  to  $A=36$  appear

to have permanent intrinsic quadrupole deformations (Pa57, Sh56b). It is possible to describe these deformations in terms of superpositions of shell-model states; in fact, in the case of many properties of  $F^{19}$ , the shell model has been used successfully to predict these properties (El55a). However, it is much simpler, both in this particular case (Pa57) and in general, to describe deformed nuclei with the development by Nilsson (Ni55) of the "strong-coupling" model of Bohr and Mottelson (Bo53). In this development, one works with single-particle wave functions defined for a deformed (spheroidal) potential well. In general, such a wave function has the projection  $\omega$  of the angular momentum on the symmetry axis as a good quantum number, but  $j$ , the total angular momentum, is not a good quantum number.

To illustrate the construction of total wave functions with Nilsson's model, we begin by describing the prediction of reduced widths for nucleon channels (Sa58, Yo54). In doing this, we follow a paper by Yoshida (Yo54). (Yoshida considered both "strong" and "weak" coupling. We do not concern ourselves here with the latter because there is no evidence at present that it is of any use in applications.) Afterwards we mention electromagnetic matrix elements. There is not sufficient practical application to warrant any discussion of alpha and deuteron processes, and no discussion of these is given.

### (a) Nucleon Channels

Let us suppose that the nucleus consists of  $A$  nucleons moving in orbits in a deformed spheroidal potential. Although  $j$  cannot be an exact quantum number for a particle in a spheroidal potential, for the present we can regard  $j$  as an *approximate* quantum number and label the particle orbits  $j_1 \cdots j_A$ . (This restriction is removed below.) Let us further suppose that the components of particle angular momentum along the body axis of symmetry are good quantum numbers  $\omega_1 \cdots \omega_A$  and let us write  $\Omega$  for  $\sum_{i=1}^A \omega_i$  and  $(j, \omega)$  for the set of orbits. We may now assert that the *internal* wave function of the system (i.e., the wave function referred to the body axes) has the form

$$X_{(j, \omega) \Omega T M T} = (A)^{-\frac{1}{2}} \sum_{(T)} (\pm) \phi_{j_1 \omega_1} \phi_{j_2 \omega_2} \cdots \phi_{j_A \omega_A}, \quad (86)$$

where  $\sum_{(T)} (\pm)$  denotes a summation over the possible permutations of the particles  $1 \cdots A$  amongst the states  $\phi_{j_1 \omega_1} \cdots \phi_{j_A \omega_A}$  such that  $T$  is a good quantum number and the state has a definite symmetry character allowed by the Pauli principle.

To construct wave functions in a space-fixed coordinate system, it only remains to introduce the quantities  $D_{MK}^{(J)}(\theta_{12})$  which enable one to transform wave functions from one set of axes to a second set whose orientation with relation to the first set is specified by Euler angles denoted by  $\theta_{12}$ . For instance, the trans-

formation of a particular particle state is

$$\phi_{jm}(\theta_1) = \sum_{\omega} D_{m\omega}^{(j)}(\theta_{12}) \phi_{j\omega}(\theta_2). \quad (87)$$

The normalization of the  $D_{MK}^{(J)}$  is

$$\int |D_{MK}^{(J)}(\theta_{12})|^2 d\theta_{12} = 8\pi^2 / (2J+1). \quad (88)$$

The wave function of a compound state of spin  $J$  and component  $M$  along a space-fixed axis is

$$X_{\lambda J M T M T} = \left( \frac{2J+1}{8\pi^2} \right)^{\frac{1}{2}} \left( \frac{1}{2} \right)^{\frac{1}{2}} \{ X_{(j, \omega) \Omega T M T} D_{MK}^{(J)} + \epsilon X_{(j, -\omega) -\Omega T M T} D_{M-K}^{(J)} \}, \quad (89)$$

where  $\epsilon$  is the sign  $\epsilon = (-1)^{J-g}$ ,  $g$  being the angular momentum of the intrinsic wave function  $X$ :

$$\mathbf{J} = \sum_i \mathbf{j}_i.$$

The presence of the second term and also the rule that the difference  $(K-\Omega)$  must be even,

$$K-\Omega = 0, \pm 2, \pm 4, \cdots, \quad (90)$$

is a consequence of the degeneracy of the system with respect to rotation by  $180^\circ$  about any axis perpendicular to the body symmetry axis. In general one may also include a vibrational wave function in (89), but we do not concern ourselves with vibrational states.

The wave function of the "channel state"

$$\psi(\alpha_1 I_1 i_1 T_1 M T_1),$$

which has one less nucleon than the compound state, has a similar form:

$$\begin{aligned} \psi(\alpha_1 I_1 i_1 T_1 M T_1) &= \left( \frac{2I_1+1}{8\pi^2} \right)^{\frac{1}{2}} \left( \frac{1}{2} \right)^{\frac{1}{2}} \{ \psi((j, \omega)_1 \Omega_1 T_1 M T_1) D_{i_1 K_1}^{(I_1)} \\ &+ \epsilon_1 \psi((j, -\omega)_1 -\Omega_1 T_1 M T_1) D_{i_1 -K_1}^{(I_1)} \}. \end{aligned} \quad (91)$$

The use of the formula

$$\begin{aligned} \int (D_{MK}^{(J)})^* D_{i_1 K_1}^{(I_1)} D_{m\omega}^{(j)} d\theta_{12} &= \frac{8\pi^2}{2J+1} (I_1 j i_1 m | JM) (I_1 j K_1 \omega | JK) \end{aligned} \quad (92)$$

immediately enables one to derive the expansion coefficients in (49) as

$$\begin{aligned} \langle \lambda | \alpha_1 j \rangle &= \frac{1}{2} \left( \frac{2I_1+1}{2J+1} \right)^{\frac{1}{2}} \sum_{\omega} \{ \langle \Omega | \Omega_1 \omega \rangle (I_1 j K_1 \omega | JK) \\ &+ \langle -\Omega | \Omega_1 \omega \rangle (I_1 j K_1 \omega | J-K) \\ &+ (-)^{J-i-I_1} \langle \Omega | -\Omega_1 \omega \rangle (I_1 j -K_1 \omega | JK) \\ &+ (-)^{J-i-I_1} \langle -\Omega | -\Omega_1 \omega \rangle \\ &\quad \times (I_1 j -K_1 \omega | J-K) \}, \end{aligned} \quad (93)$$

where the  $\langle \Omega | \Omega_1 \omega \rangle$  are the coefficients in the fractional parentage expansion of the internal wave functions

$$X_{(j,\omega)\Omega} = \sum_{\Omega_1, \omega} \langle \Omega | \Omega_1 \omega \rangle \psi_{(j,\omega)_1 \Omega_1} \phi_{j\omega}. \quad (94)$$

For brevity we have dropped the isotopic-spin labels and write  $\langle \Omega | \Omega_1 \omega \rangle$  for the full fractional parentage coefficient

$$\langle (j,\omega)\Omega T M_T | \{ (j,\omega)_1 \Omega_1 T_1 M_{T_1}, j\omega \frac{1}{2} m_i \} \rangle.$$

From (93)

$$\begin{aligned} \langle \lambda | \alpha_1 j \rangle &= \frac{1}{2} \left( \frac{2I_1+1}{2J+1} \right)^{\frac{1}{2}} \{ [\langle \Omega | \Omega_1, K-K_1 \rangle \\ &+ \langle -\Omega | -\Omega_1, -K+K_1 \rangle] (I_1 j K_1 (K-K_1) | JK) \\ &+ [\langle -\Omega | \Omega_1, -K-K_1 \rangle + \langle \Omega | -\Omega_1, K+K_1 \rangle] \\ &\times (I_1 j K_1 (-K-K_1) | J-K) \}. \quad (95) \end{aligned}$$

For nonzero  $\langle \lambda | \alpha_1 j \rangle$ , it is clear that all orbits of  $(j,\omega)_1$  must be contained in  $(j,\omega)$  or  $(j, -\omega)$  and also that

$$\Omega - K = \pm (\Omega_1 - K_1). \quad (96)$$

There are exceptional cases for which the foregoing formulas are not quite correct. For instance, the wave function (89) is not correctly normalized if

$$X_{(j,\omega)\Omega} D_{MK}^J \equiv \epsilon X_{(j,-\omega)-\Omega} D_{M-K}^{(J)}. \quad (97)$$

This implies that  $K = \Omega = 0$  and  $X_{(j,\omega)0} = \epsilon X_{(j,-\omega)0}$ . For each occupied state  $\phi_{j,\omega}$  in the total state, the state  $\phi_{j,-\omega}$  must be occupied also; thus, the total state must consist of filled two-particle "shells"  $\pm\omega$  with certain symmetry and  $J$  values. For instance, if all lowest states in an even-even ( $N=Z$ ) nucleus are filled with neutrons and protons, then only even  $J$  are allowed. If an odd-odd ( $N=Z$ ) nucleus has all lowest orbits filled and one neutron and one proton in the last orbit, then, for  $T=0$  states (symmetric in space for the last two particles), only odd  $J$  are allowed and for  $T=1$ , only even  $J$  are allowed. If an even-even ( $N=Z+2$ ) nucleus has all lowest states filled, the last two neutrons ( $T=1$ ) must be coupled antisymmetrically in space and only even  $J$  are allowed. When condition (97) holds, the wave function is

$$X_{\lambda JM} = \left( \frac{2J+1}{8\pi^2} \right)^{\frac{1}{2}} X_{(j,\omega)0} D_{M0}^{(J)},$$

and (95) becomes

$$\begin{aligned} \langle \lambda | \alpha_1 j \rangle &= \left( \frac{1}{2} \right)^{\frac{1}{2}} \left( \frac{2I_1+1}{2J+1} \right)^{\frac{1}{2}} (I_1 j K_1 - K_1 | J0) \\ &\times [\langle 0 | \Omega_1 - K_1 \rangle + \langle 0 | -\Omega_1 K_1 \rangle] \\ &= \left( \frac{1}{2} \right)^{\frac{1}{2}} (-)^{j+K_1} (J0 K_1 | I_1 K_1) \\ &\times [\langle 0 | \Omega_1 - K_1 \rangle + \langle 0 | -\Omega_1 K_1 \rangle], \quad (98) \end{aligned}$$

where it is implied that  $\Omega_1 = K_1$  for nonzero  $\langle \lambda | \alpha_1 j \rangle$ .

Evidently another exceptional case is when the channel state (91) is not correctly normalized for similar reasons. In this case,  $K_1 = \Omega_1 = 0$  and (95) becomes

$$\begin{aligned} \langle \lambda | \alpha_1 j \rangle &= \left( \frac{1}{2} \right)^{\frac{1}{2}} \left( \frac{2I_1+1}{2J+1} \right)^{\frac{1}{2}} (I_1 j 0 K | JK) \\ &\times [\langle \Omega | 0 K \rangle + \langle -\Omega | 0 -K \rangle] \\ &= \left( \frac{1}{2} \right)^{\frac{1}{2}} (-)^{j+K} (J j - K K | I_1 0) \\ &\times [\langle \Omega | 0 K \rangle + \langle -\Omega | 0 -K \rangle], \quad (99) \end{aligned}$$

where it is implied that  $\Omega = K$  for nonzero  $\langle \lambda | \alpha_1 j \rangle$ .

From (12) and (9), the reduced-width amplitudes corresponding to the expansion coefficients (95) are

$$\begin{aligned} \theta_{\lambda c} &= \sum_j U(I_1 \frac{1}{2} J l_c, s j) (T_1 \frac{1}{2} M_{T_1} m_i | T M_T) n^{\frac{1}{2}} \langle \lambda | \alpha_1 j \rangle \\ &\times (a_c/2)^{\frac{1}{2}} \phi_{j\omega}(a_c), \quad (100) \end{aligned}$$

and the reduced widths summed over channel spins,

$$\begin{aligned} \sum_s \theta_{\lambda c}^2 &= (T_1 \frac{1}{2} M_{T_1} m_i | T M_T)^2 \sum_j n \langle \lambda | \alpha_1 j \rangle^2 \\ &\times [(a_c/2) \phi_{j\omega}(a_c)]^2, \quad (101) \end{aligned}$$

where  $n$  is the number of particles that are taken into account in the parentage expansion (94) for the internal wave functions. As pointed out before, there is no need to include in the antisymmetrization those particles in close "shells" common to both compound and channel states.

At this stage we may point out the effects of dropping the assumption that  $j$  is a good quantum number. The actual orbit  $\phi_\omega$  may be expanded as

$$\phi_\omega = \sum_j \langle \omega | j \rangle \phi_{j\omega}, \quad (102)$$

the expansion coefficients  $\langle \omega | j \rangle$  being identical with Nilsson's  $c_j$  (Ni55). Thus the right-hand sides of (89) and (91) should be preceded by

$$\sum_{j_1 \dots j_A} \langle \omega_1 | j_1 \rangle \dots \langle \omega^A | j_A \rangle,$$

but the only effect on formulas (93), (95), (98), and (99) is that each term on the right-hand side is multiplied by  $\langle \omega | j \rangle$  with  $\omega$  taken appropriately for each term separately. Formulas (94) and (100) are unaffected.

The results of this section may be illustrated by the following simple example which accounts for many cases of practical interest.

(i) Channel state consists of closed shells of neutrons and protons (so  $n=1$ ,  $\Omega_1=0$ ) in the lowest rotational

state (so  $K_1=I_1=0$ ). This situation is one of the exceptional cases mentioned previously and is covered by (99) from which it follows that

$$\langle \lambda | \alpha_1 j \rangle = \left( \frac{2}{2J+1} \right)^{\frac{1}{2}} \langle K | j \rangle \delta_{jJ}. \quad (103)$$

Thus, from (101), the reduced widths for entrance channels of rotational bands of levels found in nucleon resonance reactions or  $(d, p)$  or  $(d, n)$  stripping reactions on an even-even nucleus by nucleons are proportional to  $(2J+1)^{-1}$  in the approximation in which  $j$  is a reasonably good quantum number. If there is considerable  $j$  mixing, the same result holds if  $(2J+1)^{-1}$  is replaced by  $(2J+1)^{-1} \langle K | j \rangle^2$ .

(ii) Compound state consists of closed shells of neutrons and protons (so  $n=2$ ,  $\Omega=0$ ) in the lowest state (so  $K=J=0$ ). This situation is covered by (98) from which it follows that

$$\langle \lambda | \alpha_1 j \rangle = 2^{\frac{1}{2}} (-)^{K_1+I_1} \langle K_1 | j \rangle \delta_{jI_1}. \quad (104)$$

Thus, in the approximation in which  $j$  is a good quantum number, the reduced widths of states of a rotational band found in  $(p, d)$  or  $(n, d)$  pickup reactions on even-even closed-shell targets should be all the same.

### (b) Photon Channels

From the strong-coupling wave functions of (89) and the electromagnetic operators (31)–(33), it is possible to compute electromagnetic matrix elements. The first step is to express the operators in terms of the same coordinates as those in the wave functions, viz., the Euler angles  $\theta_{12}$  of the symmetry axis relative to a space-fixed set of axes, and the internal coordinates. From the tensor nature of the electromagnetic operators, this may be done by transforming thus:

$$H_{\mathfrak{N}_1}^{(\mathcal{E})}(\theta_1) = \sum_{\mathfrak{N}_2} D_{\mathfrak{N}_1 \mathfrak{N}_2}^{(\mathcal{E})}(\theta_{12}) H_{\mathfrak{N}_2}^{(\mathcal{E})}(\theta_2), \quad (105)$$

where  $H_{\mathfrak{N}_2}^{(\mathcal{E})}(\theta_2)$  has the same functional form as  $H_{\mathfrak{N}_1}^{(\mathcal{E})}(\theta_1)$ . Unlike the corresponding evaluation of matrix elements with the usual shell model based on a spherically symmetric potential, *all* particles contribute in general. Let us break the operators  $H$  into two parts;  $H = \tilde{H} + \hat{H}$ , the part  $\tilde{H}$  corresponding to particles in closed shells that are undisturbed in the transition (each shell containing two neutrons and two protons and having  $T=0$ ), and the part  $\hat{H}$  corresponding to the "loose" particles. The internal wave functions  $X_{(j, \omega)\Omega}$  may also be broken into two parts.  $X = \tilde{X}_{((j, \omega))0(j, \omega)\Omega} + \hat{X}$  provided that we ignore antisymmetrization between the particles in the two parts. Typical matrix elements

of the operators  $\tilde{H}$  and  $\hat{H}$  are

$$\begin{aligned} & (\lambda JM | \tilde{H}_{\mathfrak{N}_1}^{(\mathcal{E})} | \lambda' J' M') \\ &= \frac{1}{2} \left( \frac{2J+1}{8\pi^2} \cdot \frac{2J'+1}{8\pi^2} \right)^{\frac{1}{2}} \sum_{\mathfrak{N}_2} \{ (\Omega | \tilde{H}_{\mathfrak{N}_2}^{(\mathcal{E})} | \Omega') \\ & \quad \times (MK | \mathfrak{N}_1 \mathfrak{N}_2 | M' K') + \epsilon (-\Omega | \tilde{H}_{\mathfrak{N}_2}^{(\mathcal{E})} | \Omega') \\ & \quad \times (M-K | \mathfrak{N}_1 \mathfrak{N}_2 | M' K') + \epsilon' (\Omega | \tilde{H}_{\mathfrak{N}_2}^{(\mathcal{E})} | -\Omega') \\ & \quad \times (MK | \mathfrak{N}_1 \mathfrak{N}_2 | M' - K') + \epsilon \epsilon' (-\Omega | \tilde{H}_{\mathfrak{N}_2}^{(\mathcal{E})} | -\Omega') \\ & \quad \times (M-K | \mathfrak{N}_1 \mathfrak{N}_2 | M' - K') \}, \\ &= \left( \frac{2J'+1}{2J+1} \right)^{\frac{1}{2}} (J' \mathcal{E} M' \mathfrak{N}_1 | JM) \{ (\Omega | \tilde{H}_{K-K'}^{(\mathcal{E})} | \Omega') \\ & \quad (J' \mathcal{E} K' (K-K') | JK) \\ & \quad + \epsilon (-\Omega | \tilde{H}_{-K-K'}^{(\mathcal{E})} | \Omega') \\ & \quad \times (J' \mathcal{E} K' (-K-K') | J-K') \}, \quad (106) \end{aligned}$$

$$\begin{aligned} & (\lambda JM | \hat{H}_{\mathfrak{N}_1}^{(\mathcal{E})} | \lambda' J' M') \\ &= \left( \frac{2J'+1}{2J+1} \right)^{\frac{1}{2}} (J' \mathcal{E} M' \mathfrak{N}_1 | JM) (J' \mathcal{E} K 0 | JK) \\ & \quad \times (0 | \hat{H}_0^{(\mathcal{E})} | 0) \delta_{KK'} \delta_{XX'}, \quad (107) \end{aligned}$$

where we have made the abbreviations

$$\begin{aligned} & (D_{MK}^{(J)} | D_{\mathfrak{N}_1 \mathfrak{N}_2}^{(\mathcal{E})} | D_{M'K'}^{(J')}) = (MK | \mathfrak{N}_1 \mathfrak{N}_2 | M' K'), \\ & (\tilde{X}_{(j, \omega)\Omega} | \tilde{H}_{\mathfrak{N}_1}^{(\mathcal{E})} | \tilde{X}_{(j, \omega')\Omega'}) = (\Omega | \tilde{H}_{\mathfrak{N}_1}^{(\mathcal{E})} | \Omega'), \quad (108) \end{aligned}$$

and where  $\delta_{XX'} = 1$  if  $\tilde{X}_{(j, \omega)\Omega}$  and  $\tilde{X}_{(j, \omega')\Omega'}$  are identical wave functions and zero otherwise.

### Electrical Multipole Transitions

The evaluation of the matrix elements of  $\tilde{H}$  proceeds as follows. Let us assume fractional parentage expansions of states  $\tilde{H}_{(j, \omega)\Omega}$  of  $n$  particles in terms of parent state  $\tilde{X}_{(j, \omega)\Omega_1}$  of  $(n-1)$  particles:

$$\begin{aligned} \tilde{X}_{(j, \omega)\Omega} &= \sum_{\substack{\Omega_1, \omega \\ M_{T1} + m_1 = M_T}} \langle \Omega | \Omega_1 \omega \rangle (T_{1\frac{1}{2}} M_{T1} \mathfrak{N} | T M_T) \\ & \quad \times \tilde{X}_{(j, \omega)\Omega_1} \phi_{j\omega}, \quad (109) \end{aligned}$$

and similarly for  $X_{(j, \omega')\Omega'}$ . It follows that

$$\begin{aligned} (\Omega | \tilde{H}_{\mathfrak{N}_2}^{(\mathcal{E})} | \Omega') &= n \sum_{\Omega \omega \omega'} \langle \Omega | \Omega_1 \omega \rangle \langle \Omega' | \Omega_1 \omega' \rangle \\ & \quad \times (\phi_{j\omega} | e r^{\mathcal{E}} Y_{\mathfrak{N}_2}^{(\mathcal{E})} | \phi_{j'\omega'}) \\ & \quad \times [\frac{1}{2} (\delta_{TT'} - \tau_1) - (Z/A^{\mathcal{E}}) \delta_{TT'}], \quad (110) \end{aligned}$$

where we have used the electric multipole operator of (31) and the definition (78) of  $\tau_1$ . On using the formula of subsections 1 and 2 for the single-particle matrix elements  $(\phi_{j\omega} | r^{\mathcal{E}} Y_{\mathfrak{N}_2}^{(\mathcal{E})} | \phi_{j'\omega'})$  and formula (106), the matrix elements of  $\tilde{H}$  are obtained. As in the problem of predicting nucleon widths, generalization to the case



when  $j$  is not a good quantum number is attained by inserting the expansion coefficients  $\langle \omega | j \rangle$  of (102) at appropriate places. The single-particle matrix elements may be evaluated with formula and numerical tables given by Nilsson (Ni55).

The evaluation of the matrix elements of  $\bar{H}$ , the closed-shell operator, is straightforward:

$$\langle 0 | \bar{H}_0^{(\mathcal{L})} | 0 \rangle = e \int \rho(\mathbf{r}) Y_0^{(\mathcal{L})} d\mathbf{r}, \quad (111)$$

where  $\rho(\mathbf{r})$  is the density distribution of protons

$$\int \rho(\mathbf{r}) d\mathbf{r} = Z, \quad (112)$$

and where the term  $Z/A^{\mathcal{L}}$  has been dropped. If we now assume that the density is uniform  $\{\rho = Z[(4\pi/3)a^3]^{-1}\}$  inside the surface given by

$$r = a[1 + \beta Y_0^{(2)}(\theta_2)], \quad (113)$$

and zero outside, it follows that, to first order in  $\beta$

$$\langle 0 | \bar{H}_0^{(\mathcal{L})} | 0 \rangle = \begin{cases} e(3Za^2\beta/4\pi) & \text{if } \mathcal{L}=2. \\ 0 & \text{otherwise.} \end{cases} \quad (114)$$

Thus the closed shells contribute only to quadrupole transitions; the reduced matrix element for the closed-shell  $E2$  transition is, from (106) and (114),

$$\langle \lambda J || \bar{H}^{(2)} || \lambda' J' \rangle = (2J'+1)^{\frac{1}{2}} (J'2K0 | JK)_{\frac{1}{2}} Q_0, \quad (115)$$

where  $Q_0$  is the intrinsic quadrupole moment of Bohr and Mottelson (Bo53) defined as

$$Q_0 = 3Za^2\beta e / (5\pi)^{\frac{1}{2}}. \quad (116)$$

For the frequently encountered case of an  $E2$  transition between the first excited state ( $J=2$ ) and the ground state ( $J'=0$ ) of an even-even nucleus,

$$\langle \lambda J || \bar{H}^{(2)} || \lambda' J' \rangle = 3Za^2\beta e / 2(5\pi)^{\frac{1}{2}} = \frac{1}{2} Q_0. \quad (117)$$

In terms of the quantity  $B_e(2)$  of Bohr and Mottelson, as defined following (37),

$$B_e(2) = (1/16\pi) Q_0^2. \quad (118)$$

#### Magnetic Dipole Transitions

The magnetic dipole operator is, from (32) and (33),

$$H_{\mathfrak{M}}^{(M1)} = \sum_{\text{all particles}} \left( \frac{e\hbar}{2mc} \right) (\nabla r Y_{\mathfrak{M}}^{(1)}) \cdot \left\{ \left( \frac{1}{2} - t_3 \right) (\mathbf{I} + g_p \mathbf{s}) + \left( \frac{1}{2} + t_3 \right) g_n \mathbf{s} \right\}, \quad (119)$$

where  $\mathbf{I}$  is the particle angular momentum relative to a space-fixed coordinate system. When the transformation (105) is made, the components of  $\mathbf{I}$  are referred to the

body-fixed system; it is important to note that  $\mathbf{I}$  is still defined as angular momentum relative to a space-fixed system. Now the internal wave functions  $X_{(j,\omega)\Omega}$  are products of single-particle wave functions  $\phi_{j\omega}$  in which  $j$  is the angular momentum relative to the *body-fixed* system. Thus one cannot directly evaluate the matrix elements  $\langle \phi_{j\omega} | h_{\mathfrak{M}}^{(M1)} | \phi_{j'\omega'} \rangle$ . The usual way of proceeding is to introduce a "collective angular momentum"  $\mathbf{R}$  defined by the equation

$$\mathbf{J} = \sum_{\text{all particles}} (\mathbf{I} + \mathbf{s})_{\text{body}} + \mathbf{R}. \quad (120)$$

Evidently,

$$\mathbf{R} = \sum_{\text{all particles}} (\mathbf{I})_{\text{space}} - (\mathbf{I})_{\text{body}}. \quad (121)$$

Now one assumes that the magnetic-moment operator corresponding to (120) is equal to (119) with  $(\mathbf{I})_{\text{body}}$  replacing  $(\mathbf{I})_{\text{space}}$ , and with a term  $g_R \mathbf{R}$  added inside the curly brackets, where  $g_R$  is the gyromagnetic ratio associated with  $\mathbf{R}$ . Usually  $g_R$  is assigned the value  $Z/A$ . By using (120), the effective  $M1$  operator is

$$H_{\mathfrak{M}}^{(M1)} = \sum_{\text{all particles}} \left( \frac{e\hbar}{2mc} \right) (\nabla r Y_{\mathfrak{M}}^{(1)}) \cdot \left\{ \left( \frac{1}{2} - t_3 \right) [(1 - g_R) \mathbf{I} + (g_p - g_R) \mathbf{s}] + \left( \frac{1}{2} + t_3 \right) [-g_R \mathbf{I} + (g_n - g_R) \mathbf{s}] \right\}, \quad (122)$$

where  $\mathbf{I}$  is taken in the body system. It is clear that the part of (122) from particles in closed shells not disturbed in a transition has zero matrix elements. It follows that the summation may be restricted to the loose particles. To evaluate the matrix elements  $\langle \Omega | H_{\mathfrak{M}}^{(M1)} | \Omega' \rangle$  of (106), one proceeds just as in the electric-multipole case by introducing the fractional parentage expansion (109) leading to (110). The evaluation of the single-particle matrix elements  $\langle \phi_{j\omega} | h_{\mathfrak{M}}^{(M1)} | \phi_{j'\omega'} \rangle$  is the only remaining problem. This may be done by using the formulas and numerical tables of Nilsson (Ni55).

As an example, let us consider the common case where there is only one loose particle and the transition is between two state  $J \rightarrow J' = J - 1$  of a rotational band  $K = K'$ ,  $\Omega = \Omega' = \omega$ :

$$\langle \phi_{j\omega} | h_0^{(1)} | \phi_{j\omega} \rangle = \left( \frac{3}{4\pi} \right)^{\frac{1}{2}} \left( \frac{e\hbar}{2mc} \right) (g_\omega - g_R) \omega, \quad (123)$$

$$g_\omega = (1/\omega) \langle (\frac{1}{2} - t_3) (l_x + g_p s_x) + (\frac{1}{2} + t_3) g_n s_x \rangle_{j\omega}. \quad (124)$$

Equation (106) then gives

$$\langle \lambda J || H^{(M1)} || \lambda' J' \rangle = \left( \frac{3}{4\pi} \right)^{\frac{1}{2}} (2J'+1)^{\frac{1}{2}} (J'1K0 | JK) \times \left( \frac{e\hbar}{2mc} \right) (g_\omega - g_R) \omega. \quad (125)$$

In terms of  $B_m(1)$  of Bohr and Mottelson as defined following (37),

$$B_m(1) = \frac{3}{4\pi} \left\{ (J1K0|J'K) \left( \frac{e\hbar}{2mc} \right) (g_\omega - g_R)\omega \right\}^2.$$

### III. Experimental Values of Reduced Widths of Resonance Levels in Light Nuclei

In Sec. II, formulas have been derived for the various reduced widths of individual energy levels. In the present section, the data on individual resonance levels in nuclei with  $A \leq 40$  is presented and some comparison with the predictions of models is made. Recently the shell model has had striking successes in predicting the level schemes of the lighter nuclei, especially those with  $A \leq 16$  (In53, El55a, Ku56). Before anticipating similar success in predicting the reduced widths of resonance levels, it must be recalled that this latter data usually concerns levels at considerably higher excitations than those levels previously discussed. Consequently there is no basis for expecting the shell model to give more than qualitative agreement with the observed reduced widths of resonance levels. As stressed in the last section, there are practical reasons for using rather different shell-model approaches to states of normal and nonnormal parity. Consequently all discussion in terms of the shell model is divided into normal and nonnormal parity states.

Although the shell model has been applied with success to nuclei in the range  $16 < A \leq 40$  [especially to  $F^{19}$  (El55a)], the limelight in this region has been taken recently by the strong-coupling version of the Bohr-Mottelson model (Bo53) [as supplemented by Nilsson (Ni55)]. This latter model has been applied with striking success to  $F^{19}$  (Pa57),  $Mg^{24}$ ,  $Al^{25}$  (Li56),  $Al^{28}$  (Sh56b) and several other nuclei (Ra57) in this region. In certain cases such as  $F^{19}$ , this model and the shell model give very similar predictions. This raises interesting problems (which do not concern us here) about the relation between the two models. In actual fact, just as the shell model has applications in the range  $16 < A \leq 40$ , so the strong-coupling model may be applied successfully in the range  $A \leq 16$  (Ku59). However, we confine discussion of nuclei of  $A \leq 16$  to the shell model and discussion of nuclei of  $16 < A \leq 40$  to the strong-coupling model. This rather arbitrary limitation may be justified by the fact that *neither* model can be expected to give a *very* good account of many of the excited levels that concern us here.

#### 1. NORMAL PARITY STATES OF THE MASS RANGE $4 < A \leq 16$

Configurations of the type  $(1s)^4(1p)^n$  may be assigned to most known normal parity states in nuclei of the  $1p$  shell. Exceptions arise for the more highly excited states of nuclei of masses 14, 15, and 16 where the

above type of configuration contains only limited number of states. For instance, in the case of mass 16, the configuration is  $(1s)^4(1p)^{12}$ , which is a closed-shell system and has only one state; hence, all excited states of positive parity must arise from other configurations.

The following discussion of the nuclear reaction data on the normal parity states is in four parts corresponding to nucleon, deuteron, alpha, and radiation processes. Where theoretical predictions about the data are made using the shell model, this is usually done only for those modes of coupling for which the necessary fractional parentage coefficients have been tabulated. There are two such modes as follows.

(i) Russel-Saunders ( $L-S$ ) coupling with no spin-exchange forces and no spin-orbit forces (Ja51): In this situation spatial symmetry is a good quantum number and therefore can be used to classify states. It so happens that, in the  $1p$  shell, the set of numbers  $T$ ,  $S$ ,  $L$ , and symmetry is sufficient to classify all states with two exceptions, viz., the  $^{13}D$  and  $^{31}D$  states of maximum symmetry [42] in  $(1p)^6$ ; each of these is doubly degenerate. The condition of no spin-exchange forces means that only force mixtures containing ordinary and Majorana (space exchange) forces are catered for. The Serber force (Se47) is such a mixture:

$$\frac{1}{2}(1+P_M) = \frac{1}{8}[3 - (\sigma_1 \cdot \sigma_2) - (\tau_1 \cdot \tau_2) - (\sigma_1 \cdot \sigma_2)(\tau_1 \cdot \tau_2)].$$

Unfortunately, it seems that those mixtures containing some spin-exchange forces are more satisfactory in shell-model calculations of nuclear spectra. In particular, there is the Rosenfeld (Ro48) mixture,

$$\begin{aligned} -0.13 + 0.93P_M + 0.46P_B - 0.26P_H \\ = -(\tau_1 \cdot \tau_2)[0.10 + 0.23(\sigma_1 \cdot \sigma_2)], \end{aligned}$$

and its "caricatured form" (In53),

$$0.80P_M + 0.20P_B = -(2/15)(2 + \tau_1 \cdot \tau_2)(1 + \sigma_1 \cdot \sigma_2),$$

which are often used in this connection. Both of these contain appreciable spin-exchange components. However, in general, it turns out that the nondiagonal elements of these components are considerably less than the diagonal separations of states. Thus, the approximation of assuming good symmetry quantum numbers is justified for most suggested central force mixtures.

(ii) Spin orbit ( $j-j$ ) coupling with (small) central forces of the ordinary and Heisenberg (charge exchange) types (Ed52): In the absence of central forces, states of a number of spin-orbit coupled nucleons are highly degenerate. Such states can be classified in many ways in principle. An especially convenient one which has been the basis of fractional parentage tables is that in which there are two quantum numbers (in addition to the usual  $J$ ,  $T$ ) called  $s$  and  $t$ , the seniority and reduced isotopic spin. It so happens that any mixture of ordinary and Heisenberg forces is diagonal in this representation. However, as in the previous case of  $L-S$  coupling, the "natural" types of force for the representation do not

correspond to those which succeed best in nuclear-structure calculations. In the present case, we notice that the Rosenfeld mixture and its caricature contain large Majorana components which are nondiagonal, in general, in the  $(s, t)$  representation. Nevertheless, again as in the previous case, the suggested representation can provide a good approximation to the wave functions. This is because any type of zero-range force always can be written as a combination of ordinary and Heisenberg forces (because zero-range Majorana and Bartlett forces are equivalent to ordinary and Heisenberg forces, respectively). Since the actual range of nuclear forces (compared with nuclear dimensions) is fairly small, the quantum numbers  $s$  and  $t$  should be preserved even in the presence of strong Majorana and Bartlett forces.

Neither of the foregoing two extreme types of coupling seems to be a good description of the actual mode of coupling in the  $1p$  shell, which is believed to be intermediate between the two (El57a, Im53, Ku56). Although in general we compare only the observed values with the pairs of predicted values from the extreme modes, in certain special cases we actually examine data in the intermediate region between the two extremes. The mode of coupling in this intermediate region can be specified by a ratio  $\xi/K$ , the so-called "intermediate coupling parameter" (In53). In this ratio,  $\xi$  is a measure of the strength of the spin-orbit forces tending to produce a state of spin-orbit coupling, and  $K$  is a measure of the strength of the central forces that tend to produce Russell-Saunders coupling.

In the following discussions, experimental references are only given if they are not to be found in the compilations of data by Ajzenberg and Lauritsen (Aj52, Aj55, Aj59).

### (a) Nucleon Channels

At present there are some 30 or so experimental values of reduced widths for compound states of normal parity in the  $1p$  shell and channel states consisting of a nucleon and a residual nucleus. With few exceptions the residual nucleus is in its ground state in these processes. A few of the values are for compound states that do not belong to the ground-state configurations  $(1s)^4(1p)^n$ ; these cases occur in  $N^{14}$ ,  $N^{15}$ , and  $O^{16}$ . All values are listed in Table V along with the theoretical predictions, where possible, of the two extreme coupling modes of the shell model. The observed relative orbital angular momentum of separation is almost always  $p$  wave. We now discuss the entries in the table and other nucleon data on normal parity states according to the mass numbers of the compound nuclei.

#### Mass 5

The mirror nuclei  $He^5$  and  $Li^5$  are very similar. In both nuclei the ground state is unbound against nucleon emission and possesses a large natural width. Furthermore, each nucleus is known to have a very broad state

a few Mev above the ground state making, with the ground state, the  $1p_{3/2}-1p_{1/2}$  inverted doublet expected from the shell model. In view of the large widths, it is somewhat unnatural to use the one-level resonance reaction theory for relating experimental phase shifts to the shell model, especially for the upper state. Rather it seems more appropriate to compare the observed phase shifts directly to those expected in nucleon scattering from a potential well with a spin-orbit force included. Both programs have been carried through. The former approach (Ad52, Do52, Mi 58c) leads to fits of the data in terms of the reduced widths of the two states. That of the lower state is determined to be approximately the single-particle value, but the reduced width of the upper state is undetermined except insofar that it be large. The second approach (Sa54) is more precise. Adequate fits of the observed phase shifts have been obtained with the square, Gaussian, and exponential well shapes  $V$  and a spin-orbit force of the Thomas type:  $\text{const } (1/r)(dV/dr)(\mathbf{l} \cdot \mathbf{s})$ . Given some well shape, the various parameters seem to be fairly well determined in the fitting. For the three wells mentioned, the fitting gives

$$\text{Square well: } [1+0.1031(\mathbf{l} \cdot \mathbf{s})r_0\delta(r-r_0)](19.65 \text{ Mev}) \\ (r_0=3.21 \times 10^{-13} \text{ cm}),$$

$$\text{Gaussian well: } [1+0.2468(\mathbf{l} \cdot \mathbf{s})](47.32 \text{ Mev}) \\ \times \exp[-(r/a)^2] \quad (a=2.30 \times 10^{-13} \text{ cm}),$$

$$\text{Exponential well: } [1+0.4765(\mathbf{l} \cdot \mathbf{s})(r/b)](155.5 \text{ Mev}) \\ \exp(-2r/b) \quad (b=1.924 \times 10^{-13} \text{ cm}).$$

It is rather unfortunate that no analysis has been reported for a cutoff oscillator well because this has the unique characteristic of having a Thomas-type spin-orbit term that does not depend on radial distance. Most shell-model structure calculations assume this latter type of spin-orbit term for convenience. Thus, at present, no immediate comparison is possible of the strength of spin-orbit force needed in structure calculations with that needed to explain the alpha-nucleon scattering. However, we can make a rough comparison by taking the expectation value of the spin-orbit force in the radial wave function for each of the above three cases. The value obtained in units of  $(\mathbf{l} \cdot \mathbf{s})$  is, in each case, about 3 or 4 Mev. This is to be compared with the strength of approximately 2 Mev needed in structure calculations on the mass 6 nuclei (In53, Ga55).

#### Mass 7

A normal parity state of spin  $\frac{5}{2}$  has been found in  $Be^7$  in  $Li^6+p$  bombardment and a similar state has been found in  $Li^7$  in  $Li^6+n$  bombardment. There is little doubt that these two states are mirror states. Not only do they have the same spin and almost the same excitation energy, but their reduced widths for nucleon emission are roughly the same, namely  $\theta^2 \sim 0.35$ , when an interaction radius of  $1.45(6^{\frac{1}{2}}+1) \times 10^{-13} = 4.09 \times 10^{-13}$

TABLE V. Nucleon widths of normal parity states of nuclei in the mass range  $4 < A \leq 16$ .<sup>a</sup>

Compound nucleus	Excitation in Mev	Spin and isotopic spin	Channel: residual nucleus + nucleon + $l_c$ <sup>c</sup>	Obs channel width (kev, in center of mass)	Obs $\theta^2$ <sup>d</sup>	Compound nucleus in $L-S$ coupling	Residual nucleus in $L-S$ coupling	$\Lambda^2$ in $L-S$ coupling <sup>e</sup>	Compound nucleus in $j-j$ coupling	Residual nucleus in $j-j$ coupling	$\Lambda^2$ in $j-j$ coupling <sup>e</sup>
He <sup>6</sup>	0	$\frac{3}{2}-, \frac{1}{2}$	He <sup>4</sup> + $n+1$	~700	~1	<sup>22</sup> P	<sup>11</sup> S	1	$(p_{\frac{1}{2}}^1(1s_{\frac{1}{2}})^4)$	$(1s_{\frac{1}{2}})^4$	1
Li <sup>6</sup>	0	$\frac{3}{2}-, \frac{1}{2}$	He <sup>4</sup> + $p+1$	~1500	~1	<sup>22</sup> P	<sup>11</sup> S	1	$(p_{\frac{1}{2}}^1(1s_{\frac{1}{2}})^4)$	$(1s_{\frac{1}{2}})^4$	1
Li <sup>7</sup>	7.46	$\frac{5}{2}-, \frac{1}{2}$	Li <sup>6</sup> + $n+1$	61	0.39	<sup>24</sup> P[3]	<sup>22</sup> P[2]	$\frac{2}{3}$	$(p_{\frac{1}{2}}^4(p_{\frac{1}{2}})^2)$	$(p_{\frac{1}{2}})^2$	0
Be <sup>7</sup>	7.16	$\frac{5}{2}-, \frac{1}{2}$	Li <sup>6</sup> + $p+1$	670	0.36	<sup>24</sup> P[3]	<sup>22</sup> P[2]	$\frac{2}{3}$	$(p_{\frac{1}{2}}^4(p_{\frac{1}{2}})^2)$	$(p_{\frac{1}{2}})^2$	0
Li <sup>8</sup>	2.28	$3+, 1$	Li <sup>7</sup> + $n+1$	28	0.11	<sup>33</sup> P[31]	<sup>22</sup> P[3]	$\frac{2}{3}$	$(p_{\frac{1}{2}}^4)^2$	$(p_{\frac{1}{2}})^3$	5/15
Be <sup>8</sup>	17.63	$1+, 1$	Li <sup>7</sup> + $p+1$	10	0.13	<sup>33</sup> P[31]	<sup>22</sup> P[3]	$\frac{2}{3}$	$(p_{\frac{1}{2}}^4)^2$	$(p_{\frac{1}{2}})^3$	2/15
Be <sup>10</sup>	19.18	$3+, 1$	Li <sup>7</sup> + $p+1$	~180	~0.06	<sup>33</sup> P[31]	<sup>22</sup> P[3]	$\frac{2}{3}$	$(p_{\frac{1}{2}}^4)^2$	$(p_{\frac{1}{2}})^3$	2/15
	7.37	$3+, 1$	Be <sup>9</sup> + $n+1$	23	0.021	<sup>31</sup> F[42]	<sup>22</sup> P[41]	0	$(p_{\frac{1}{2}})^5 p_{\frac{1}{2}}$	$(p_{\frac{1}{2}})^5$	0
Be <sup>10</sup>	7.54	$(2+), 1$	Be <sup>9</sup> + $n+1$	7	0.0051	<sup>31</sup> D[42]	<sup>22</sup> P[41]	?	$(p_{\frac{1}{2}})^5 p_{\frac{1}{2}}$	$(p_{\frac{1}{2}})^5$	?
						or <sup>33</sup> P[33]		0			
B <sup>10</sup>	7.46	$2+, (0)$	Be <sup>9</sup> + $p+1$	80	0.15	<sup>18</sup> D[42]	<sup>22</sup> P[41]	?	$(p_{\frac{1}{2}})^5 p_{\frac{1}{2}}$	$(p_{\frac{1}{2}})^5$	?
	7.56	$0+$	Be <sup>9</sup> + $p+1$	3	0.006	<sup>33</sup> P[33]		0	$(p_{\frac{1}{2}})^5 p_{\frac{1}{2}}$	$(p_{\frac{1}{2}})^5$	0
B <sup>10</sup>	8.89	$2+, 1$	{Be <sup>9</sup> + $p+1$ B <sup>9</sup> + $n+1$ }	8	0.0048	or <sup>18</sup> P[321] <sup>31</sup> D[42]	<sup>22</sup> P[41]	0	$(p_{\frac{1}{2}})^5 p_{\frac{1}{2}}$	$(p_{\frac{1}{2}})^5$	?
	8.89	$3+, 1$	{Be <sup>9</sup> + $p+1$ B <sup>9</sup> + $n+1$ }	75	0.039	or <sup>33</sup> P[33] <sup>31</sup> F[42]	<sup>22</sup> P[41]	0	$(p_{\frac{1}{2}})^5 p_{\frac{1}{2}}$	$(p_{\frac{1}{2}})^5$	0
C <sup>11</sup>	9.70	$\frac{3}{2}-, (\frac{1}{2})$	B <sup>10</sup> + $n+1$	{225 or 75}	{0.12 or 0.04}						
B <sup>12</sup>	3.76	$2+, 1$	B <sup>11</sup> + $n+1$	37	0.054	<sup>33</sup> P[431]	<sup>22</sup> P[43]	$\frac{1}{10}$	$(p_{\frac{1}{2}})^6(p_{\frac{1}{2}})^2$	$(p_{\frac{1}{2}})^7$	0
C <sup>12</sup>	16.10	$2+, 1$	B <sup>11</sup> + $p+1$	0.006	0.08	<sup>33</sup> P[431]	<sup>22</sup> P[43]	$\frac{5}{18}$	$(p_{\frac{1}{2}})^7 p_{\frac{1}{2}}$	$(p_{\frac{1}{2}})^7$	$\frac{1}{2}$
	(17.80) <sup>b</sup>	$(0+)$	B <sup>11</sup> + $p+1$	≤140	≤0.05	<sup>18</sup> P[431]	<sup>22</sup> P[43]	$\frac{1}{3}$	$(p_{\frac{1}{2}})^6(p_{\frac{1}{2}})^2$	$(p_{\frac{1}{2}})^7$	0
N <sup>13</sup>	3.51	$\frac{1}{2}-, \frac{1}{2}$	C <sup>12</sup> + $p+1$	67	0.06	or <sup>33</sup> P[431]		$\frac{1}{3}$			
	8.62	$0+, (1)$	C <sup>13</sup> + $p+1$	6	0.02	<sup>22</sup> P[441]	<sup>11</sup> S[44]	$\frac{1}{3}$	$(p_{\frac{1}{2}})^7(p_{\frac{1}{2}})^2$	$(p_{\frac{1}{2}})^8$	0
N <sup>14</sup>	8.98	$1+, 1$	C <sup>13</sup> + $p+1$	7	0.007	<sup>33</sup> P[422]	<sup>22</sup> P[441]	0	$(p_{\frac{1}{2}})^6(p_{\frac{1}{2}})^4$	$(p_{\frac{1}{2}})^8 p_{\frac{1}{2}}$	0
	9.72	$1+, 1$	C <sup>13</sup> + $p+1$	15	0.007	<sup>11</sup> P[433]	<sup>22</sup> P[441]	0	$(p_{\frac{1}{2}})^6(p_{\frac{1}{2}})^4$	$(p_{\frac{1}{2}})^8 p_{\frac{1}{2}}$	0
	12.79	$4+, 1$	C <sup>13</sup> + $p+3$	0.18	0.00018						
			C <sup>13</sup> + $p+4$	0.085	0.04						
			C <sup>13</sup> + $p+3$	0.44	0.045						
			C <sup>13</sup> + $p+2$	9.6	0.07						
			N <sup>13</sup> + $n+3$	0.59	0.0024						
N <sup>15</sup>	$\frac{1}{2}-, \frac{1}{2}$	C <sup>14</sup> + $p+1$	9.7	0.03							
		N <sup>14</sup> + $n+1$	1.5	0.002							
		C <sup>14</sup> + $p+3$	0.03	0.002							
		N <sup>14</sup> + $n+1$	22.0	0.01							
N <sup>15</sup>	$\frac{1}{2}-, \frac{1}{2}$	C <sup>14</sup> + $p+1$	0.3	0.0003							
		N <sup>14</sup> + $n+1$	20.0	0.009							
N <sup>15</sup>	$\frac{5}{2}-, \frac{1}{2}$	C <sup>14</sup> + $p+1$	0.8	0.03							
		N <sup>14</sup> + $n+1$	16.0	0.007							
O <sup>15</sup>	7.61	$(\frac{5}{2}-)$	N <sup>14</sup> + $p+1$	<2	<10						
	9.03	$\frac{3}{2}, \frac{1}{2}-$	N <sup>14</sup> + $p+1$	4	0.0045						
	13.65	$1+, 1$	N <sup>15</sup> + $p+1$	10	0.012						

<sup>a</sup> References to the data used in the table are given in the discussions in the text except where the data is cited in the published compilations (Aj52, Aj55, Aj59).

<sup>b</sup> Uncertain entries are bracketed ( ).

<sup>c</sup> The residual nucleus in the fourth column is always in the ground state except where a subscript  $n$  denotes that it is in the  $n$ th excited state.

<sup>d</sup> The observed values of  $\theta^2$  are corrected for variation of the partial level shift. The interaction radius is always assumed to be  $1.45(A_1^{1/3}+1) \times 10^{-3}$  cm.

<sup>e</sup> The ninth and 12th columns list theoretical values of  $\Lambda^2 = \theta^2/\theta_p^2$ . For comparison with the experimental values of  $\theta^2$  in the sixth column, we try  $\theta_p^2 = 0.6$  [see the discussion in Sec. II.2(a)].

cm is assumed (Ba51, Jo54b, Wi56a, Ma56e).<sup>2</sup> The state was originally identified in a shell-model scheme as a <sup>22</sup>P[3] state of  $L-S$  coupling and a  $(p_{\frac{1}{2}})^3$  state of  $j-j$  coupling (La55a). Lately, however, these assignments have been revised in the light of new experimental evidence (Ma57b) and further theoretical considerations (So57, Ma57a, Me56); the new assignments are <sup>24</sup>P[21] and  $(p_{\frac{1}{2}})^2 p_{\frac{1}{2}}$ . The residual nucleus Li<sup>6</sup> is <sup>18</sup>S[2] in  $L-S$  coupling and arises from  $(p_{\frac{1}{2}})^2$  in  $j-j$

<sup>2</sup> An unusually small interaction radius is used in (Jo54b).

coupling. The reduced width for  $p$ -wave emission in  $L-S$  coupling is  $\frac{2}{3}$  of the single-particle value; in  $j-j$  coupling it is zero. By taking the value 0.60 for  $\theta_p^2$ , agreement between experiment and theory is achieved (So57) at a mode of coupling characterized by  $\xi \sim 2K$ .

The ratio of the yields to the ground ( $\frac{3}{2}-$ ) and first excited ( $\frac{1}{2}-$ ) states of Li<sup>7</sup> in the Li<sup>6</sup>( $d, p$ )Li<sup>7</sup> stripping reaction indicates that the ratio of the two reduced widths is roughly 0.7 (Ho53, Le55). In  $L-S$  coupling, the states arise from the <sup>22</sup>P[3] doublet and the pre-

dicted ratio of the two reduced widths is unity. In  $j-j$  coupling, both states arise from  $(p_{\frac{3}{2}})^3$  and the ground state is predicted to have a smaller reduced width than the excited one by a factor  $\frac{3}{10}$ . The observed ratio lies in between the two predictions, and intermediate-coupling calculations (Au55, Fr57) give agreement centered at the mode characterized by  $\xi \sim 3K$ . It is also possible to analyze the relative yield to the ground ( $1+$ ) and first excited ( $3+$ ) states of  $\text{Li}^6$  in the  $\text{Li}^7(p,d)\text{Li}^6$  reaction (Re56a) and find a reduced width ratio of  $\sim 1.4$ , which agrees with an intermediate-coupling mode of  $\xi \sim 1.8K$  (Au55). (The predictions of  $L-S$  and  $j-j$  coupling for the ratio are  $25/14$  and  $3/7$ , respectively.)

#### Mass 8

There is good isobaric correspondence between the observed states of  $\text{Li}^8$  and  $\text{Be}^8$  if the 16.72-Mev level in  $\text{Be}^8$  is paired off with the ground state of  $\text{Li}^8$ . The 17.63- and 19.2-Mev states in  $\text{Be}^8$  then pair off in energy with the 0.93- and 2.28-Mev states in  $\text{Li}^8$ . The spins of these various states, as far as they are known, support this pairing. The nucleon reduced width of any pair of isobaric states should be the same. Since any nucleon width of a  $\text{Be}^8$  state is shared equally between neutrons and protons, the neutron (or proton) reduced width of a state in  $\text{Be}^8$  should be one-half of the neutron reduced width of the isobaric state in  $\text{Li}^8$ , i.e., the total nucleon widths of corresponding states should be the same.

The observed proton reduced width of the 17.63 state in  $\text{Be}^8$  is  $\theta^2 = 0.13$ . This state, which is the first  $T=1$  state of spin  $J=1$ , is identified as coming from  ${}^{33}P[31]$  in  $L-S$  coupling and from  $(p_{\frac{3}{2}})^4$  in  $j-j$  coupling. The  $L-S$  state predicts  $\theta^2 = \frac{1}{3}\theta_p^2$  and the  $j-j$  state predicts  $\theta^2 = (2/15)\theta_p^2$ . On taking  $\theta_p^2 \approx 0.60$ , the observed value lies between the predicted values. An additional item of experimental information on this state is the channel spin ratio, which is known to be  $1:5$  for  $s=1:s=2$  (De49). Theoretically, the predictions of such quantities do not contain the uncertain single-particle width  $\theta_p^2$  which drops out in the ratio. Both  $L-S$  and  $j-j$  coupling predict precisely the observed value of  $1:5$  (Ch53).

There is a state of 18.14 Mev in  $\text{Be}^8$  which has been suggested to be  $1+$ . It is presumably  $T=0$  since no isobar is found in  $\text{Li}^8$ . If the main decay of this state is supposed to be to the ground state of  $\text{Li}^7$ , its reduced width for this process is  $\theta^2 \sim 0.3$ . In  $L-S$  coupling the state is most likely  ${}^{13}P[31]$ , which has a reduced width  $\theta^2 = \frac{1}{3}\theta_p^2$  and a channel spin ratio of  $1:5$ . In  $j-j$  coupling, the state would be  $(p_{\frac{3}{2}})^3 p_{\frac{3}{2}}$ , but there are two states of  $J=1+$ ,  $T=0$  in this configuration, and finding the relative amplitude of each in the actual state involves diagonalizing the central interaction.

The observed widths of the state at 19.18 Mev in  $\text{Be}^8$  and the isobaric  $3+$  state at 2.28 Mev in  $\text{Li}^8$  can be fitted with roughly the same value of the total nuclear

reduced width as expected for isobaric states (Ad54) [see, however, (Ne57)]. The total nucleon reduced width for either level is  $\theta^2 = 0.12$  (Th54, Th56, Wi56a). In  $L-S$  coupling the state is  ${}^{33}P[31]$  and in  $j-j$  coupling it comes from  $(p_{\frac{3}{2}})^3$ . The predicted values of  $\theta^2$  in the two extreme modes are  $\frac{2}{3}\theta_p^2$  and  $(4.15)\theta_p^2$ , respectively. This reduced width has also been investigated in intermediate coupling (La55a). However, there is no such nearly sensitive dependence on the degree of intermediate coupling as was found in a similar instance in the mass 7 nuclei (So57, La55a). It has been suggested (Ma56a) that the 19.18 state in  $\text{Be}^8$  is not the analog of the  $3+$  level at 2.28 in  $\text{Li}^8$ . This suggestion comes from an analysis of the evidence on  $\text{Li}^7+p$  scattering in this vicinity, which points to an analog level at 19.0 Mev.

The relative yields to the ground and 0.93 states in  $\text{Li}^8$  in the  $\text{Li}^7(d,p)$  reaction (Le55, Re56a) indicate a ratio of 1.83 for the reduced widths for breakup of these states into  $\text{Li}^7+n$  [see also (Fr57)].  $L-S$  and  $j-j$  coupling give the ratios  $5/3$  and  $4$ , respectively (assuming the two states to be  $2+$  and  $1+$  and to arise from the  ${}^{33}P[31]$  state in  $L-S$  coupling).

#### Mass 9

Very little can be inferred about the spins of the known states in  $\text{Be}^9$  at present. There are four definite or suggested low-lying excited states at 1.8-, 2.43-, 3.1-, and 4.8-Mev excitation. The 2.43 state is very sharp [ $\Gamma < 1$  kev, (Go55b)], the 4.8 state is broad ( $\Gamma = 0.5-1$  Mev), and the widths of the other two are uncertain but probably  $< 100$  kev. There is qualitative agreement with expectation. One expects low-lying normal parity states of spin  $\frac{1}{2}$ ,  $\frac{3}{2}$  arising from  ${}^{22}P[41]$  and  ${}^{22}D[41]$ , respectively, in  $L-S$  coupling and from  $(p_{\frac{3}{2}})^5$  in  $j-j$  coupling. The reduced widths expected are  $\frac{2}{3}\theta_p^2$  and zero, respectively, in  $L-S$  coupling and both are zero in  $j-j$  coupling. Thus the 2.43 state (which would have an observed  $\theta^2 < 0.001$  for  $p$ -wave neutron emission) might be identified as the  $\frac{3}{2}$  state. This can decay only by  $f$ -wave emission. The observed state at 3.1 could be the predicted  $\frac{1}{2}$  state. Because of its possibly large width, the 1.8 state may be an  $s$ -wave state since it is unbound only by 0.14 Mev or so, and a state formed by other waves would be sharpened by the penetrability. Since  $\text{C}^{13}$  is a  $(4n+1)$ -type nucleus like  $\text{Be}^9$ , we might expect certain similarities in their structures. In particular, the single-particle  $s$ - and  $d$ -wave states of the type found in  $\text{C}^{13}$  may occur in  $\text{Be}^9$ . The 1.8 and 4.8 states of  $\text{Be}^9$  would be the most likely candidates. It is interesting that an analysis of the  $\text{Be}^9(\gamma,n)\text{Be}^8$  and  $\text{Be}^9(\gamma,n)\text{Be}^{8*}$  reactions (Gu49, Ma56b) has been made with an  $s$ -wave state near 1.7 Mev and a broad  $d$ -wave state at 4.8 Mev. The ratio between the two cross sections is sensitive to the value of the intermediate-coupling parameter  $\xi/K$ . The observed ratio corresponds to  $\xi = 1.4K$ .

The  $\text{B}^{10}(n,d)\text{Be}^9$  and  $\text{B}^{10}(p,d)\text{B}^9$  reactions (Ri54,

Re56a) yielding the ground and 2.4 states of the mass 9 nuclei have been analyzed to give the ratio of reduced widths of the  $B^{10}$  ground state for break up into these states. The ratio is 1.40 from the first reaction, 0.93 from the second. The prediction of  $j-j$  coupling is  $\frac{7}{3}$ ; that of  $L-S$  coupling depends on the exchange nature of the central forces.

#### Mass 10

The first unbound state in the mass 10 isobars that is believed to have normal parity is the 7.46 level in  $B^{10}$ , whose spin is inferred to be  $2+$  (Mo56). The second state is the  $0+$  state at 7.56 whose isotopic spin is undetermined. If  $T=1$  for this state, then it must appear in the spectrum of  $Be^{10}$ . From the parity assignments of the  $Be^9(d,p)Be^{10}$  stripping reaction (Gr56a), the only eligible state at about the analogous energy in  $Be^{10}$  is the state that at 6.18 Mev whose parity is undetermined because of the weakness of the group leading to it. The 7.56 Mev state has a small reduced width against proton emission, namely,  $\theta^2 \sim 0.008$ . In  $L-S$  coupling the state would be  $^{33}P[33]$  if  $T=1$  and  $^{13}P[321]$  if  $T=0$ . Both assignments give  $\theta^2=0$ . In  $j-j$  coupling, for either isotopic spin, the state would be  $(p_{\frac{3}{2}})^5 p_{\frac{1}{2}}$  with the  $(p_{\frac{3}{2}})^5$  group in the spin  $\frac{1}{2}$  state. Since  $Be^9$ , the residual nucleus, has spin  $\frac{3}{2}$ , again  $\theta^2$  is predicted to be zero. The smallness of the observed  $\theta^2$  is thus not surprising.

There is a state in  $B^{10}$  at 8.89 Mev whose spin is believed to be  $2+$ ,  $T=1$  (Ma54, Ma56c). There is a known level at about the analogous energy in  $Be^{10}$  which is also believed to have spin 2, although the parity is unknown; this is the 7.54-Mev level. According to an analysis of the  $Be^9(p,\alpha)Li^{6*}$  reaction, the observed reduced width of the  $B^{10}$  level for nucleon emission is  $\theta^2=0.016$  or  $0.0048$  (Ma54). (This is the sum of the neutron and proton reduced widths assuming them to be equal.) If the 7.54 level in  $Be^{10}$  is assumed to be  $2+$ , its reduced width is  $\theta^2=0.0051$  in nice agreement with the second of the two possibilities for the  $B^{10}$  level. In fact, a recent analysis of the data on the  $B^{10}$  level has confirmed that the second value should be taken (Ma56c). In  $L-S$  coupling the level would be  $^{31}D[42]$  or  $^{33}P[33]$ . The former can give a large reduced width, and the latter gives zero. (N.B. The  $^{31}D[42]$  level contains two components that are split by diagonalizing the central interaction. Since its structure is in this way ambiguous, we do not quote a precise prediction for the reduced width.) In  $j-j$  coupling the state arises from  $(p_{\frac{3}{2}})^5 p_{\frac{3}{2}}$ , and it could have a large range of reduced widths values from zero upwards depending on the relative amounts of  $(p_{\frac{3}{2}})^5_{J_1=\frac{3}{2}}$  and  $(p_{\frac{3}{2}})^5_{J_1=\frac{1}{2}}$  in its parentage. Finally we discuss the 7.37 state in  $Be^{10}$  that is believed to be  $3+$ . If the spin is indeed  $3+$ , the state can be identified as the  $^{31}F[42]$  state in  $L-S$  coupling and as arising from  $(p_{\frac{3}{2}})^5 p_{\frac{3}{2}}$  [with the  $(p_{\frac{3}{2}})^5$  group in a spin  $\frac{3}{2}$  or  $\frac{5}{2}$  state] in  $j-j$  coupling. Both extreme modes clearly predict  $\theta^2=0$  which is satis-

factory in view of the small observed value of  $\theta^2=0.021$  (Wi55a).

For some time there was speculation on the apparent absence of a level corresponding to this latter one in the spectrum of  $B^{10}$ . From the known width of the  $Be^{10}$  level, one could easily calculate that the isobaric state in  $B^{10}$  should be of reasonable width ( $\sim 50$  kev or so), not too sharp and not too broad to escape observation. Thus the absence of such in a state seemed mysterious. The mystery has been resolved by a recent analysis of new data (Ma56c) which finds that the 8.89-Mev level of  $B^{10}$  actually consists of two levels of widths  $\sim 40$  and  $\sim 80$  kev. The former of these is associated with the  $2+$  level at 7.54 Mev in  $Be^{10}$ , as we have already discussed. The latter width is attributed to the missing  $3+$  level. The total nucleon reduced widths of the  $3+$  states in  $Be^{10}$  and  $B^{10}$  are  $\theta^2 \sim 0.021$  and  $\sim 0.038$ , respectively. The difference of a factor of almost two is a little disturbing but not sufficiently to throw serious doubt on the interpretation of the levels as an isobaric pair.

#### Mass 11

The only resonance data on these nuclei comes from the  $Li^7+\alpha$  and  $B^{10}+p$  bombardments. The  $B^{10}(p,\alpha)Li^7$  reaction reveals a state of spin  $\frac{3}{2}-$  in  $C^{11}$  at 9.70 Mev with a proton reduced width of either  $\theta^2=0.12$  or  $0.04$  (Cr56a). It does not seem possible to identify this state unambiguously with the shell model.

#### Mass 12

There is considerable isobaric correspondence between the levels of  $B^{12}$  and  $C^{12}$ . Pairing off the ground state of  $B^{12}$  with the 15.09 state of  $C^{12}$  enables a number of other pairs to be associated in energy and spin. The first of these is the 16.10-Mev state in  $C^{12}$  which corresponds to the 0.95-Mev state of  $B^{12}$  and has spin  $2+$ . In  $L-S$  coupling this state would be  $^{33}P[431]$  which has  $\theta^2=(5/18)\theta_p^2$ . In  $j-j$  coupling it would be  $(p_{\frac{3}{2}})^7 p_{\frac{3}{2}}$  which has  $\theta^2=\frac{1}{2}\theta_p^2$ . The observed value is  $\theta^2 \sim 0.08$  which is less than both of the predicted values when  $\theta_p^2$  is taken as 0.6.

A rather doubtful  $0+$  state occurs at 17.80 Mev in  $C^{12}$ . Its isotopic spin is undetermined. In  $L-S$  coupling it would be  $^{13}P[431]$  or  $^{33}P[431]$  and, in  $j-j$  coupling  $(p_{\frac{3}{2}})^6(p_{\frac{3}{2}})^2$ . Both  $L-S$  states predict  $\theta^2=\frac{1}{9}\theta_p^2$  and the  $j-j$  state predicts  $\theta^2=0$ . The observed total width of 150 kev corresponds to  $\theta^2=0.05$ , but this value must be taken as an upper limit since no alpha width has been subtracted.

The  $2+$  state at 3.76 Mev in  $B^{12}$  has a reduced width of  $\theta^2=0.05$ , and may have an analog in the 18.86 state in  $C^{12}$  or possibly in the 18.39 state which has been suggested to be  $2+$ . In  $L-S$  coupling the state is  $^{33}D[431]$  with a reduced width  $\theta^2=0.10\theta_p^2$ . In  $j-j$  coupling, the state is  $(p_{\frac{3}{2}})^6(p_{\frac{3}{2}})^2$  and this has  $\theta^2=0$ . Taking  $\theta_p^2=0.60$ , the observed value again lies between

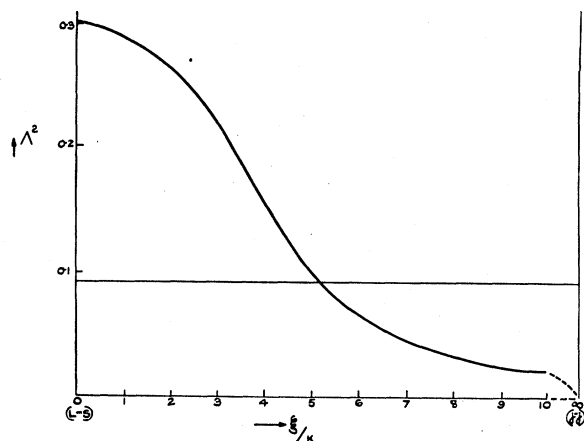


FIG. 2. The value of  $\Lambda^2 = \Gamma/\Gamma_p$  for the proton emission process  $N^{13}(\frac{3}{2}^-) \rightarrow C^{12}(0^+)$ . The horizontal line is the experimental value (assuming  $\theta_p^2 = 0.60$ ). Rosenfeld forces were used in the calculation of the theoretical curve.

the predictions of the extreme coupling modes. An analysis of neutron scattering on  $B^{11}$  indicates a channel spin ratio (the ratio of the reduced widths for the two channel spins 1 and 2) of zero or infinity (Wi55a). The foregoing  $L-S$  assignment implies a ratio one and the  $j-j$  assignment makes no prediction since both reduced widths separately are zero. [The most likely impurity in the  $j-j$  case,  $(p_{\frac{3}{2}})^7(p_{\frac{1}{2}})$ , predicts a ratio one.] Note that the 18.86-Mev state in  $C^{12}$  has a width of about 100 kev. If this is mostly made up of the width for proton emission to  $B^{11}$  in its ground state, the reduced width for this latter process is  $\theta^2 \sim 0.03$  which is about a half the value for the  $B^{12}$  state, as would be expected if these states are isobars.

### Mass 13

There is only one well-established normal parity state in the mass 13 nuclei that is unbound. This is the 3.51 Mev ( $\frac{3}{2}^-$ ) state in  $N^{13}$  which has a reduced width of  $\theta^2 = 0.06$  (Se51, Ja53). In  $L-S$  coupling this state forms with the ground state, the  $^{22}P[441]$  doublet and has  $\theta^2 = \frac{1}{3}\theta_p^2$ . In  $j-j$  coupling, the state is  $(p_{\frac{3}{2}})^7(p_{\frac{1}{2}})^2$  and this implies  $\theta^2 = 0$ . Taking  $\theta_p^2 = 0.6$ , the observed value falls between the two predicted values. This example has been analyzed in intermediate coupling (La53) and the result is shown in Fig. 2. Agreement between theory and experiment is achieved at a mode of coupling characterized by  $\xi = 5K$ . This is a rather higher value of  $\xi$  than is obtained on fitting a reduced width in  $Li^7$  (So57), but such a trend in  $\xi$  with  $A$  often has been remarked on (In53, Ku56).

### Mass 14

The state at 8.62 Mev in  $N^{14}$  has spin  $0^+$  and is probably  $T=1$  since it is not produced in the  $N^{14}(\alpha, \alpha')-N^{14*}$  reaction (Mi56). If indeed it has  $T=1$ , it should have one of the states at 6.59, 6.72, and 6.89 in  $C^{14}$

as its analog. The  $C^{13}(d, p)C^{14}$  reaction suggests the 6.89 state on grounds of parity (McG55). By accepting  $T=1$ , it can be assigned to the normal configuration  $(1p)^{10}$  with the structure  $^{33}P[433]$  in  $L-S$  coupling and  $(p_{\frac{3}{2}})^{-2}$  in  $j-j$  coupling. In both cases  $\theta^2$  is predicted to be zero and it is satisfactory to find that the observed value is small (0.020). [If the state is not  $T=1$ , it must arise from a configuration higher than  $(1p)^{10}$ . The most likely configurations are  $(1p)^8(2s, 1d)^2$  and these imply  $\theta^2 = 0$ .]

A second unbound normal parity state is found at 8.98 in  $N^{14}$  with spin  $1^+$ . If this is assigned to the normal configuration  $(1p)^{10}$ , it is  $^{11}P[433]$  in  $L-S$  coupling and  $(p_{\frac{3}{2}})^{-2}$  in  $j-j$  coupling. Again, in both cases,  $\theta^2$  is predicted to be zero and the observed value is small (0.007). Another  $1^+$  level with the same reduced width has been reported at 9.72 Mev (Zi57).

At high excitation, there occur two  $4^+$  states (at 12.79 and 12.92). These must be assigned to higher configurations. The reduced widths of the lower state for  $f$ -wave proton emission to the  $\frac{1}{2}$  ground state in  $C^{13}$  and for  $f$ -wave neutron emission to the  $\frac{1}{2}$  ground state of  $N^{13}$  are  $\theta^2 = 0.00018$ , and 0.0024, respectively (Sh53, Sh55a). It is significant that these values differ by more than a factor of 10 or so. Small differences in reduced widths for mirror processes can arise from the different boundary conditions for neutrons and protons, but a factor of five must be ascribed to a breakdown of neutron-proton symmetry, that is, to the impurity of isotopic spin as a quantum number. The two observed  $4^+$  states occur only 130 kev apart, which is within the estimates one can make of Coulomb mixing energy (Ra53, McD56), so it is not surprising that isotopic spin is not preserved.

It is also significant that the 12.79-Mev state emits  $g$ -wave protons to the 3.09 ( $\frac{3}{2}^+$ ) state of  $C^{13}$  with appreciable probability ( $\theta^2 = 0.04$ ) signifying that configurations that are four quanta above the normal configuration of  $N^{14}$  are already contributing to the structure of these states.

Finally, the absolute cross section of the pickup reaction  $N^{14}(p, d)N^{13}$  has been analyzed to give the reduced width of the ground state of  $N^{14}$  for breakup into  $N^{13}$  and a neutron (St56). The value obtained is said to be qualitatively in agreement with that expected from the intermediate-coupling shell model. In addition, some theoretical predictions of a rather general nature have been made about reduced widths involving the lowest states of  $N^{14}$  and  $N^{15}$  (Fr56, Fr57, El56b).

### Mass 15

The levels in  $O^{15}$  at 6.14, 7.61, and 9.03 Mev (Ha56, Fe59b) have tentatively been assigned normal parity (for example, the 7.61-Mev state is probably  $\frac{5}{2}^-$ ). The  $N^{14}(d, p)N^{15}$  stripping reaction indicates that the levels in  $N^{15}$  at 6.33, and 9.06 Mev (Gr56a) correspond to the first and last of the three levels in  $O^{15}$ . There are several

TABLE VI. Alpha-particle widths of levels of the mass range  $4 < A \leq 16$ .<sup>a</sup>

Compound nucleus	Excitation in Mev	Spin and isotopic spin	Channel: residual nucleus + $\alpha$ <sup>b</sup>	Observed channel width (kev in center of mass)	Obs $\theta^2$ <sup>i</sup>
Li <sup>7</sup>	4.63	$7-, \frac{1}{2}$	He <sup>3</sup> +3	93	0.32
Be <sup>7</sup>	7.46	$7-, \frac{1}{2}$	H <sup>3</sup> +3	38	0.012
	4.58	$7-, \frac{1}{2}$	He <sup>3</sup> +3	102	0.54
	6.4	$\left\{ \begin{array}{l} 3+, \frac{1}{2} \text{ or} \\ 3+, \frac{1}{2} \end{array} \right.$	(He <sup>3</sup> +0 or He <sup>3</sup> +2)	$\left\{ \begin{array}{l} 120 \text{ or} \\ 60 \end{array} \right.$	$\left\{ \begin{array}{l} 0.02 \text{ or} \\ 0.04 \end{array} \right.$
	7.16	$3-, \frac{1}{2}$	He <sup>3</sup> +3	50	0.072
Be <sup>8</sup> <sup>b</sup>	0	0+, 0	He <sup>4</sup> +0	$4.5(\pm 3) \times 10^{-3}$	0.07
	2.90	2+, 0	He <sup>4</sup> +2	$\sim 2.0 \times 10^3$	$\sim 1.0$
	10.8	4+, 0	He <sup>4</sup> +4	$\sim 6.7 \times 10^3$	$\sim 1.5$
	16.06	2+, 0 or 4+	He <sup>4</sup> +4 or He <sup>4</sup> +2	$0.47 \times 10^3$	$\left\{ \begin{array}{l} 0.05 \text{ or} \\ 0.06 \end{array} \right.$
	16.72	(2+, 1) <sup>g</sup>	He <sup>4</sup> +2	150	0.016
B <sup>10</sup> <sup>c</sup>	4.77	2+, 0	Li <sup>6</sup> +2	$< 10, > 10^{-3}$	$< 10, > 10^{-3}$
	5.11	2-, 0	Li <sup>6</sup> +1	1.2	0.036
	5.16	2+, 1	Li <sup>6</sup> +2	$\sim 0.4$	$\sim 0.1$
	6.89 <sup>d</sup>	1-, 0	Li <sup>6</sup> +1	...	$\sim 0.15$
	7.48 <sup>e</sup>	2-, 1	Li <sup>6</sup> +1	$\sim 15$	$\sim 0.008$
	8.89	2+, 1	Li <sub>2</sub> <sup>6</sup> +2	28	0.50
B <sup>11</sup> <sup>c</sup>	8.92	$\left( \frac{3}{2}, \frac{5}{2} \right) \frac{1}{2}$	{ Li <sup>7</sup> +0 or Li <sup>7</sup> +1 or Li <sup>7</sup> +2	$< 10^{-2}$	$< 0.1$ or $< 0.4$ or $< 5$
	9.19	$\frac{5}{2}-, \frac{1}{2}$	Li <sup>7</sup> +2	$> 10^{-3}$	$> 1.2 \times 10^{-3}$
C <sup>11</sup>	9.28	$\frac{3}{2}+, \frac{3}{2}$	Li <sup>7</sup> +1	6	0.28
	9.70	$\frac{3}{2}-, \left( \frac{1}{2} \right)$	Li <sup>7</sup> +0	75 or 225	$\left\{ \begin{array}{l} 0.012 \text{ or} \\ 0.037 \end{array} \right.$
	10.06	$\frac{7}{2}-, \left( \frac{1}{2} \right)$	Li <sup>7</sup> +3	56 or 100	$\left\{ \begin{array}{l} 0.24 \text{ or} \\ 0.48 \end{array} \right.$
C <sup>12</sup>	15.09	1+, 1	Be <sub>1</sub> <sup>8</sup> +2	0.020	$7 \times 10^{-6}$
	16.10	2+, 1	{ Be <sup>8</sup> +2 or Be <sub>1</sub> <sup>8</sup> +0	0.1	$3 \times 10^{-5}$
	16.57	2-, 1	Be <sub>1</sub> <sup>8</sup> +1	5	$10^{-3}$
	17.22	1-	{ Be <sup>8</sup> +1 or Be <sub>1</sub> <sup>8</sup> +1	140	0.03
				$\sim 35$	$\sim 0.008$
				$\sim 900$	$\sim 0.2$
N <sup>14</sup>	12.69	3-	B <sup>10</sup> +1	1.7	0.09
	12.79	4+	B <sup>10</sup> +2	1.0	0.12
O <sup>16</sup>	9.58	1-, 0	C <sup>12</sup> +1	645	1.3 <sup>+</sup>
	9.835	2+, 0	C <sup>12</sup> +2	0.75	0.0022 <sup>+</sup>
	10.36	4+, 0	C <sup>12</sup> +4	27	0.39 <sup>+</sup>
	11.25	0+, 0	C <sup>12</sup> +0	2400	1.1 <sup>+</sup>
	11.51	2+, 0	C <sup>12</sup> +2	77	0.05 <sup>+</sup>
	11.62	3-, 0	C <sup>12</sup> +3	1200	1.1 <sup>+</sup>
	12.43	(1-, 0)	C <sup>12</sup> +1	172	0.06 <sup>+</sup>
	12.51 <sup>f</sup>	2-	C <sub>1</sub> <sup>12</sup> +1	{ 0.9 or 0.03	{ 1.2 or 0.04
	12.95	2-, 1	C <sub>1</sub> <sup>12</sup> +1	1.0	0.04
	13.09	1-, 1	{ C <sup>12</sup> +1 or C <sub>1</sub> <sup>12</sup> +1	27	0.008
	13.24	3-, 1	{ C <sup>12</sup> +3 or C <sub>1</sub> <sup>12</sup> +1	12	0.006
13.65	1+, 0	{ C <sub>1</sub> <sup>12</sup> +1 or C <sub>1</sub> <sup>12</sup> +2	6	0.074	
			57	0.57	

<sup>a</sup> References to data used in the table are given in the discussions in the text except where the data is cited in the published compilations (Aj52, Aj55, Aj59).

<sup>b</sup> The limits on the width of the ground state of Be<sup>8</sup> are taken from estimates of the lifetime (He56, Ru56).

<sup>c</sup> The limits in the entries in B<sup>10</sup> and B<sup>11</sup> can be imposed according to whether the states concerned decay preferentially by gamma or alpha emission [D. H. Wilkinson (private communication); (Jo54a, Me59)].

<sup>d</sup> The entry for the 6.89-Mev level in B<sup>10</sup> assumes  $\Gamma_p < \Gamma_\alpha, \Gamma_d$ .

<sup>e</sup> The entry for the 7.48-Mev level in B<sup>10</sup> is discussed in Sec. III.2(a) under "Mass 10."

<sup>f</sup> The larger of the two possible values of the partial width in the case of the 12.51 level in O<sup>16</sup> is preferred because the smaller one would imply a very large proton reduced width ( $\theta^2 \gg 1$ ) for the state (see Table X).

<sup>g</sup> Uncertain entries are bracketed ( ).

<sup>h</sup> The residual nucleus in the fourth column is in the ground state unless a subscript  $n$  denotes that it is in the  $n$ th excited state.

<sup>i</sup> An interaction radius of  $1.45(A^{1/3} + 4^{1/3}) \times 10^{-13}$  cm has been used in extracting values of reduced widths, except in the cases of O<sup>16</sup> marked + where a radius constant of 1.40 was assumed in the published analysis of the data (Bi54), and the 0, 2.9, and 10.8 levels in Be<sup>8</sup> where the radii used were 5.7, 5.0, and  $4.5 \times 10^{-13}$  cm (Ru56).

levels in N<sup>15</sup> between 9 and 13 Mev to which normal parity has been definitely or tentatively assigned (Ba54, Fo55, Ba55b, Sh55a, Gr56a, Fe59a). The normal configuration of these mass 15 nuclei is  $(1p)^{11}$  which has only one excited state, and this is identified at 6.3-Mev excitation. Thus all the normal parity states above

must come from higher configurations such as  $(1p)^9(2s, 1d)^2$  or possibly  $(1p)^{10}(2p, 1f)$ . The first possibility gives zero reduced widths. The observed values for all the above states are small. Some of the spin assignments in (Fo55) do not agree with those of (Ba55b). We quote the latter assignments in Table V.



## Mass 16

There is a state at 12.43 Mev in  $O^{16}$  whose spin has alternately been suggested as being  $0+$  and  $1-$  (Co53, Bi54, Ho55). The former possibility implies  $p$ -wave formation and the corresponding value of the reduced width is very large  $\theta^2 \gg 1$  (Co53). The only possible theoretical explanation of a large  $p$ -wave reduced width lies in assigning the configuration  $(1p)^{11}2p$ . However, even this gives only  $\theta^2 \sim 0.30$  when the value 0.60 is assumed for  $\theta_p^2$ , and so the correct spin is probably  $1-$ .

Another unbound state of normal parity exists at 13.65. The spin is  $1+$  (Ha57a) and this implies  $p$ -wave nucleon emission. However, the partial width of the state for this emission is unknown.

## (b) Alpha Particle Channels

In Table VI, we list the observed reduced alpha widths for both normal and nonnormal parity states in the  $1p$  shell. The most striking feature of the reduced widths is the great variation. However, this is due in some measure to the fact that the very small values (for instance, those in  $C^{12}$ ) correspond to transitions forbidden by the isotopic-spin selection rule. In such cases, the magnitude of the alpha width gives an estimate of isotopic-spin impurity (Wi53a).

Another feature is the occurrence of some large widths in  $Li^7$  (Mi58b) but especially in the  $4n$  nuclei  $Be^8$  (Tr55, Ru56) and  $O^{16}$  (Bi54). Theoretically, large widths are expected on the alpha-particle model. Whether the shell model can give such magnitudes is more debatable. There is no basic reason why it should not. It has been pointed out (Pe56) that the totally antisymmetric shell-model ground states of  $(1s)^4(1p)^n$  with  $n=4, 8, 12$  and with oscillator wave functions can be written in such a way as to show that the systems are divided spatially into groups of four nucleons separated by node planes. Thus, there is less difference between the two models than might appear at first sight. In particular,  $(1s)^4(1p)^4$ , the configuration of  $Be^8$ , has been examined from this point of view, and it has been shown that, in  $L-S$  coupling with oscillator wave functions, the  $^{11}S[44]$  ground-state wave function can be rewritten as a product of the two internal wave functions of two groups of four particles times a wave function of relative motion. This means that the shell-model state can have an appreciable alpha width, the precise value being controlled by the overlap between the alpha wave functions and the foregoing internal wave functions.

It would be interesting to predict the  $O^{16}$  widths with the alpha model, especially in view of the success the model has in predicting the  $O^{16}$  spectrum (De54b).

## (c) Deuteron Channels

Table VII lists the observed deuteron widths for normal and nonnormal parity states in the  $1p$  shell. There are only a few entries because the deuteron

 TABLE VII. Deuteron widths of levels in the mass range  $4 < A \leq 16$ .<sup>a</sup>

Compound nucleus	Excitation in Mev	Spin and isotopic spin	Channel: residual nucleus $+L$ <sup>d</sup>	Obs. channel width (kev in center of mass)	Assumed radius $a$ ( $10^{-13}$ cm)	Obs $\theta^2$
$He^6$	16.69	$\frac{3}{2}+, \frac{1}{2}$	$He^3+2$	...	5	$1.4^e$
$Li^6$	16.80	$\frac{3}{2}+, \frac{1}{2}$	$He^3+2$	...	$\left\{ \begin{array}{l} 5 \\ 7.6 \end{array} \right.$	$\left\{ \begin{array}{l} 0.1^e \\ 0.7^e \end{array} \right.$
$Li^6$ <sup>b</sup>	2.189	$3+, 0$	$He^4+2$	20	$\left\{ \begin{array}{l} 3.5 \\ 4.0 \end{array} \right.$	$\left\{ \begin{array}{l} 1.20^e \\ 0.75^e \end{array} \right.$
	4.52	$2+, 0$	$He^4+2$	600	3.5	$11.5^e$
	5.4	$1+, 0$	$He^4+0$	broad	3.5	$0.3-1.5^e$
$B^{10}$	6.89	$1-, 0$	$Be^8+1$	...	4.73	$\sim 1.2$
	7.48 <sup>c</sup>	$2-, 1$	$Be^8+1$	$\sim 15$	4.73	$\sim 0.012$
$N^{14}$	12.41	$4-$	$C^{12}+3$	22	5.15	0.20
	12.60	$3+$	$C^{12}+2$	30	5.15	0.02
	12.69	$3-$	$C^{12}+3$	0.93	5.15	0.0039
	12.79	$4+$	$C^{12}+4$	2.0	5.15	0.059

<sup>a</sup> References to data used in the table are given in the discussions in the text except where the data is cited in the published compilations (Aj52, Aj55, Aj59).

<sup>b</sup> The  $Li^6$  values have been deduced from the  $He^4+d$  data (Ga55) with rather a small interaction radius ( $3.5 \times 10^{-13}$  cm). Note that limits on the ground-state reduced width were also deduced in this analysis.

<sup>c</sup> For discussion of the values given for the 7.48-Mev level in  $B^{10}$ , see "Mass 10" of Sec. III.2(b).

<sup>d</sup> The residual nucleus in the fourth column is always in the ground state unless a subscript  $n$  indicates that it is the  $n$ th excited state.

<sup>e</sup> An interaction radius of  $1.45 (A^{1/3}+2^{1/3})$  is not used in these entries.

thresholds are usually high in excitation in the continuum where individual levels are not resolved. One noteworthy point is the size of the widths in  $Li^6$  (Ga55); as we have seen in Sec. II, such large widths are quite consistent with the nuclear shell model and are, in fact, expected because of the large overlap between the wave function of two nucleons moving in  $1p$  orbits and a deuteron separating from the well-center with orbital angular momentum zero or two.

## (d) Photon Channels

Table VIII lists the known  $M1$  radiation widths observed between states of normal parity in the  $1p$  shell. It is an extended and corrected version of a previous table.<sup>3</sup> Many entries are taken from a recent compilation (Wi56b), and we refer to this paper for the many experimental references. The initial and final states in nearly every case can be ascribed to the normal configuration  $(1p)^n$ , and so theoretical predictions can be made about the observed magnitudes. Such predictions for  $L-S$  and  $j-j$  coupling are listed in the table along with the assignments to the character of the initial and final states. In every case the radiation is supposed to come only from the  $1p$  nucleons and the possible effects of recoil motion of the  $(1s)^4$  core are ignored. Such effects are presumably more important

<sup>3</sup> See (La54) but notice: (i)  $\Lambda$  is defined differently in this reference; (ii) in Formulas (4) to (7), errors occur in the relative phases of the space and spin contributions to  $\Lambda(M1)$ . This invalidates the last column of Table 2 in this reference.

TABLE VIII.  $M1$  transitions of known width in nuclei of the mass range  $4 < A \leq 16$ .<sup>a</sup>

Nucleus	Excitation of initial state in Mev	Spin and isotopic spin of initial state	Excitation of final state in Mev	Spin and isotopic spin of final state	Obs width in ev	Experimental value of $\Lambda^2$	Initial state in $L-S$ coupling	Final state in $L-S$ coupling	$\Lambda^2$ in $L-S$ coupling	Initial state in $j-j$ coupling	Final state in $j-j$ coupling	$\Lambda^2$ in $j-j$ coupling
Li <sup>7</sup> <sup>b</sup>	0.477	$\frac{1}{2}^-, \frac{1}{2}$	0	$\frac{3}{2}^-, \frac{1}{2}$	$\sim 0.0057$	$\sim 0.84$	$^{22}P[3]$	$^{22}P[3]$	0.80	$(p_1)^3$	$(p_1)^3$	0.31
Be <sup>7</sup>	0.430	$\frac{1}{2}^-, \frac{1}{2}$	0	$\frac{3}{2}^-, \frac{1}{2}$	$\sim 0.0024$	$\sim 0.48$	$^{22}P[3]$	$^{22}P[3]$	0.59	$(p_1)^3$	$(p_1)^3$	0.31
Be <sup>8</sup>	17.63	$1^+, (1)^d$	0	$0^+, 0$	17	0.048	$^{33}P[31]$	$^{11}S[4]$	0	$(p_1)^4$	$(p_1)^4$	0.21
	18.14 <sup>e</sup>	$(1^+)$	0	$0^+, 0$	8.3	0.040	$^{11}D[4]$	$^{11}D[4]$	0	$(p_1)^4$	$(p_1)^4$	0
B <sup>10</sup>	4.78	$(1^+, 0)$	0.72	$1^+, 0$	0.15	0.035	$^{13}D_{11}[42]$	$^{13}S[42]$	0	$(p_1)^5 p_1$	$(p_1)^6$	
	5.16	$(2^+, 1)$	0	$3^+, 0$	0.03	0.0034	$^{31}D_1[42]$	$^{13}D_1[42]$	1.32	$(p_1)^6$	$(p_1)^6$	0.65
			0.72	$1^+, 0$	0.15	0.026	$^{13}S[42]$	$^{13}S[42]$	0	$(p_1)^6$	$(p_1)^6$	0.74
			2.15	$1^+, 0$	0.4	0.23	$^{13}D_1[42]$	$^{13}D_1[42]$	0.57	$(p_1)^5 p_1$	$(p_1)^6$	
	7.56	$(0^+, 0$ or $1)$	0.72	$1^+, 0$	4.8	0.23	$^{33}P[33]$ or $^{13}P[321]$	$^{13}S[42]$	0.019 or 0	$(p_1)^5 p_1$	$(p_1)^6$	0.0080 or 1.00
		2.15	$1^+, 0$	1	0.12		$^{13}D_1[42]$	0.032 or 0		$(p_1)^5 p_1$		
	8.89	$2^+, 1$	0.72	$1^+, 0$	8	0.34	$^{31}D[42]$ or $^{33}P[33]$	$^{13}S[42]$	0 or 0.019	$(p_1)^5 p_1$	$(p_1)^6$	
B <sup>11</sup>	4.46	$(\frac{5}{2}^-, \frac{1}{2})$	0	$\frac{3}{2}^-, \frac{1}{2}$	0.66	0.115	$^{22}D[43]$	$^{22}P[43]$	0.13	$(p_1)^6 p_1$	$(p_1)^7$	
	9.19	$(\frac{5}{2}^-, \frac{1}{2})$	0	$\frac{3}{2}^-, \frac{1}{2}$	0.01	$2 \times 10^{-4}$	$^{22}F[43]$	$^{22}P[43]$	0	$(p_1)^6 p_1$	$(p_1)^7$	
	9.19	$(\frac{5}{2}^-, \frac{1}{2})$	4.46	$(\frac{5}{2}^-, \frac{1}{2})$	1.3	0.062	$^{22}F[43]$	$^{22}D[43]$	$2 \times 10^{-4}$	$(p_1)^6 p_1$	$(p_1)^6 (p_1)$	
	9.19	$(\frac{5}{2}^-, \frac{1}{2})$	6.81	$(\frac{5}{2}^-, \frac{1}{2})$	0.23	0.080	$^{22}F[43]$	$^{22}D[43]$	0.0028	$(p_1)^6 p_1$	$(p_1)^6 (p_1)$	
C <sup>11</sup>	9.70	$(\frac{3}{2}^-)$	0	$\frac{3}{2}^-, \frac{1}{2}$	2.3	0.040	$^{22}P[421]$	$^{22}P[43]$	0.0079	$(p_1)^6 p_1$	$(p_1)^7$	
C <sup>12</sup>	15.10	$1^+, 1$	0	$0^+, 0$	100	0.45	$^{33}P[431]$	$^{11}S[44]$	0	$(p_1)^7 p_1$	$(p_1)^8$	0.59
	15.10	$1^+, 1$	4.43	$2^+, 0$	$\sim 3$	0.04	$^{33}P[431]$	$^{11}D[44]$	0	$(p_1)^7 p_1$	$(p_1)^7 p_1$	0.21
	16.10	$2^+, 1$	4.43	$2^+, 0$	152	1.4	$^{33}P[431]$	$^{11}D[44]$	0	$(p_1)^7 p_1$	$(p_1)^7 p_1$	0.37
N <sup>13</sup>	3.51	$\frac{3}{2}^-, \frac{1}{2}$	0	$\frac{1}{2}^-, \frac{1}{2}$	0.66	0.244	$^{22}P[441]$	$^{22}P[441]$	0.40	$(p_1)^6 (p_1)^2$	$(p_1)^8 p_1$	0.124
N <sup>14</sup>	8.62	$0^+, (1)$	0	$1^+, 0$	0.73	0.0176	$^{33}P[433]$	$^{13}S[442]$	0.028	$(p_1)^6 (p_1)^4$	$(p_1)^2$	0
			3.95	$1^+, 0$	3.1	0.47	$^{13}D[442]$	$^{13}D[442]$	0.035	$(p_1)^7 (p_1)^3$	$(p_1)^7 (p_1)^3$	0.50
N <sup>15</sup>	8.98	$1^+, (0)$	0	$1^+, 0$	0.17	0.0036	$^{11}P[433]$	$^{13}S[442]$	0	$(p_1)^6 (p_1)^4$	$(p_1)^2$	
	10.70	$\frac{3}{2}^-, \frac{1}{2}$	0	$\frac{1}{2}^-, \frac{1}{2}$	0.12	0.0015	$^{22}P[443]$	$^{22}P[443]$		$(p_1)^3$	$(p_1)^3$	
	10.81	$\frac{3}{2}^-, \frac{1}{2}$	0	$\frac{1}{2}^-, \frac{1}{2}$	0.010	$1.2 \times 10^{-4}$	$^{22}P[443]$	$^{22}P[443]$		$(p_1)^3$	$(p_1)^3$	
	11.29	$\frac{3}{2}^-, \frac{1}{2}$	0	$\frac{1}{2}^-, \frac{1}{2}$	0.29	0.0031	$^{22}P[443]$	$^{22}P[443]$		$(p_1)^3$	$(p_1)^3$	

<sup>a</sup> References to the data used in the table are to be found in published compilations (Aj52, Aj55, Aj59, and especially W56b).

<sup>b</sup> The observed value quoted for Li<sup>7</sup> is a new one [C. P. Swann, V. K. Rasmussen, and F. R. Metzger, Phys. Rev. 114, 862 (1959)].

<sup>c</sup> Only the total radiation width of the 18.14-Mev state in Be<sup>8</sup> is known along with the fact that  $E \gtrsim 12$  Mev.

<sup>d</sup> All uncertain spin assignments are bracketed ( ).

<sup>e</sup> The absence of an entry in the theoretical columns implies that the evaluation of the entry is too ambiguous.

when there are only a few "loose" nucleons outside the core to absorb the recoil, such as in the mass 7 nuclei. Values of the single-particle widths  $\Gamma_p$  that are needed in order to obtain values for  $\Lambda^2 = \Gamma/\Gamma_p$  are estimated as explained in Sec. II.2(c).

The table shows that the theoretical prediction of  $\Lambda^2$  vary greatly from case to case, as do the experimental values. Also, although neither  $L-S$  nor  $j-j$  coupling gives an adequate account of the observed values, there is in several cases a correlation between the observed values and the pairs of predicted values that is suggestive of an intermediate-coupling situation. (See especially the transitions in N<sup>14</sup>.) In a few cases, namely, the transitions in Li<sup>7</sup>, Be<sup>7</sup> (La55a, Bu56), N<sup>13</sup> (La53), Be<sup>8</sup>, B<sup>10</sup>, B<sup>11</sup>, and C<sup>12</sup> (Ku57), calculations have been done in intermediate coupling. The mass 7 results cannot be taken too seriously in view of the previously mentioned neglect of core motion and large experimental uncertainties. The N<sup>13</sup> transition (Fig. 3) is fitted in intermediate coupling with Rosenfeld forces at a point where  $\xi = 5K$ , which is the expected coupling mode for this nucleus (In53, Ku56).

There exists two  $E0$  transitions in the mass range

$A \leq 16$ . They are  $0^+ - 0^+$  transitions between the 7.68 and ground state of C<sup>12</sup> and the 6.06 and ground state of O<sup>16</sup>. These have been discussed in the literature (Sc55, El56c, Sh56a). They are both quite strong transitions ( $\Lambda^2 \sim \frac{1}{2}$ ) and are informative in revealing properties of levels. The O<sup>16</sup> transition is allowed for  $(1p)^{11}2p \rightarrow (1p)^{12}$  but is forbidden for the two-particle transition  $(1p)^{10} (2s, 1d)^2 \rightarrow (1p)^{12}$ . The C<sup>12</sup> transition is forbidden according to the shell model because of an interesting selection rule (Sh56a) arising from the nature of the  $E0$  operator:  $\sum_i (\frac{1}{2} - t_{3i}) r_i^2$ . This rule forbids all  $E0$  transitions between states of equivalent particles like  $(1p)^8 \rightarrow (1p)^8$ . The nice thing about this rule is that it is quite independent of the nature of the forces between particles, that is, it is purely a selection rule on orbital configurations. The finiteness of the C<sup>12</sup> transition is thus direct evidence for configuration impurity in the initial or final states. The most likely impurity is  $(1p)^7 2p$ ; it may be that quite a small amount of impurity is sufficient to give an appreciable transition strength, but this speculation should be checked by calculation.

There are a few suspected  $E2$  transitions in the  $1p$  shell, but the widths are generally not well known. Four

cases are:

$$0.72(1+) \rightarrow 0(3+) \text{ in } B^{10}, \quad \Gamma = 10^{-6} \text{ ev}, \quad \Lambda^2 = 0.9 \\ \text{(Th53, Bl57, Se56),}$$

$$4.44(2+) \rightarrow 0(0+) \text{ in } C^{12}, \\ \begin{cases} \Gamma = 0.025 \text{ ev}, & \Lambda^2 = 2.5 \text{ (De56),} \\ \Gamma = 0.01 \text{ ev}, & \Lambda^2 = 1 \text{ (Sw57),} \end{cases}$$

$$16.10(2+) \rightarrow 0(0+) \text{ in } C^{12}, \\ \begin{cases} \Gamma = 3 \text{ ev}, & \Lambda^2 = 0.4, \text{ (Wi56b),} \\ \Gamma = 7 \text{ ev}, & \Lambda^2 = 1 \text{ (Ke59),} \end{cases}$$

$$6.91(2+) \rightarrow 0(0+) \text{ in } O^{16}, \\ \Gamma > 0.026 \text{ ev}, \quad \Lambda^2 > 0.28 \text{ (De56).}$$

In extracting values of  $\Lambda^2$  we have used (83) along with the entries of Table III and  $b = 1.65 \times 10^{-13}$  cm. Some predictions about  $\Lambda^2(E2)$  for unmeasured transitions have been made previously by Lane and Radicati (La54). Note that (i) all theoretical values in Table III of this reference should be divided by six because of an error; (ii)  $\Lambda$  in this reference is equivalent to  $\Lambda^2$  of the present work in the case of  $E2$  transitions.

### (e) Concluding Remarks

In this section the shell model has been used to predict about 30 or so experimental data involving normal parity states in the  $1p$  shell. Apart from the question of agreement between experiment and theory, an important feature of the predictions of  $\Lambda^2$  is that this quantity may have values from zero (forbidden transitions) up to unity (single particle transitions). In fact,  $\Lambda^2$  can be larger than unity in certain cases. As an example, the reduced width of  $C^{12}$  in  $j-j$  coupling for nucleon emission is eight times the single-particle value, i.e.,  $\Lambda^2 = 8$ .

The general conclusion from comparing all the experimental values with the pairs of predicted values in the two extreme coupling modes is that there is good evidence in support of the shell model with the freedom of intermediate coupling. In the cases where the data has been investigated in intermediate coupling, agreement is obtained for  $\xi/K$  between three and five with the suggestion of an increase between these values with increasing mass. Such values of  $\xi/K$  are in good agreement with those used in nuclear-structure calculations (In53, Ku56).

## 2. NONNORMAL PARITY STATES OF THE MASS RANGE $4 < A \leq 16$

In Sec. II.2(b), we set up a simplified shell model of nonnormal parity states. This model is used in the present discussion as a guide in the analysis of the experimental data on reduced widths. The model predicts that the first states of nonnormal parity of a mass  $A$  nucleus in the  $1p$  shell consist of an  $2s$  or a  $1d$  particle coupled on to the ground state of the mass  $(A-1)$  nucleus or, alternatively, a  $1s$  nucleon hole

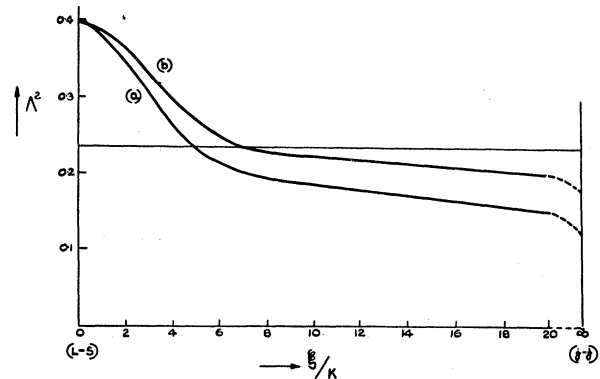


FIG. 3. The value of  $\Lambda^2 = \Gamma/\Gamma_p$  for the  $M1$  radiation width in  $N^{13}$ :  $3.51(\frac{3}{2}-) \rightarrow 0(\frac{1}{2}-)$ .  $\Gamma_p$  is the single-particle width for a proton as defined in Sec. II.2(c). The horizontal line ( $\Lambda^2 = 0.244$ ) is the experimental value. Curve (a) is computed with the Rosenfeld central force mixture and curve (b) with the Serber mixture.

coupled on to the ground state of the mass  $(A+1)$  nucleus. It is clear that, if states of the former structure occur near the nucleon thresholds, they produce strong effects in the cross sections when the mass  $(A-1)$  nucleus is bombarded with  $s$ - or  $d$ -wave incident particles. The nature of these effects depends on just where the states are located relative to the thresholds. There are three possibilities.<sup>4</sup>

(i) *States occur below the nucleon thresholds, i.e., they are bound against nucleon emission.* In this case, they manifest themselves in the scattering cross sections above the thresholds by producing strong deviations from hard-sphere scattering. In particular, the thermal-neutron scattering lengths are *greater* than the interaction radius. The last prediction is verified in the data presented in the  $Li^6+n$ ,  $Be^9+n$ ,  $C^{12}+n$ , and  $N^{14}+n$  scatterings.

(ii) *States occur above the nucleon thresholds and also above the barriers in the nucleon channels.* Single-particle states are expected to be usually too broad to be observed as isolated resonances when no barrier (Coulomb or angular momentum) exists to sharpen up the widths. Thus, if the  $2s$  and  $1d$  state occur above the barriers, they are not distinguishable for the nonresonant backgrounds in the bombardment of mass  $(A-1)$  nuclei by nucleons. Nevertheless, they should produce anomalous background effects, and the presence of the  $2s$  state again affects the thermal-neutron scattering length which should now be *less* than the interaction radius. This latter situation is observed in the  $He^4+n$  and  $Li^7+n$  scatterings.

(iii) *States occur above the nucleon thresholds but below the barriers in the nucleon channels.* When the single-particle levels occur in such energy regions, they appear

<sup>4</sup> In all three situations, the single-particle states should manifest themselves in stripping reactions by giving large yields;  $(d,n)$  reactions leading to final nuclei  $Be^8$ ,  $B^{10}$ ,  $C^{12}$ ,  $N^{14}$  would be especially interesting in this connection.

as resonances in excitation curves and so can be very conveniently investigated. It is a fortunate fact that the  $2s$  and  $1d$  levels do seem to often occur like this experimentally. For instance, single-particle resonances for  $s$  and  $d$  waves are found in mass 10, 12, 13, and 14 nuclei.

In contrast to the single-particle states, states of the  $1s$ -hole type in the mass  $A$  nucleus are not expected to influence the bombardment of the mass  $(A-1)$  nucleus with nucleons. Consequently, the latter type of reaction is not expected to reveal anything about the states of  $1s$  hole (unless, of course, one allows for some impurity in their structure, i.e., allows for interaction with the particle states which would amount to deviations from the simplified shell model). This may help to explain why much less is known about states of the  $1s$ -hole type than about particle states. In most nuclei, no states have been identified as being of this type mainly because one does not know for which properties to look. In particular, it would be of great help in trying to determine these states to have some idea of their energies. For this purpose, we can appeal to the simplified shell model which gives a method for predicting the required energies. This method, which seems to work in the few cases where it has been tested empirically (for instance, see "Mass 5" in the following), is based on the neglect of interaction between different orbits. (This is a rather stronger requirement than is strictly necessary for the validity of the simplified model, which only requires that the *polarizing* interaction between

different orbits be small.) With this neglect, it follows that the binding of a  $1s$ -hole type state of the mass  $A$  nucleus in the ground state of the mass  $(A-1)$  nucleus is equal to the binding of  $\text{He}^3$  in  $\text{He}^4$ . Thus one can directly estimate the required positions of the states of  $1s$  hole.

In Table IX are listed the spins and energies of the lowest states of nonnormal parity expected in nuclei of the  $1p$  shell on the basis of the simplified shell model. The energies of the lowest states of the  $1s$ -hole type ( $D$ ) are estimated as just described. The energies of the  $2s_{1/2}$ ,  $1d_{3/2}$ , and  $1d_{5/2}$  particle states are estimated by assuming that their binding energies are always the same and equal to the observed binding energies in  $\text{C}^{13}$ , namely 1.87, 1.06, and  $-1.92$  Mev, respectively. This method for the particle states is a semiempirical one, since it is an experimental fact that the lowest-particle states always have about the same binding, to within a Mev or so. Almost independently of whether the ground state of a given nucleus is loosely or tightly bound, the particle states first seem to appear near the nucleon dissociation energy. This fact indicates that the positions of these states are determined mainly by the mean potential well (which varies smoothly with mass number) rather than the actual interaction with other nucleons which effectively can fluctuate considerably with mass number. For instance, the symmetry effect tends to make the binding in  $4n$ -type nuclei considerably larger than in the other nuclei.

This latter effect is well known for states of normal

TABLE IX. Spins and energies of the lowest states of nonnormal parity expected in nuclei of the  $1p$  shell.<sup>a</sup>

Nuclei	Expected positions of lowest states of type (A)	Spins	Expected positions of lowest states of type (B)	Spins	Expected positions of lowest states of type (C)	Spins	Expected positions of lowest states of type (D)	Spins
$\text{He}^5, \text{Li}^5$		$\frac{1}{2}$		$\frac{5}{2}$		$\frac{3}{2}$	15	$\frac{1}{2}, \frac{3}{2}$
$\text{Li}^6$	3.6	1, 2	4.4	1 to 4	7.4	0 to 3	13.3	1, 2
	6.1	0, 1	6.9	2, 3	12.9	1, 2	13.8	0, 1
$\text{Li}^7, \text{Be}^7$	5.4	$\frac{1}{2}, \frac{3}{2}, \frac{5}{2}$	6.2	$\frac{3}{2}, \frac{5}{2}, \frac{7}{2}$	9.2	$\frac{1}{2}, \frac{3}{2}, \frac{5}{2}$	1.7	$\frac{1}{2}$
	7.6	$\frac{1}{2}, \frac{3}{2}, \frac{5}{2}$	8.8	1/2 to 11/2	11.4	3/2 to 9/2	3.7	$\frac{3}{2}, \frac{5}{2}$
$\text{Be}^8$	17.0	1, 2	17.8	1 to 4	20.8	0 to 3	18.9	1, 2
	17.5	0, 1	18.3	2, 3	21.0	1, 2	21.2	?
$\text{Be}^9, \text{B}^9$	-0.2	$\frac{1}{2}$	0.6	$\frac{5}{2}$	3.6	$\frac{3}{2}$	12.1	$\frac{5}{2}, \frac{7}{2}$
	1.8	$\frac{3}{2}, \frac{5}{2}$	2.6	1/2 to 9/2	5.6	$\frac{1}{2}$ to $\frac{7}{2}$	12.8	?
$\text{B}^{10}$	6.6	1, 2	7.4	1 to 4	10.4	0 to 3	9.1	1, 2
	9.0	?	9.8	?	12.4	?	11.1	?
$\text{B}^{11}, \text{C}^{11}$	9.6	$\frac{3}{2}, \frac{5}{2}, \frac{7}{2}$	10.4	1/2 to 11/2	13.4	3/2 to 9/2	1.9	$\frac{1}{2}$
	10.3	$\frac{1}{2}, \frac{3}{2}, \frac{5}{2}$	11.1	$\frac{3}{2}, \frac{5}{2}, \frac{7}{2}$	14.1	$\frac{1}{2}, \frac{3}{2}, \frac{5}{2}$	6.3	$\frac{3}{2}, \frac{5}{2}$
$\text{C}^{12}$	16.8	1, 2	17.8	1 to 4	20.8	0 to 3	15.6	0, 1
	18.8	?	19.8	?	22.8	?	19.3	1, 2
$\text{C}^{13}, \text{N}^{13}$	3.1	$\frac{1}{2}$	3.9	$\frac{5}{2}$	6.9	$\frac{3}{2}$	10.0	$\frac{1}{2}, \frac{3}{2}$
	7.5	$\frac{3}{2}, \frac{5}{2}$	8.3	1/2 to 9/2	11.3	$\frac{1}{2}$ to $\frac{7}{2}$	12.3	$\frac{1}{2}$
$\text{N}^{14}$	8.7	0, 1	9.5	2, 3	12.5	1, 2	9.7	0, 1
	12.4	1, 2	13.2	1 to 4	16.2	0 to 3	16.0	1, 2
$\text{N}^{15}, \text{O}^{15}$	8.9	$\frac{1}{2}, \frac{3}{2}$	9.7	$\frac{3}{2}, \frac{5}{2}, \frac{7}{2}$	12.7	$\frac{1}{2}, \frac{3}{2}, \frac{5}{2}$	5.0	$\frac{1}{2}$
	11.2	$\frac{1}{2}$	12.0	$\frac{5}{2}$	15.0	...	...	...
$\text{O}^{16}$	13.7	0, 1	14.5	2, 3	17.5	1, 2	...	...
	20.0	1, 2	20.7	1 to 4	23.8	0 to 3	...	...

<sup>a</sup> We list the four types of states (A), (B), (C), and (D) as defined in the text. The positions of the  $2s_{1/2}$ ,  $1d_{3/2}$ , and  $1d_{5/2}$  particle states (A), (B), and (C) are estimated by the condition that the binding of a neutron be the same as for the observed lowest states of these types in  $\text{C}^{13}$ , namely, 1.87, 1.06, and  $-1.92$  Mev, respectively. The positions of the first states of the  $1s$ -hole type (D) are determined as described in the text; that is, essentially, using the assumption that the binding of such a state in the ground state of the next heavier nucleus is equal to the binding of  $\text{He}^3$  in  $\text{He}^4$  (20.56 Mev). All energies are expressed as excitation above the ground states in Mev.

parity, but, for nonnormal parity states, any such effect is much less indicating that the odd nucleon effectively couples weakly to other nucleons compared to their coupling amongst themselves. This is just the kind of evidence that supports the simplified shell model for nonnormal parity states because, as discussed in the last section, this model is based on the weakness of interaction between different orbits. Thus the application of the simplified model has some self-consistency, although it should be stressed again that its theoretical basis is very uncertain.

Finally, Yoshida (Yo54) has interpreted the nucleon widths of nonnormal parity states in terms of the strong-coupling model. We do not discuss his work here, but, in Sec. II.3, the connection between the simplified model and the strong-coupling model is mentioned.

### (a) Nucleon Channels

There are some 20 or 30 unbound states of nonnormal parity for which nucleon reduced widths are known. These are listed in Table X. We now discuss this and other data according to the mass numbers of the compound nuclei.

#### Mass 5

The  $s$ -wave phase shift up to 20 Mev in the scattering of neutrons from  $\text{He}^4$  has roughly the energy dependence expected from hard-sphere scattering:  $\delta_0 = -k_n R$  (Hu52). Since this holds down to thermal energies, the constant  $R$  defined by this equation can be identified as the thermal scattering length. The value of  $R$  is  $2.4 \times 10^{-13}$  cm, which is considerably less than the interaction radius from the usual formula  $1.45(4^{\frac{1}{2}} + 1) \times 10^{-13} = 3.71 \times 10^{-12}$  cm. This implies, as we have seen, the existence of an unbound broad  $s$ -wave level. It must be centered at an excitation  $E_n \gtrsim 20$  Mev, since otherwise it would affect the observed energy dependence of the phase shift. The  $s$ -wave phase shift for proton scattering up to 18 Mev is consistent with scattering from a hard sphere of radius  $2.0 \times 10^{-13}$  cm (Mi58c).

There is evidence for anomalous  $d$ -wave phase shifts and a  $\frac{3}{2}^+$  resonance emitting  $d$ -wave neutrons is found in the  $\text{H}^3 + d$  reaction at 16.69 Mev excitation in  $\text{He}^5$ . The reduced width is small,  $\theta^2 \sim 0.03$ , so this is clearly not the single-particle  $1d_{\frac{3}{2}}$  level. The simplest explanation of this state is that it arises from the configuration  $(1s)^3(1p)^2$ ; that is, a  $1s$  hole in  $\text{Li}^6$ , presumably in its ground state. On the simplified shell model (see Table IX), such a state is predicted at 15 Mev, which is within 2 Mev of the observed position. The reduced width of the pure state is zero, and the finite observed value indicates the degree of impurity in the state. The surprising fact is that the impurity is so small. The broad  $1d_{\frac{3}{2}}$  single-particle state must occur somewhere in the vicinity of the 16.69-Mev state; yet, in spite of

that, there appears to be little interaction between the two states.

A similar  $\frac{3}{2}^+$  state is found at 16.80 excitation in  $\text{Li}^5$  from the  $\text{He}^3 + d$  reaction. To some extent its detailed properties confirm that it is the mirror of the foregoing state in  $\text{He}^5$ . For instance, the nucleon reduced widths are about the same. The deuteron reduced widths for the two states, on the other hand, may differ considerably for certain choices of interaction radius (for instance, they differ by a factor of 10 if the radius  $5 \times 10^{-13}$  cm is used). Since the values of the reduced widths are very sensitive to choice of radius, such differences cannot be taken as serious evidence against the mirror nature of the two levels.

Recently there has been evidence for states above the 16.69 state in  $\text{He}^5$  from the  $T(d, n)$  reaction (Ga56) and from neutron scattering (Bo57).

#### Mass 7

A broad level (or levels) of nonnormal parity is found at about 6.5 Mev in both  $\text{Li}^7$  and  $\text{Be}^7$ . The breadth of the  $\text{Li}^7$  levels must be ascribed to breakup into  $\text{H}^3 + \text{He}^4$ , since its position is below the neutron threshold. The  $\text{Be}^7$  levels, on the other hand, can break up by proton emission so that its breadth is composed of a width for  $\text{He}^3 + \text{He}^4$  and a width for  $p + \text{Li}^5$ . A rough analysis (Ba51) of the latter level indicates the width for  $\text{He}^3 + \text{He}^4$  decay to  $\sim 0.12$  (if  $J = \frac{1}{2}$ ) or  $\sim 0.06$  Mev (if  $J = \frac{3}{2}$ ). The width for the mirror decay of  $\text{Li}$  into  $\text{H}^3 + \text{He}^4$  is greater than these values by a factor equal to the ratio of the barrier penetrabilities ( $s$  wave if  $J = \frac{1}{2}$ ;  $d$  wave if  $J = \frac{3}{2}$ ). The reduced proton width of the  $\text{Be}^7$  level is not very well determined but it is large, that is, of the order of the single-particle value. Thus it seems that at least one of the two single-particle  $2s$  levels of spins  $\frac{3}{2}$  and  $\frac{1}{2}$  occurs at 6.5 Mev. This surmise is supported in the case of  $\text{Li}^7$  by the size of the  $\text{Li}^6 + n$  coherent thermal-neutron scattering length ( $7 \times 10^{-13}$  cm), which far exceeds the interaction radius of  $4.2 \times 10^{-13}$  cm and therefore demands at least one strong bound  $s$ -wave state. However, there is a possible error of 50% in the thermal-neutron cross section (Sh51) and also, at higher energies, the  $s$ -wave potential scattering is anomalously small rather than large (Jo54b, Wi56a). Thus the situation is not a simple one. From a theoretical point of view one anticipates a complicated situation involving many states. Besides expecting  $2s$  and  $1d$  single-particle states (since the energy is near the nucleon threshold where such levels are found to occur empirically in other cases), we also expect a low-lying  $1s$ -hole ( $\frac{1}{2}^+$ ) state. By using the simple means of estimating the positions of such a level, we find (Table IX) that it is predicted at 1.5-Mev excitation. This estimate can only be taken to suggest the fact that a low-lying  $\frac{1}{2}^+$  level of this type can be expected, but it may be significant that a similarly estimated position in the mass 5 nuclei (see "Mass 5" above) was apparently

TABLE X. Nucleon widths of nonnormal parity states of the mass range  $4 < A \leq 16$ .<sup>a</sup>

Compound nucleus	Excitation in Mev	Spin and isotopic spin	Channel: residual nucleus + nucleon + $\rho$ <sup>c</sup>	Obs width (keV in center of mass)	Obs $\theta^2$ <sup>e</sup>
He <sup>5</sup>	16.69	$\frac{3}{2}^+, \frac{1}{2}$	He <sup>4</sup> + $n$ + 2	...	0.03
Li <sup>6</sup>	16.80	$\frac{3}{2}^+, \frac{1}{2}$	He <sup>4</sup> + $p$ + 2	...	0.03
Be <sup>7</sup>	~6.5	$(\frac{3}{2}, \frac{3}{2}^+), \frac{1}{2}^e$	Li <sup>6</sup> + $p$ + 0	...	~0.75
B <sup>10</sup>	6.89	1-, 0	Be <sup>9</sup> + $p$ + 0	...	~1.5
	7.48	2-, 1	Be <sup>9</sup> + $p$ + 0	57	0.02
	7.81	2-	Be <sup>9</sup> + $p$ + 0	260	0.15
C <sup>11</sup>	10.06	$\frac{7}{2}^+, (\frac{1}{2})$	B <sup>10</sup> + $p$ + 0	160 or 90	0.20 or 0.09
B <sup>12</sup>	4.53	3-, 1	B <sup>11</sup> + $n$ + 2	120	0.42
C <sup>12</sup>	16.57	2-	B <sup>11</sup> + $p$ + 0	~140	~0.21 <sup>h</sup>
	17.22	1-	B <sup>11</sup> + $p$ + 0	~50	~0.03
C <sup>13</sup>	6.87	$\frac{5}{2}^+, \frac{1}{2}$	C <sup>12</sup> + $n$ + 2	...	0.008
	7.64 <sup>b</sup>	$\frac{3}{2}^+, \frac{1}{2}$	C <sup>12</sup> + $n$ + 2	~90	~0.04
	~8.5 <sup>b</sup>	$\frac{3}{2}^+, \frac{1}{2}$	C <sup>12</sup> + $n$ + 2	~1000	~0.4
N <sup>13</sup>	2.37	$\frac{1}{2}^+, \frac{1}{2}$	C <sup>12</sup> + $p$ + 0	33	0.81
	3.56	$\frac{3}{2}^+, \frac{1}{2}$	C <sup>12</sup> + $p$ + 2	61	0.32
	6.38	$\frac{5}{2}^+, \frac{1}{2}$	C <sup>12</sup> + $p$ + 2	11	0.005
	6.60	$\frac{1}{2}^+, \frac{1}{2}$	C <sup>12</sup> + $p$ + 0	75	0.022
	6.85	$\frac{3}{2}^+, \frac{1}{2}$	(C <sup>12</sup> + $p$ + 2)	41	0.02
			(C <sup>12</sup> + $p$ + 0)	73	0.5
	7.42	$\frac{5}{2}^+, \frac{1}{2}$	C <sup>12</sup> + $p$ + 2	85	0.03
	8.15	$\frac{3}{2}^+, \frac{1}{2}$	C <sup>12</sup> + $p$ + 2	350	0.17
C <sup>14</sup>	~11.5	$\frac{3}{2}^+, \frac{3}{2}^+, 1$	C <sup>13</sup> + $n$ + 2	~1000	~0.4
N <sup>14</sup>	8.06	1-, 1	C <sup>13</sup> + $p$ + 0	31	0.15
	8.70	0-, 1	C <sup>13</sup> + $p$ + 0	470	0.29 <sup>h</sup>
	8.90	3-, (1)	C <sup>13</sup> + $p$ + 2	19	0.18
	9.18 <sup>e</sup>	(2-, 1)	(C <sup>13</sup> + $p$ + 2)	<0.4	<0.002
	9.39	1-	C <sup>13</sup> + $p$ + 0	18	0.10
	9.49	2-, 1	C <sup>13</sup> + $p$ + 2	37	0.15
	10.43	(2-, 1)	C <sup>13</sup> + $p$ + 2	≤ 28	≤ 0.03
	12.69	3-	N <sup>13</sup> + $n$ + 2	4.3	0.0028
			C <sup>13</sup> + $p$ + 2	0.62	0.00018
			C <sub>1</sub> <sup>13</sup> + $p$ + 3	0.17	0.0044
			C <sub>2</sub> <sup>13</sup> + $p$ + 2	0.70	0.0046
			C <sub>3</sub> <sup>13</sup> + $p$ + 1	5.6	0.0070
N <sup>15</sup>	11.43	$\frac{1}{2}^+, \frac{1}{2}$	(C <sup>14</sup> + $p$ + 0)	15	0.005
			(N <sup>14</sup> + $n$ + 0)	24	0.014
	11.61	$\frac{1}{2}^+, \frac{3}{2}$	(C <sup>14</sup> + $p$ + 0)	500	0.23
			(N <sup>14</sup> + $n$ + 0)	18	0.0014
	11.77	$\frac{3}{2}^+, \frac{1}{2}$	(C <sup>14</sup> + $p$ + 2)	0.5	0.003
			(N <sup>14</sup> + $n$ + 0)	34.0	0.01
	12.14	$\frac{3}{2}^+, \frac{1}{2}$	(C <sup>14</sup> + $p$ + 2)	14	0.04
			(N <sup>14</sup> + $n$ + 2)	36	0.008
	12.32	$\frac{5}{2}^+, \frac{1}{2}$	(C <sup>14</sup> + $p$ + 2)	0.3	0.006
			(N <sup>14</sup> + $n$ + 0)	2.1	0.007
O <sup>15</sup>	8.00	$\frac{1}{2}^+, \frac{3}{2}^+, \frac{1}{2}$	N <sup>14</sup> + $p$ + 0	93	0.36 <sup>h</sup>
	8.33	$\frac{3}{2}^+, \frac{1}{2}$	N <sup>14</sup> + $p$ + 0	3	0.0045
	8.79	$\frac{1}{2}^+, \frac{1}{2}$	N <sup>14</sup> + $p$ + 0	34	0.024
	9.77	$\frac{1}{2}^+, \frac{3}{2}^+, \frac{1}{2}$	N <sup>14</sup> + $p$ + 0	1180	0.33 <sup>h</sup>
O <sup>16</sup>	12.43	(1-)	N <sup>15</sup> + $p$ + 0	...	0.15 <sup>h</sup>
	12.51 <sup>d</sup>	2-	N <sup>15</sup> + $p$ + 2	0.033	0.13 <sup>h</sup>
	12.78	0-, 1	N <sup>15</sup> + $p$ + 0	40	0.17 <sup>h</sup>
	12.95	2-, 1	N <sup>15</sup> + $p$ + 2	1.2	0.15 <sup>h</sup>
	13.09	1-, 1	N <sup>15</sup> + $p$ + 0	112	0.15 <sup>h</sup>
	13.24	3-, 1	N <sup>15</sup> + $p$ + 2	4.7	0.11 <sup>h</sup>

<sup>a</sup> References to data used in the table are given in the discussions in the text except where the data is cited in the well-known compilations (Aj52, Aj55, Aj59).

<sup>b</sup> The neutron widths of the 7.64- and 8.5-Mev states in C<sup>13</sup> are taken from the data of C<sup>12</sup> +  $n$  scattering (Bu55). Rather larger values are indicated in the C<sup>12</sup>( $d, p$ ) reaction (McG55).

<sup>c</sup> The spin of the 9.18-Mev level in N<sup>14</sup> has been recently reported as 2+, and the width as 70 ev [S. S. Hanna and L. Meyer-Schutzmeister, Phys. Rev. 115, 986 (1959)].

<sup>d</sup> The proton width of the 12.5-Mev level in O<sup>16</sup> is the smaller of two possibilities (0.033 or 0.9) and is chosen because the larger value implies  $\theta^2 \gg 1$ .

<sup>e</sup> When an entry is bracketed ( ), there is some doubt about it.

<sup>f</sup> The residual nucleus of the fourth column is always in the ground state unless a subscript  $n$  indicates the  $n$ th excited state.

<sup>g</sup> An interaction radius of  $1.45(A^{1/3} + 1) \times 10^{-13}$  cm is used except the case of the levels in N<sup>14</sup>, where published graphs of penetrabilities (Ch48) based on a radius  $1.41(A^{1/3} + 1) \times 10^{-13}$  cm are used.

<sup>h</sup> The reduced width has not been corrected for the variation of the level shifts with energy.

verified to within a few Mev. Such a state would have zero reduced width for nucleon emission, but it may have a large one for alpha emission. By virtue of the latter, it could be broad and overlap and interact with the single-particle states to give rise to a complicated

type of situation such as seems to be observed (see Ma57a).

### Mass 8

There are no known bound states of nonnormal parity in the mass 8 nuclei. For that matter there are

no free states either, at least none that appear as discrete resonances. On the other hand, there are several indications of strong  $s$ -wave effects just above the nucleon thresholds which suggest that the  $2s$  single-particle levels (four in all;  $J=1, 2$ ;  $T=1, 2$ ) are located a short way above the neutron thresholds. In particular, both thermal-neutron scattering lengths in  $\text{Li}^{7+n}$  are either very small or negative, and this indicates strong free  $s$ -wave levels. The  $s$ -wave phase shifts near  $E_n=0.25$  Mev are positive (Wi56a). An analysis of the  $\text{Li}^7(nn')\text{Li}^{7*}$  reaction reveals very strong  $s$ -wave effects in the region about 1 Mev bombarding energy (Fr55). Also, the reactions  $\text{Li}^7(p,\gamma)\text{Be}^8$  show considerable evidence for  $s$ -wave effects both in angular distributions and excitation curves (Wi54).

#### Mass 9

No nonnormal parity states have been definitely established as yet in  $\text{Be}^9$ , but we wish to point out that there is evidence for the existence of low-lying single-particle  $2s$  and  $1d$  states as one might expect from analogy with  $\text{C}^{13}$ , another  $(4n+1)$  nucleus. As mentioned in discussing normal parity states, the breadth of the 1.8-Mev anomaly, taken in conjunction with its proximity to threshold, may establish it as the expected  $\frac{1}{2}+$   $s$ -wave state. This anomaly is revealed in the inelastic scattering of protons (Go55b, Bo56) deuterons, and alphas (Ra55a) on  $\text{Be}^9$ . In each case a broad inelastic group (width  $\sim 200$  kev) is found corresponding to an excess energy of the residual system of  $\sim 1.8$  Mev. [Notice that evidence for a similar anomaly in  $\text{B}^9$  is found from the  $\text{Be}^9(p,n)\text{B}^9$  reaction (Ma55).] The shape of the anomaly can be fitted with a Breit-Wigner type resonance formula, and this may be taken to suggest that the inelastic particles leave behind a compound state of  $\text{Be}^9$  with excitation 1.8 Mev. Unfortunately, the fittings do not really give separate values of the two parameters (reduced width, resonance energy). Nevertheless it is possible to conclude that the reduced width is large, probably about the single-particle value and certainly greater than one-fifth of it (Go55b, Ra55a). Such a large reduced width for an  $s$ -wave state implies that the neutron is released by the inelastically scattered particles without much appreciable intrinsic time delay, so that the process may be more realistically described as a three-body breakup rather than two consecutive two-body ones. This makes the analysis in terms of a Breit-Wigner formula somewhat artificial. An alternative analysis has been made (Ra55a, Su58, Mi58a) in which one first attempts to fit the shape of the anomaly in terms of phase-space factors of the three particles alone. Then one improves the fit by taking into account the  $\text{Be}^8$ -neutron interaction (final state interaction). This fitting yields a value of the scattering length for this interaction which is large ( $13 \times 10^{-13}$  cm). Such a large value implies the presence of a strong (single particle)  $s$ -wave interaction

centered below the threshold, which is just the conclusion of the other analysis.

#### Mass 10

The scattering lengths of the  $\text{Be}^9+n$  scattering are large ( $7.8 \times 10^{-13}$  cm) compared with the interaction radius ( $4.5 \times 10^{-13}$  cm) and this indicates strong bound  $s$ -wave levels of both spins  $1-$  and  $2-$ . These may well be the two states at 5.96 and 6.26 Mev that are established as  $s$  wave in the  $\text{Be}^9(d,p)\text{B}^{10}$  reaction (Gr56a). One is tempted to associate the 5.96-Mev state with the believed  $2-$  state of  $T=1$  near the analogous energy in  $\text{B}^{10}$ . This is the 7.48-Mev level. On the other hand, the reduced width of this state for  $s$ -wave nucleon emission is only  $\theta^2=0.04$  or less, and this means that it is a "weak" state and hardly capable of producing strong effects at the neutron threshold in  $\text{Be}^{10}$ .

As far as  $T=0$  states of nonnormal parity are concerned, the first level is the one at 5.11 Mev in  $\text{B}^{10}$ , which is believed to be  $2-$ . The next one is the 6.89 Mev state. A recent analysis (Mo56) of the  $\text{Be}^9(p,p)$ ,  $\text{Be}^9(p,\alpha)$ , and  $\text{Be}^9(p,d)$  reactions indicates that the spins of this state are  $1-$  or  $2-$ , and that the ratio  $\Gamma_p/\Gamma$  is 0.30 or 0.18, respectively, as  $J=1, 2$ . The fact that the state radiates strongly to the 1.74-Mev state of  $\text{B}^{10}$  which has spin  $0+$  (Table XI) suggests that the spin is  $J=1$ . Since the state is broad, and the level shift varies significantly through the width of the state (as does the proton penetration factor), one must not fit the cross section through the state in terms of a simple Breit-Wigner formula with constant widths. Instead, one must use the general resonance formula with the reduced widths as parameters. Such a fitting is not completely unambiguous, but there seems to be no doubt (Mo56) that  $\theta^2$  for the proton channel is of order unity, as expected for a single-particle state.

A special feature of the 6.89-Mev state as revealed by study of the  $\text{Be}^9(p,\gamma)$  reaction is that it decays by the emission of  $E1$  radiation to both  $T=0$  and  $T=1$  states with fair probability (Ca54a, Ca55, Lo55, Cl56). This may indicate a composite structure. Certainly there is no lack of predicted levels in this energy region. The coupling of  $2s$  and  $1d$  particles to the ground state of the mass 9 system gives 20 states altogether. The low excited states of the mass 9 system give rise to similar numbers, and, in addition, states involving a  $1s$  hole are predicted to occur not far above the nucleon thresholds.

A large number of possible structures could explain the small  $s$ -wave reduced width of the 7.48 level we have mentioned. It could have an excited state of the mass 9 system as parent; it could involve a  $1s$  hole coupled to the mass 11 ground state; or it could be mainly a  $1d$  particle coupled to the mass 9 ground state. The last possibility is given some credence by the observed fact that, in spite of the high  $d$ -wave barrier, an appreciable amount of  $d$ -wave admixture is needed

to fit the angular distributions from this level (De49). The proton width of the 7.48 level is only 65% of the total width which is reported to be 88 keV from proton capture work and  $150(\pm 50)$  keV from elastic scattering (Mo56). Thus there appears to be a width of 35 keV for alpha and deuteron decay in spite of the implied violation of the isotopic spin selection rule. In fact, the  $\text{Be}^9(p,\alpha)$  and  $\text{Be}^9(p,d)$  reactions show a resonance of about the right width (We56) but apparently centered at a few tens of kilovolts below the  $\text{Be}^9(p,\gamma)$  resonance. At present it is not quite certain that the resonances are the same, although it seems very likely; the shift in energy may be due (Mo56) to the interference with the second  $2-$  level at 7.81 MeV.

There is considerable interest in the results of a study of the pair conversion electrons from the radiation emitted near the 7.48 level (De54a). If one level is assumed responsible, the radiation is reported to be  $E3$  or  $M2$ . Since a  $2s \rightarrow 1p$  transition is forbidden for such radiation, this might be taken as support for the suggestion that the 7.48 state has configuration  $(1p)^2 1d$ . However, the value of  $\Lambda^2$  for the transition ( $10^3$ ) is much too large to permit such an interpretation. One must conclude that either the pair conversion theory on which the radiation assignment is based is at fault or else at least two levels are involved. It has been shown recently that the pair conversion data can be fitted in terms of two states, one emitting  $E1$  radiation and the other  $M1$  (Mo56). The one emitting  $M1$  radiation is believed to have spin  $2+$  and to occur at 7.46 MeV; its existence is independently suggested by the elastic proton scattering data (Mo56).

Recent investigations have suggested a very tentative correspondence between states in the range 5.7–7.6 MeV in  $\text{Be}^{10}$  and those in the corresponding range 7.4–9.3 MeV in  $\text{B}^{10}$ . In the energy range in  $\text{Be}^{10}$ , there are states at 5.96, 6.18, 6.26, 7.37, and 7.54. As mentioned in the discussion of normal parity states, the 6.18, 7.37, and 7.54 states may be associated with the 7.56 and 8.89 states of  $\text{B}^{10}$ , the 8.89 state being interpreted as a close doublet (Ma56c). There is some doubt about identifying the 5.96 state with the 7.48 state in  $\text{B}^{10}$ . Accepting this assignment leaves only the 6.26 state which had no apparent analog in  $\text{B}^{10}$ , until recently when two investigations (De57, Mo56) revealed a broad  $s$ -wave state ( $\Gamma \sim 0.5$  MeV) in  $\text{B}^{10}$  at an excitation energy of 7.81 MeV. The most disturbing feature of this correspondence is that it involves *all* the known states of  $\text{B}^{10}$  in the range 7.4–9.3 MeV, except the 7.46 state, thereby implying that all except one are  $T=1$ . Since it is very unlikely that there is only one  $T=0$  state in this range, one must conclude that either the correspondence is incorrect or that there exist  $T=0$  states that have not been found experimentally.

#### Mass 11

There is little evidence on any nonnormal parity free states in the mass 11 nuclei. We only mention them to

point out that the simple estimate (Table IX) for the positions of the  $1s$ -hole states indicates that the lowest should occur about 2 MeV and have spin  $\frac{1}{2}+$ . This raises the interesting question as to whether this state is one of the established ones (at 2.1 or 4.4 MeV?) or whether it has not yet been observed. Such a state should not be found in the  $\text{B}^{10}(d,p)\text{B}^{11}$  stripping reaction because it has zero nucleon reduced width.

An analysis of the  $\text{B}^{10}(p,\alpha)\text{Li}^7$  reaction at the 10.06 MeV level in  $\text{C}^{11}$  assigns nonnormal parity to this state and an  $s$ -wave proton reduced width of either 0.20 or 0.09 (Cr56a).

#### Mass 12

In  $\text{C}^{12}$  we find the first clear demonstration of  $2s$  single-particle levels occurring as resonances. Altogether, four states can be made by coupling a  $2s$  nucleon to the ground state of the mass 11 system  $J=2$ ,  $1-$ ;  $T=0$ ,  $1$ . The  $2-$  level at 16.57 may well be one of these because it has an  $s$ -wave reduced width for proton emission of about the value  $\frac{1}{2}\theta_p^2$ . Experimentally, some doubt existed as to the spin, but the assignment  $2-(T=1)$  now appears as satisfactory as others (De57). The parity assignment to the 16.57 state also has some support from the believed negative parity of 1.67 state in  $\text{B}^{12}$  which is the energy analogue. It was originally thought that the 17.22 ( $1-$ ,  $T=1$ ) state was also a single-particle level; recently, however, Dearnaley has shown that the proton width of this state is the smaller part ( $\sim 5\%$ ) of the total widths, so the reduced width is small (De57). The absence of the two  $T=0$  levels need not be disturbing. Analogy with normal parity states tells us that, other things being equal,  $T=0$  states are more bound than  $T=1$ . This means that the two states could occur below the nucleon threshold, where several states with no spin and parity assignments are, in fact, known to exist. Furthermore, the  $1-$  state can decay by alpha emission; if the reduced alpha width were large, the state might be so broad as to be indistinguishable from the background.

Another nonnormal parity state is found in  $\text{B}^{12}$  at 4.53 MeV. This has spin  $3-$  and is a  $d$ -wave state with a large reduced width of 0.42, which makes it likely that this is a  $1d$  single-particle state. The angular distribution of the  $\text{B}^{11}+n$  scattering (Wi55a) has been fitted with a channel spin ratio ( $s=2:s=1$ ) of 10, assuming the potential  $s$ -wave scattering to contain a statistical mixture of the two channel spins. The latter assumption may be wrong and this may help to explain the discrepancy between the ratio 10 and the ratio of  $\frac{3}{2}$  predicted by the simplified shell model in which the  $\text{B}^{12}$  state is considered to be a  $1d\frac{1}{2}$  nucleon coupled to the ground state of the mass 11 nucleus.

#### Mass 13

The nuclei  $\text{C}^{13}$  and  $\text{N}^{13}$  manifest the success of the simplified shell model in a striking way. Both the reduced widths and the spectrum itself lend strong



support to the model. According to the model, the spectrum of states in  $C^{12}$  should be reproduced in  $C^{13}$  and  $N^{13}$ , with the addition of  $2s_{3/2}$ ,  $1d_{3/2}$ , and  $1d_{5/2}$  particles. Once we specify the relative spacings of these single-particle levels, we can "predict" the spectrum of the mass 13 nuclei by superposing the three families as in Fig. 4(a). In addition, the spectrum of  $N^{14}$  should be reproduced in states containing a  $1s$  hole, but the simple estimate (Table IX) indicates that such a family only begins at  $\sim 10$  Mev. If we take the observed  $2s_{3/2}$ ,  $1d_{3/2}$ ,  $1d_{5/2}$  ordering from  $O^{17}$ , we obtain the spectrum shown in Fig. 4(b). On comparing with the observed spectrum, the most striking agreement is in the gap of 3 Mev above the first two states. The most obvious differences are: (1) the inversion of the  $2s_{3/2}-1d_{3/2}$  order; (2) there are too many predicted levels, especially as some of the observed levels must have normal (-) parity.

The first difference can be trivially attributed to a change in well-shape between  $C^{13}$  and  $O^{17}$ . The second difference is more illuminating. One should really compare only experimental and theoretical spectra with reference to the particular reactions used. Let us first consider the scattering of nucleons by  $C^{12}$ . This reveals only those compound states with nonzero reduced nucleon widths. It so happens that, of all the states we predict, only three have nonzero reduced widths, namely, those states formed by adding a  $2s_{3/2}$ ,  $1d_{3/2}$  and  $1d_{5/2}$  to  $C^{12}$  in its ground state. These three should have single-particle widths. This is completely borne out by experiment. In the  $C^{12}+p$  reaction,  $s$ - and  $d$ -wave states are found at 2.37 and 3.56 Mev in  $N^{13}$  with large reduced widths. From phase-shift analyses of the  $C^{12}+n$  and  $C^{12}+p$  scattering (Bu55, Sc56), a broad  $d_{3/2}$  level is identified at 8.5 Mev excitation in  $C^{13}$  and a corresponding one at 8.15 Mev in  $N^{13}$ .

Now let us consider what is to be expected when we relax the model somewhat, that is, we allow some mixing interaction between states. Such mixing affects close neighbors first and, amongst other things, leads to a sharing of reduced width properties. Both the  $2s_{3/2}$

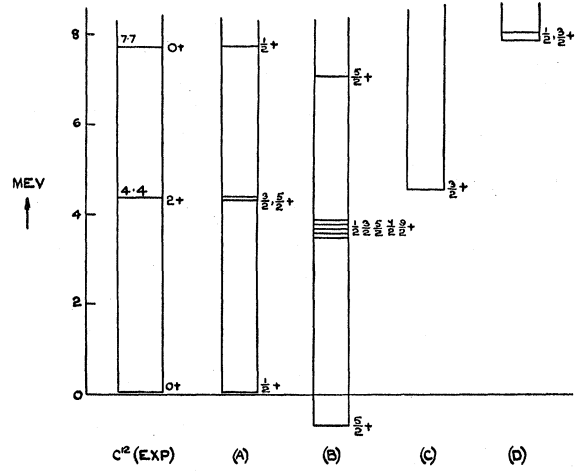
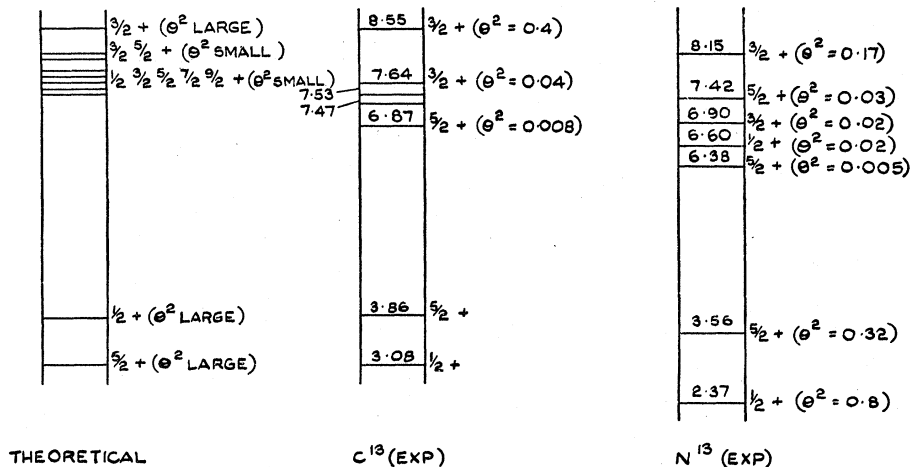


FIG. 4(a). The prediction of positive parity states in carbon-13 according to the simplified shell model discussed in the text. The first spectrum is the experimental one of carbon-12. The next four are predicted spectra of carbon-13 of states of the types (A), (B), (C), and (D).

and  $d_{3/2}$  single-particle states are predicted to be separated by 3 Mev or so from their nearest neighbors of the same spin, and so these latter should have small  $\theta^2$ . There are two states of spin  $5/2+$  and one state of spin  $3/2+$  reported at 6.38, 7.42, and 6.60 Mev in  $N^{13}$  from  $C^{12}+p$  scattering and their reduced widths are 0.005, 0.03, and 0.022, respectively (Sc56, Li57, Re56b). The  $5/2+$  state of 6.87 Mev in  $C^{13}$  found in  $C^{12}+n$  scattering may be the mirror of the 6.38 state in  $N^{13}$ . Its reduced width is 0.008 (Bu55, Sc56, Wi56c, Co56). The  $d_{3/2}$  state, on the other hand, is predicted to occur close to two other  $3/2+$  states. Thus we expect these states to acquire only small reduced widths when the mixing interactions are introduced [Fig. 4(b)]. This expectation is confirmed experimentally by the identification of a comparatively sharp  $3/2+$  state at 7.64 Mev in  $C^{13}$  (Bu55) near the broad state is  $\sim 8.5$  Mev, and a similar state at 6.90 in  $N^{13}$  (Sc56, Re56b) near the broad  $N^{13}$

FIG. 4(b). The positive parity states of the mass 13 systems. The spectrum on the left is the expected one and those on the right are experimental. Reduced widths for emission to the ground state of  $C^{12}$  are indicated in brackets by each state.



state at 8.15 Mev. (The reduced widths of these widths of these states are  $\sim 0.04$  and  $0.02$ , so they may be mirror states.) The two predicted  $\frac{3}{2}$  states consist of an  $s_{\frac{1}{2}}$  and a  $d_{\frac{3}{2}}$  nucleon coupled to the first excited state of  $C^{12}$ . It is significant that the observed  $N^{13}$  state at 6.90 has a large  $s$ -wave reduced width for emission to the excited state of  $C^{12}$  (Sc56, Re56b), viz.,  $\theta^2 \sim 0.5$ . It is thus apparent that the simple model gives a surprisingly good representation of the experimental situation.

The  $C^{12}(d,p)C^{13}$  reaction is subject to the same selection rules in the observation of levels as the  $C^{12}+n$  scattering if it proceeds by stripping. This is because the reduced width is a multiplying factor in the stripping cross section. On the other hand, if the compound nucleus mechanism is operative, there is no such selection rules. The reaction proceeds by stripping to the three single-particle levels and it also excites with less intensity several other levels as well (McG55).

The interpretation of the lowest  $\frac{1}{2}+$  state as a  $2s$  single-particle state has received further corroboration from an analysis of the  $C^{12}+n$  scattering results at energies  $\lesssim 1$  Mev (Th52). Not only is the scattering length larger ( $6.11 \times 10^{-13}$  cm) than the interaction radius ( $4.77 \times 10^{-13}$  cm), indicating a strong bound state, but also the precise numerical values of the scattering length and "effective range" ( $3.3 \pm 0.3 \times 10^{-13}$  cm) can be shown to be consistent with a single-particle model of the  $\frac{1}{2}+$  state. To be more specific, these two quantities are related to the logarithmic derivative  $f$  of the radial wave function and its energy derivative evaluated at zero neutron energy:

$$f = \left(1 - \frac{1}{\alpha a}\right)^{-1}; \quad \left(\frac{\mathcal{L}^2}{ma^2}\right) \left(\frac{df}{dE}\right) = \frac{1 - \alpha a + \frac{1}{2}a^2 - r_0/2a}{(1 - \alpha a)^2},$$

where  $1/\alpha$  is the scattering length, and  $r_0$  is the effective range. These two quantities and the binding energy of the 3.08 state in  $C^{13}$  are, for example, consistent with a single-particle  $2s$  state in a square well, depth 35.23 Mev, radius  $4.062 \times 10^{-13}$  cm (La52).

#### Mass 14

The situation in  $N^{14}$  is like that in  $C^{12}$  inasmuch as  $s$ -wave states with large reduced widths occur as resonances. These are the 8.06 ( $1-$ ,  $T=1$ ) and 8.70 ( $0-$ ,  $T=1$ ) states. The latter has a proton reduced width of the order of  $\frac{1}{2}\theta_p^2$  expected for a  $2s$  single-particle state. Although the former has quite a large reduced  $s$  width (0.15), it does not appear to be a single-particle  $2s$  state but rather (Br57) a mixture of  $2s$  and  $1d$  states. Further evidence for this comes from the fact that the 9.39 Mev state (see below) has an equally large reduced width. Both the 8.06 and 8.70 states may have their analogs in  $C^{14}$  amongst the four reported states at 6.09, 6.59, 6.72, 6.89 Mev. One analysis of the  $C^{13}(d,p)C^{14}$  stripping reaction assigns negative parity to

the first three of these (McG55). Another analysis (El56a) confirms the first one to be  $s$ -wave capture. The two expected  $T=0$  states of  $2s$  single-particle structure may well occur amongst the several unidentified states below the nucleon thresholds in  $N^{14}$ . (The state at 4.91 is believed to have spin  $0-$ .)

There is also a  $d$ -wave ( $3-$ ) state at 8.90 which has a large proton reduced width of the order  $\frac{1}{2}\theta_p^2$ , and so presumably has the structure of a  $1d$  particle coupled to the ground state of the mass 13 system (Wa59).

At 9.18 there occurs a state of possible spin  $2-$  (Ma56d). Accepting this spin, the reduced width (for  $d$  waves) is very small ( $\theta^2 < 0.002$ ), and this indicates that the ground state of the mass 13 system is not the main parent of this state. The isotopic spin of the state is in doubt; the strong  $E1$  radiation from it to the ground state suggests  $T=1$ ; on the other hand, the observation of the state in the  $N^{14}(\alpha,\alpha')N^{14*}$  reaction suggests  $T=0$  (Mi56).

A  $1-$  state has been reported at 9.39 Mev (Zi57) with a quite strong width ( $\theta^2 \sim 0.10$ ).

It has been suggested that the 9.49 state in  $N^{14}$  is  $2-$  and formed by  $d$  waves (Wi56b, Zi57, Zi58, Wa59). If we attribute the observed width entirely to  $d$ -wave formation,  $\theta^2 \sim 0.15$  for this state.

The 10.43 state is reported to be  $2-$  (Wi55b, Wi57). The small observed ( $d$  wave) width of 28 kev implies a small reduced width  $\theta^2 \sim 0.05$ , which in turn implies that the main parentage of this state comes from excited states in the mass 13 system. The observed channel spin ratio for the  $s=0$  to the  $s=1$  channel is  $\frac{3}{2}$ , and this suggests that the amount of parentage from the mass 13 ground state is associated with a  $d_{\frac{3}{2}}$  rather than a  $d_{\frac{5}{2}}$  nucleon. (These two single-particle states imply channel spin ratios of  $\frac{3}{2}$ ,  $4/9$ , respectively.)

At higher energies, a ( $3-$ ) state is found at 12.69 Mev. Like the  $4+$  state discussed in Sec. III.1(a), this has very small reduced widths for nucleon emissions, and its neutron and proton reduced widths also differ by a factor of five or so, indicating strong isotopic spin impurity (Sh53, Sh55a).

The  $C^{13}(d,p)C^{14}$  reaction reveals a strong  $d$ -wave level (or levels) centered at about 11.5 Mev in  $C^{14}$  (McG55). This may well be the expected doublet of single-particle levels  $J=1, 2-$ ;  $T=1$  formed by coupling a  $1d_{\frac{3}{2}}$  particle on to the ground state of the mass 13 system.

#### Mass 15

This mass is of special interest. Experimentally, several levels of positive parity have been found in the  $N^{14}(d,p)N^{15}$  reaction (Sh55b, Gr56a) at 5.28, 5.31, 7.16, 7.32, 7.57, 8.32, and 8.57 Mev. Theoretically, Halbert and French (Ha57b) have made an attempt to predict the energies of the levels, together with their spins and reduced widths, by diagonalizing interactions within the configurations ( $1s^4 1p^{10} 2s$ ), ( $1s^4 p^{10} 1d$ ), and ( $1s^3 1p^{12}$ ). Amongst other reasons, this calculation is

interesting because it gives insight into the simplified shell model that we have been using.

The comparison between experiment and theory is, on the whole, very good. Experimental values of the reduced widths vary over nearly two orders of magnitude, but they are reproduced satisfactorily by the calculation.

Comparison with the simplified model shows that the model certainly *cannot* be used reliably in the mass 15 systems. Although there is a tendency for each state to have a pure configuration (i.e., one of the three quoted above dominates), the assumption of "unique parentage" breaks down seriously for some states. As Halbert and French point out, the four lowest predicted states have comparable amounts of parent states of  $T=0$  and  $T=1$ . Furthermore, the two lowest states (5.28 and 5.31) have small reduced widths instead of the large ones predicted by the simplified model. The suggested explanation for the 5.31 state—that it comes from the  $(1s^3 1p^{12})$  configuration (In55)—is not supported by the calculations or by recent experimental data on  $C^{15}$  decay (Al59). This fact means that the simple recipe for predicting the position of hole-type states also fails in mass 15 [from Table IV(b), the recipe predicts 5 Mev, which is near the 5.31 state].

The failure of the simplified model in mass 15 probably applies also to other  $(4n+3)$  type nuclei like mass 11. However, in nuclei of other types, the model must work rather better. Not only is this an experimental fact (see Mass 12, 13, 14 above) but it is also theoretically reasonable, since the amount of parentage mixture must vary inversely as the energy spacing of low-lying parent levels. In the  $(4n+2)$  type parents of  $(4n+3)$  type nuclei, this spacing is least.

In  $O^{16}$ , unbound states are reported at 8.00 ( $\frac{1}{2}^-, \frac{3}{2}^+$ ), 8.33 ( $\frac{3}{2}^+$ ) (Ha56), 8.79 ( $\frac{1}{2}^+$ ) (Fe59b), 9.77 ( $\frac{1}{2}^-, \frac{3}{2}^+$ ). The 8.00 and 8.33 states have large and small widths, respectively, and are probably isobars of the 8.32 and 8.57 states in  $N^{15}$ . The former is found in calculation to be mainly of the structure  $[N^{14}(\text{ground})+2s]$  (i.e., the simplified model applies to this case). Presumably the 9.77 state, which also has a large reduced width, accounts for most of the remainder of this parentage.

Higher in the spectrum of  $N^{15}$ , several positive parity states are found in the reactions  $C^{14}+p$  (Ba54, Ba55b, Fe59a),  $N^{14}+n$  (Fo55) and  $B^{11}+\alpha$  (Sh55a). These have uniformly small reduced widths except for the 11.57 state of spin  $\frac{1}{2}^+$ , where the value is very large (Ba55, Fe59a). This state probably has  $T=\frac{3}{2}$  (it does not decay by neutron emission to the ground state of  $N^{14}$ ), and it is naturally identified at the 2s single-particle state whose "core" or "parent" is the first excited ( $T=1, J=0$ ) state of the mass 14 system.

### Mass 16

The addition of 2s and 1d nucleons to the ground state of the mass 15 system gives 6 states of spin 0,

1, 1, 2, 2, 3— for  $T=0$  and another 6 for  $T=1$ . There are several states below the proton threshold in  $O^{16}$  of odd parity, and these are presumably members of the  $T=0$  group. Above threshold are found a 0—, a 1—, and two 2— states (at 12.78, 13.09, and 12.51, 12.95, respectively) and also a possible 1— state at 12.43 (He58b) and a possible 3— state at 13.24 (Ha56). The 0— and 1— (*s* wave) and the two 2— (*d* wave) states have reduced widths rather less than but of the order of  $\frac{1}{2}\theta_p^2$ , and this suggests their interpretation as 2s and 1d single-particle states. The suspect 1— state would have a fairly large reduced width although rather less than the single-particle value. The suspect 3— state emits alpha particles to the 2+ excited state of  $C^{12}$  and the width for this process is unknown so that the proton width can only be given as an upper limit.

There is a certain center-of-mass effect to be taken into account in constructing states of nonnormal parity on the basis of the usual shell model (E155b). Besides demanding a certain mixing of configurations, this effect actually excludes some states being spurious in the sense that they are not new states of internal motion but only of the center-of-mass motion. Some of the 12 states that we mention above are excluded in this interpretation.

### (b) Alpha-Particle and Deuteron Channels

These have been discussed generally for both normal and nonnormal parity states in Secs. III.1(b) and (c). The experimental data is included in Tables VI and VII.

### (c) Photon Channels

In Table XI we list the observed electric-dipole electromagnetic transitions of known width in the 1p shell (Wi56b). In every case only one of the two states involved is of nonnormal parity (usually the initial state). In addition to these  $E1$  transitions, an  $E3$  transition is found in  $O^{16}$  (see below).

A very useful criterion for an initial analysis of the strength of an  $E1$  transition is provided by the vanishing of the  $E1$  matrix elements taken between states of the same isotopic spin in self-conjugate nuclei [in other words, the "isotopic spin selection rule" for  $E1$  transitions (McD 55)]. This selection rule enables one to extract information about the isotopic spin of the states involved in an  $E1$  transition from the transition width. For instance, the extreme smallness of the  $E1$  widths from the 5.11 state in  $B^{10}$  of spin 2— establishes this state as almost pure  $T=0$ . In contrast, the occurrence of strong  $E1$  transitions from the 6.89 state in the same nucleus to states of  $T=0$  and  $T=1$  implies that this state contains both  $T=0$  and  $T=1$  components (Wi56d).

In order to discuss the observed  $E1$  widths further, it is convenient to extract, for each width, the value of the quantity  $\Lambda^2$ . As discussed in Sec. II, this is defined, for any transition, as the ratio of the transition width

TABLE XI. *E1* transitions of known width in nuclei of the mass range  $4 < A \leq 16$ .<sup>a</sup>

Nucleus	Excitation of initial state in Mev	Spin and isotopic spin of initial state	Excitation of final state in Mev	Spin and isotopic spin of final state	Obs. width in ev	Experimental value of $A^2$	Initial state in <i>L-S</i> coupling <sup>d</sup>	Final state in <i>L-S</i> coupling <sup>d</sup>	$A^2$ in <i>L-S</i> coupling <sup>d</sup>	Initial state in <i>j-j</i> coupling	Final state in <i>j-j</i> coupling	$A^2$ in coupling
Li <sup>6</sup>	16.80	$\frac{3}{2}^+, \frac{1}{2}$	0	$\frac{3}{2}^-, \frac{1}{2}$	11	0.044	$(^{13}S_1)(1s_1)^{-1}$	$^2P$	0	$(p_1)^2(1s_1)^{-1}$	$p_1$	1/12
Be <sup>7</sup>	6.35	$(\frac{1}{2}, \frac{3}{2}^-), \frac{3}{2}^+$	0	$\frac{3}{2}^-, \frac{1}{2}$	$2/2J+1$	$0.08/2J+1$	$(^{13}S_1)(2s_1)$	$^2P$	5/9 or 5/18	$(p_1)^2(2s_1)$	$(p_1)^3$	1/6 or 1/15
B <sup>10</sup>	5.11	$2^-, 0$	0	$3^+, 0$	$1/2J+1$	$0.04/2J+1$	$(^{13}S_1)(2s_1)$	$^2P$	5/18 or 5/36	$(p_1)^2(2s_1)$	$(p_1)^3$	4/9 or 1/36
			0.72	$1^+, 0$	0.012	0.001	$(^{13}S_1)(1s_1)^{-1}$	$^2P$	0 <sup>e</sup>	$(p_1)^2(1s_1)^{-1}$	$p_1$	0 <sup>e</sup>
			2.15	$1^+, 0$			$(^{13}S_1)(2s_1)$	$^2P$	0 <sup>e</sup>	$(p_1)^2(2s_1)$	$(p_1)^3$	0 <sup>e</sup>
	6.89	$1^-, 0$	0.72	$1^+, 0$	1.0	0.03	$(^{13}S_1)(1d_{5/2})$	$^3S$	0 <sup>e</sup>	$(p_1)^2(1d_{5/2})$	$(p_1)^6$	0 <sup>e</sup>
			1.74	$0^+, 1$	2.6	0.11	$(^{13}S_1)(2s_1)$	$^3S$	0 <sup>e</sup>	$(p_1)^2(2s_1)$	$(p_1)^6$	0 <sup>e</sup>
			2.15	$1^+, 0$	0.52	0.027	$(^{13}D_1)$	$^3D_1$	16/81	$(p_1)^2(2s_1)$	$(p_1)^6$	4/15
	7.48	$2^-, 1$	0	$3^+, 0$	$\leq 21$	$\leq 0.30$	$(^{13}D_1)$	$^3D_1$	1/500	$(p_1)^2(1d_{5/2})$	$(p_1)^5(p_1)$	0 <sup>e</sup>
			0.72	$1^+, 0$	$\leq 2$	$\leq 0.04$	$(^{13}D_3)(2s_1)$	$^3D_3$	28/45	$(p_1)^2(2s_1)$	$(p_1)^6$	3/125
B <sup>11</sup>	9.28	$(\frac{3}{2}^+, \frac{1}{2})$	0	$\frac{3}{2}^-, \frac{1}{2}$	0.8	0.005	$(^{13}D_3)(2s_1)$	$^3D_3$	0.0135	$(p_1)^2(2s_1)$	$(p_1)^7$	189/250
			4.46	$(\frac{3}{2}^-), \frac{1}{2}$	1.9	0.090	$(^{13}D_3)(2s_1)$	$^3D_3$	0.37	$(p_1)^2(2s_1)$	$(p_1)^6(p_1)$	...
			6.81	$(\frac{3}{2}^-), \frac{1}{2}$	0.6	0.20	$(^{13}D_3)(2s_1)$	$^3D_3$	0.027	$(p_1)^2(2s_1)$	$(p_1)^5(p_1)$	...
	16.57	$2^-, 1$	4.43	$2^+, 0$	$\sim 15$	$\sim 0.05$	$(^{13}D_3)(2s_1)$	$^3D_3$	0	$(p_1)^2(2s_1)$	$(p_1)^7(p_1)$	1/6
	17.22	$1^-$	0	$0^+, 0$	$\sim 800$	$\sim 1.0$	$(^{13}D_3)(2s_1)$	$^3D_3$	...	$(p_1)^2(2s_1)$	$(p_1)^8$	...
			4.43	$2^+, 0$	$\sim 400$	$\sim 1.0$	$(^{13}D_3)(2s_1)$	$^3D_3$	...	$(p_1)^2(2s_1)$	$(p_1)^7(p_1)$	...
	2.37	$\frac{1}{2}^+, \frac{1}{2}$	0	$\frac{1}{2}^-, \frac{1}{2}$	0.67	0.35	$(^{11}S_0)(2s_1)$	$^2P$	1/9	$(p_1)^2(2s_1)$	$(p_1)^7(p_1)$	...
	3.51	$\frac{3}{2}^+, \frac{1}{2}$	2.37	$\frac{3}{2}^+, \frac{1}{2}$	0.04	0.56	$(^{11}S_0)(2s_1)$	$^2P$	1/3	$(p_1)^2(2s_1)$	$(p_1)^6(p_1)$	1/3
	8.06	$1^-, 1$	0	$1^+, 0$	10.2	0.12	$(^{11}S_0)(2s_1)$	$(^{11}S_0)(2s_1)$	20/81	$(p_1)^2(2s_1)$	$(p_1)^2(2s_1)$	0
N <sup>14</sup> <sup>b</sup>			2.31	$0^+, 1$	0.05	0.0015	$(^{11}S_0)(2s_1)$	$(^{11}S_0)(2s_1)$	0 <sup>e</sup>	$(p_1)^2(2s_1)$	$(p_1)^2$	4/9
			3.95	$1^+, 0$	1.26	0.11	$(^{11}S_0)(2s_1)$	$^3S$	0 <sup>e</sup>	$(p_1)^2(2s_1)$	$(p_1)^2$	0 <sup>e</sup>
	8.70	$0^-, 1$	0	$1^+, 0$	46	0.42	$(^{11}S_0)(2s_1)$	$^3D$	4/81	$(p_1)^2(2s_1)$	$(p_1)^7(p_1)^3$	0
	9.17	$(2^-, 1)$	0	$1^+, 0$	10.7	0.082	$(^{11}S_0)(2s_1)$	$^3S$	10/27	$(p_1)^2(2s_1)$	$(p_1)^2$	2/3
	9.49	$2^-, 1$	3.95	$1^+, 0$	0.30	0.005	$(^{11}S_0)(2s_1)$	$^3S$	8/9	$(p_1)^2(1d_{5/2})$	$(p_1)^2$	0
	10.43	$(2^-, 1)$	0	$1^+, 0$	17	0.067	$(^{11}S_0)(2s_1)$	$^3D$	0	$(p_1)^2(1d_{5/2})$	$(p_1)^2$	0
	11.43	$\frac{1}{2}^+, \frac{1}{2}$	0	$\frac{1}{2}^-, \frac{1}{2}$	5.66	0.027	$(^{11}S_0)(2s_1)$	$^3S$	10/27	$(p_1)^2(1d_{5/2})$	$(p_1)^2$	...
	11.61	$\frac{3}{2}^+, \frac{3}{2}$	0	$\frac{3}{2}^-, \frac{3}{2}$	26.3	0.12	$(^{11}S_0)(2s_1)$	$^3P$	25/192	$(p_1)^2(2s_1)$	$(p_1)^3$	25/32
	8.33	$\frac{3}{2}^+, \frac{3}{2}$	0	$\frac{3}{2}^-, \frac{3}{2}$	0.59	0.006	$(^{11}S_0)(2s_1)$	$^3P$	...	$(p_1)^2(2s_1)$	$(p_1)^3$	...
	8.79	$\frac{1}{2}^+, \frac{1}{2}$	0	$\frac{1}{2}^-, \frac{1}{2}$	0.33	0.003	$(^{11}S_0)(2s_1)$	$^3P$	...	$(p_1)^2(2s_1)$	$(p_1)^3$	...
	9.77	$(\frac{3}{2}, \frac{3}{2}^+)$	0	$\frac{3}{2}^-, \frac{3}{2}$	$276/2J+1$	$0.34/2J+1$	$(^{13}S_1)(2s_1)$	$^2P$	...	$(p_1)^2(2s_1)$	$(p_1)^3$	...
	13.09	$1^-, 1$	0	$0^+, 0$	150	0.40	$(^{13}S_1)(2s_1)$	$^2P$	1/6 or 1/12	$(p_1)^2(2s_1)$	$(p_1)^3$	1/9 or 4/9
			6.05	$0^+, 0$	$< 0.2$	$< 0.003$	$(^{13}S_1)(2s_1)$	$^2P$	4/9	$(p_1)^2(2s_1)$	$(p_1)^4$	4/9
							$(1p)^{-2}(2s, 1d)$		0	$(1p)^{-2}(2s, 1d)$		0

<sup>a</sup> References to the data used in the table are to be found in the published compilations (AJ52, AJ53, AJ59, and especially W156b).  
<sup>b</sup> The 9.18 state in N<sup>14</sup> has been assigned spin 2<sup>+</sup> [S. Hanna and L. Meyer-Schutzmeister, Phys. Rev. 115, 986 (1959)].  
<sup>c</sup> All uncertain spin assignments are bracketed ( ).  
<sup>d</sup> The *L-S* coupling implied in columns 8 to 10 is not pure *L-S* coupling of the whole system but only *L-S* coupling of the "core" of "like" particles. The "odd" particle in the states of nonnormal parity is always assumed to be spin-orbit coupled before being coupled to the core [see Sec. II.2(b), Eq. (67)].  
<sup>e</sup> The entry is zero by virtue of the isotopic spin selection rule for *E1* transitions (McD55) and so does not provide any test of a specific nuclear model such as the shell model used here.  
<sup>f</sup> The absence of an entry in the theoretical columns implies that the evaluation of the entry is too ambiguous.

to that of a corresponding single-particle transition:  $\Lambda^2 = \Gamma/\Gamma_p$ . In the same discussion, a conventional definition of "single-particle transition" was made in which the matrix elements (assuming an oscillator well) are essentially given by the integrals  $I(\mathcal{L}, 1, 1')$  of Table III. The final formula for  $\Lambda^2$  in terms of  $\Gamma$  and these integrals was given at the end of the section. The entries of column 7 in Table XI are obtained from direct use of this formula, assuming a value for the oscillator-well size constant  $b$  of  $1.65 \times 10^{-13}$  (Ca54b, Ja54). Columns 10 and 13 of Table XI give the theoretical values of  $\Lambda^2$  based on the assumption of  $L-S$  and  $j-j$  coupling, respectively, and these are to be compared with column 7. For the states of nonnormal parity, i.e., those containing an "odd" particle, the odd particle is always assumed to be spin-orbit coupled before being coupled on to the "core," irrespective of whether  $L-S$  and  $j-j$  coupling applies inside the core.

The qualitative conclusions that we can draw in comparing the observed and predicted transitions are much the same as for the  $M1$  transitions in Table VIII. The theoretical predictions vary greatly from case to case as do the experimental values. Also in some cases, there is a certain correlation between the observed values and the pairs of predicted ones that may be taken to corroborate our simplified shell model for nonnormal parity states. (Impurities in a wave function of the simplified model type have a more serious effect on the prediction of  $E1$  widths than on the prediction of nucleon widths of nonnormal parity states, since admixtures of other wave functions of the simplified model give rise to interference terms in the former case but not in the latter case. Thus, we do not expect the predictions of the model to be so good for  $E1$  widths.)

The  $E3$  transition in  $O^{16}$  that we mentioned previously is between the 6.14 ( $3-$ ) state and the ground state. The width of the transition is  $\Gamma = 0.7(\pm 0.3)10^{-4}$  ev (De55, Ko58), which corresponds to  $\Lambda^2(E3) = 6(\pm 3)$  (if the single-particle matrix element is evaluated for a  $1d \rightarrow 1p$  transition using Table III with  $b = 1.65 \times 10^{-13}$  cm). In  $j-j$  coupling  $(1d_{3/2})(1p_{3/2})^2 \rightarrow (1p_{3/2})^4$ ,  $\Lambda^2 = 5/21$ ; in  $L-S$  coupling ( $^{11}F \rightarrow ^{11}S$ ),  $\Lambda^2 = 5/7$ . Both theoretical values are considerably less than the experimental ones. In extracting the experimental values of  $\Lambda^2$ , the single-particle matrix element may have been underestimated but surely not so much as to account for the required factor of 10 or so. Some suggestion has been made for the occurrence of radiation from the neighborhood of the 7.48 state in  $B^{10}$  which would be  $E3$  in nature if the state were responsible (De54a). However, the  $\Lambda^2$  value for the transition would be  $\gg 10$ , and so the suggestion is probably incorrect.

Several thermal-neutron capture cross sections are known (Table XII). If the  $s$ -wave levels responsible for capture and their neutron reduced widths could be established, these cross sections would yield many radiation widths, mostly  $E1$ . However, an analysis of the capture in  $Li^8$  (Th51) and  $C^{12}$  (Th52, Wo54) indi-

 TABLE XII. Thermal-neutron cross sections of nuclei in the  $1p$  shell.\*

Compound nucleus	Coherent scattering cross section in barns	Total scattering cross section in barns	Thermal capture cross section in millibarns	Final states and their percentage capture
$Li^7$	$\sim 6$	...	$28 \pm 8$	
$Li^8$ <sup>b</sup>	$0.80 \pm 0.05$	$1.5 \pm 0.4$	$33 \pm 5$	
$Be^{10}$	$6.04 \pm 0.03$	$6.04 \pm 0.03$	$9.0 \pm 0.5$	0(0+):75 3.37(2+):25
$B^{11}$	...	$3.3 \pm 0.5$	$450 \pm 200$	
$B^{12}$	...	3.76	<2	
$C^{13}$	...	$4.70 \pm 0.05$	4.7	0( $\frac{1}{2}-$ ):70 3.68( $\frac{3}{2}-$ ):30 3.09( $\frac{1}{2}+$ ):<10 3.86( $\frac{3}{2}+$ ):<6
$C^{14}$	$4.5 \pm 0.6$	$5.5 \pm 1.0$	$0.9 \pm 0.2$	
$N^{15}$	$11.1 \pm 0.3$	$11.4 \pm 0.5$	$80 \pm 20$	0( $\frac{1}{2}-$ ):20 5.30(+):40 6.33( $\frac{3}{2}-$ ):17 7.16(+):4 7.32(+):12 8.28(+):4 9.16:2

\* References to the data are to be found in the compilations (Aj59, Aj55), except for the limit of 2 mb in the case of  $B^{12}$  (Harwell, unpublished work) and the thermal capture cross sections of  $Li^8$ ,  $B^{10}$ ,  $N^{14}$  (Ba57).  
<sup>b</sup> In  $Li^8$  the coherent scattering amplitude is observed to be negative. In other cases the sign is not known.

cates that considerable  $E1$  capture can occur outside the interaction radius in these and probably other cases. Such capture interferes with the usual internal contribution and thereby makes the extraction of the latter from the data uncertain. This may explain in apparent paradox in the case of capture in  $C^{13}$ . If we assume that the  $\frac{1}{2}+$  (3.09) state is responsible for this capture (Ki54), the ratio of the  $E1$  widths for the  $\frac{1}{2}+ \rightarrow \frac{1}{2}-$  and  $\frac{1}{2}+ \rightarrow \frac{3}{2}-$  transitions is 7:3 or, if we extract the  $E^3$  factor, 1:25. Now if there is no  $T_1=1$  parentage in the  $1+$  state (as would be implied by our simplified shell model, which says that  $C^{12}$  is its unique parent), we expect this ratio to be the same in  $N^{13}$ . The two relevant  $E1$  widths in  $N^{13}$  are known, and the ratio (when corrected for the  $E^3$  factor and the spin of the emitting state in the  $\frac{1}{2}+ \rightarrow \frac{3}{2}-$  transition) is 1:1. Thus, there is a discrepancy of 25 in the two ratios. A freak interference between the internal and external contributions in either  $N^{13}$  or  $C^{13}$  may be responsible.

#### (d) Concluding Remarks

The present section has established that we can usefully exploit the simplified shell model of nonnormal parity states as a guide for analyzing the data. Considering that the model has little theoretical foundation as mentioned, its usefulness is somewhat surprising. It is significant that its best results are achieved for mass 13 for the states in which a single particle is coupled to the states of the mass 12 "core" and the worst for mass 15 with a mass 14 "core." Since the states of  $C^{12}$  are widely spaced ( $\sim 4$  Mev or so), the core has a special stability against being excited or polarized. This fact certainly contributes strongly to the success of the model in this case. We have seen that the triplet of  $\frac{3}{2}+$

states near 7 Mev actually enables us to estimate the power of the interactions between states. The mixing of pure states within an Mev or so of each other is of the order of 20% which is remarkably small. The situation we are discussing here has some correspondence with the fine structure interpretation of the complex-potential model of heavy nuclei (La55b). According to this model a zero-order single-particle level is mixed into the multitude of surrounding states but only over a limited energy range. In light nuclei, such as mass 13, there are very few states to do the sharing or absorbing, so few in fact that we can study levels and their sharing ability on an individual basis. However, the mixing range is just about the same in both situations, namely, a Mev or so.

It is certainly very desirable that a theoretical examination of the simplified shell model be undertaken in some special cases in order to find out whether the model is implied by the usual shell-model assumptions for normal parity states or whether some new assumptions are needed. Probably the nonnormal parity states can be more informative about the nature of the forces coupling nucleons to each other than the normal parity states. In atoms, for instance, where forces are long range, our model is a recognized one and can be shown to be consistent with normal Coulomb forces, etc. In the nucleus, forces are taken to be of short range in discussing normal parity states. For nonnormal parity states, it may be that forces have to be taken with longer range to justify the simple model and so fit the observed data. Such speculation can be checked only by calculation, and calculations have been made so far only for the mass 15 systems (Ha57b; see "Mass 15" above).

### 3. NUCLEI IN THE MASS RANGE $16 < A \leq 40$

There is a growing amount of reaction data on nuclei between oxygen and calcium, that is, nuclei of the ( $2s$ ,  $1d$ ) shell (En54, En57). The data on widths for nucleon, alpha, and radiation processes are listed in Tables XIII, XIV, and XV. On attempting any detailed theoretical analysis of most of this data, one soon finds this to be impracticable in view of the ambiguities in the identification of individual states. Because of this, most of the ensuing discussion of the tables consists of qualitative remarks. We first make some general observations about normal and nonnormal parity states, and then we discuss some specific entries in the tables in the light of these observations.

#### (a) Normal Parity States

The mass 17 nuclei,  $O^{17}$  and  $F^{17}$ , exhibit three states corresponding to the expected  $1d_{3/2}$ ,  $2s_{1/2}$ , and  $1d_{5/2}$  single-particle states. In  $O^{17}$ , these are the ground, 0.87, and 5.08 states, respectively (Ad53). The identification of these states as the single-particle states is supported by their positions (Fo58), their spins, the  $M1$  and  $E2$

moments of the ground state of ( $O^{17}$ ), the strength (large reduced width) of the  $2s_{1/2}$  state [as revealed by its strong influence on the  $O^{16}+p$  and  $O^{16}+n$  scattering at low energy (La52, Th52)], and the large reduced width of the  $1d_{3/2}$  state as measured in  $O^{17}$  by the  $O^{16}+n$  resonance scattering. The only experimental fact in apparent disagreement with the assignment of the single-particle states is the width of the  $\frac{1}{2}+ \rightarrow \frac{5}{2}+E_2$  transition in  $O^{17}$ . This transition is theoretically forbidden between the two single-neutron states prescribed by the shell model [there is not even a contribution from the recoiling  $O^{16}$  core provided that properly antisymmetrized wave functions are used (El55b)]; experimentally, the transition is allowed (Th53). Recently, the observed width has been fitted simultaneously with the observed  $E2$  moment of the ground state by modifying the shell-model picture to include weak collective effects [weak excitation of a quadrupole phonon oscillation in the  $O^{16}$  core (El55b, Ba56a, Am57)].

Recent successful shell-model work on the mass 18 and mass 19 systems (Re55, El55a) show that the structures of low-lying individual states of even these two- and three-particle nuclei are quite complicated in a shell-model description. We may expect that, for highly excited states and for heavier nuclei, the states are even more complicated. Qualitatively this leads one to expect small reduced widths for nucleon channels since the most likely overlap between any given compound and final states is a small one. This expectation is confirmed by the smallness of the  $s$ - and  $d$ -wave reduced widths in Table XIII. In fact, the smallness of  $\theta^2$  and the closeness of the spacing of many levels in Table XIII means that one may begin to apply statistical considerations. In several nuclei, one can make order-of-magnitude estimates of  $\gamma^2/D$ , the strength functions, and confirm that the values are of the order of the predicted value  $10^{-1}$  (La57).

The striking success of the strong-coupling model of Bohr and Mottelson (Bo53) for the mass 25 system (Li56, Li58) has led to an examination of the low-lying states of  $F^{19}$  with the same model (Pa57). The simplest considerations with the strong-coupling model already give qualitative agreement with the observed spectrum. More refined considerations, which take into account the  $j$  mixing of single-particle states due to the deformation (Ni55) and  $K$  mixing due to the rotation-particle coupling (Ke56), give very good agreement with observed data [even including the large width of the  $E2$  transition  $0.197 (\frac{5}{2}+) \rightarrow 0(\frac{1}{2}+)$ , which the shell-model calculations fail to give unless supplemented by collective effects (El55a, Ba56a)]. It is an impressive fact that the predictions with the strong-coupling model can be made in a few hours, whereas the shell-model calculations take months to perform. In spite of the absence of apparent similarity between the two models, they do ultimately make nearly the same predictions. This fact suggests an underlying similarity between the two; in

other words, the configuration mixing between the  $d_{3/2}$ ,  $d_{5/2}$ , and  $s_{1/2}$  orbits that results from the complicated shell-model calculations is essentially the simple type of mixing that is induced by deforming the spherical potential well into a spheroidal shape. Recently, Elliott has examined this situation (El58) and has exposed the connection between the two models.

This discovery of the applicability of the strong-coupling model does not imply any revision of the above statement that little may be said of the individual resonance (i.e., unbound) levels in nuclei like  $F^{19}$ . However, it does mean that one may now make predictions about resonance levels of nuclei like  $Al^{25}$  where these levels occur at low excitations. From the shell-model point of view, it is effectively impossible to make predictions about  $Al^{25}$  which has nine loose particles outside the closed shell  $O^{16}$ . With the strong-coupling model, in contrast, predictions are immediate (see Sec. II.3). All the lowest states are members of rotational bands, the internal wave functions consist of the closed ( $\omega$ ) shell  $Mg^{24}$  and a single particle.

So far we have mentioned only "single-particle" states as opposed to "single-hole" states. Certain evidence for the existence of the latter type states is found in the nuclei  $O^{17}$  and  $F^{19}$ . The interpretation of the 0.114 ( $\frac{1}{2}^-$ ) state in  $F^{19}$  as a  $1p_{3/2}$ -hole state leads to the correct energy of this state when we make use of the simplified model discussed previously. It has been suggested (Ch54) that the odd-parity states in  $O^{17}$  should be regarded as states of three holes  $(1p_{3/2})^{-3}$ , but one may also try a single hole,  $(1p_{3/2})^{-1}$ , interpretation. The first four states of odd parity in  $O^{17}$  are at 3.06 ( $\frac{1}{2}^-$ ), 3.85 ( $\frac{3}{2}^-$ ), 4.56 ( $\frac{5}{2}^-$ ), and 5.23. The last state has been found recently as a weak group in the  $O^{16}(d,p)O^{17}$  reaction with a stripping-type angular distribution best fitted with  $l_n=3$  (Pa55a). The ground state of  $F^{18}$  is  $1+$ ,  $T=0$  and, according to the shell-model theory (El55a), there should be a state about 1 Mev higher with  $J=3+$ ,  $T=0$ . If we consider making a  $1p_{3/2}$  hole in these two states, then we expect to produce four states of spins  $\frac{1}{2}$ ,  $\frac{3}{2}$ , and  $\frac{5}{2}$ ,  $\frac{7}{2}$ . If we identify the above four states with these, then their energies are only about 2 Mev below the predicted positions. In addition, notice that all four states have small reduced widths as expected (Table XIII), according to the present interpretation. (The 5.23 state is so sharp that it is not found in the  $O^{16}+n$  scattering.)

### (b) Nonnormal Parity States

First we discuss the approach to these states in terms of the shell model; it is recalled that, in discussion of nuclei in the mass-range  $4 < A \leq 16$ , it was found that proper shell-model calculations for states of nonnormal parity required prohibitive labor. In the case of the mass range  $16 < A \leq 40$ , even most normal parity states have not been treated because of the labor involved. Consequently, we are again forced to adopt the sim-

plified shell model for discussion of low-lying non-normal parity states. The only nuclei in which such states are found are  $Na^{21}$ ,  $Al^{25}$ ,  $P^{29}$ , and  $Cl^{33}$  (see Table XIII). The best example is  $Al^{25}$ , as investigated in the proton bombardment of  $Mg^{24}$  (Mo51, Ko52, Li56). In this nucleus, the simplified model seems to be readily applicable. The levels at 3.08 ( $\frac{3}{2}^-$ ), 3.72 ( $\frac{7}{2}^-$ ), and 3.85 ( $\frac{1}{2}^-$ ) all have large widths and would appear to be the expected  $2p_{3/2}$ ,  $1f_{7/2}$ ,  $2p_{3/2}$  single-particle states. (In contrast with these levels, the normal parity levels at 3.88, 4.22, and 4.60 have very small widths; however, the normal parity states at 2.51 and 2.70 probably have larger ones.) The nuclei  $Na^{21}$ ,  $P^{29}$ , and  $Cl^{33}$  also exhibit "strong"  $p$ -wave states.

We recall that the simplified model of nonnormal parity states was introduced because the usual shell-model calculations are much too complicated to be of practical use for such states. In contrast, the strong coupling model deals with states of normal and non-normal parity with equal facility; in particular, it predicts that the lowest states of either parity in a nucleus of  $A$  particles should have large reduced widths for channels involving the ground state of the nucleus of  $(A-1)$  particles. [Referring to Sec. II.3, the predicted values of  $\theta^2/\theta_p^2$  for the levels of a compound nucleus consisting of a closed-shell nucleus plus one particle are  $2(2J+1)^{-1}$ , where  $J$  is the spin of the compound state.] From this point of view, we may say that the strong-coupling model provides an alternative basis for the large reduced widths of nonnormal parity states, a basis which has the merit of not requiring special assumptions over and above those for normal parity states. Furthermore, the observed widths, although large, are usually rather less than  $\theta^2/\theta_p^2=1$  or  $\frac{1}{2}$  which is predicted by the simplified shell model. This is in qualitative accord with the extra factors like  $2(2J+1)^{-1}$  implied by the strong-coupling model. Yoshida (Yo54) has reinterpreted the observed widths of nonnormal parity states of nuclei with  $A < 16$  in terms of the strong-coupling model and found reasonable agreement. In the following discussion, we describe a similar application to nuclei in the mass range  $16 < A \leq 40$ .

### (c) Nucleon Channels

From considerations of excitation energy and level density, the only widths in Table XIII about which individual predictions can possibly be made are those of  $O^{17}$  and  $F^{17}$ ,  $Na^{21}$ ,  $Al^{25}$ ,  $P^{29}$ , and  $Cl^{33}$ , i.e., the  $(4n+1)$ -type nuclei.

The nuclei  $O^{17}$  and  $F^{17}$  presumably must be discussed in terms of the shell model since it is unlikely that nuclei so close to the closed shell  $O^{16}$  have a permanent deformation. On this basis, the 5.08-Mev state of  $O^{17}$  is the expected  $d_{3/2}$  single-particle state (as is the 4.6 state of  $F^{17}$ ). This assignment is supported by the large widths. All the other states (which have small widths) must be attributed to core excitation.

TABLE XIII. Nucleon widths of states in the mass range  $16 < A \lesssim 40$ .

Compound nucleus	Excitation in Mev	Spin and parity	Channel: residual nucleus + nucleon + l	Obs channel width (kev in center of mass)	Obs value of $\theta^2$ <sup>b</sup>	Reference <sup>c</sup>
O <sup>17</sup>	4.56	$\frac{3}{2}^-$	O <sup>16</sup> +n+1	42	0.057	
	5.08	$\frac{1}{2}^+$	O <sup>16</sup> +n+2	95	0.39	
	5.39	$\frac{1}{2}^-$	O <sup>16</sup> +n+1	33	0.014	
	5.94	$\frac{3}{2}^-$	O <sup>16</sup> +n+1	28	0.0084	
	6.37	$\frac{1}{2}^+$	O <sup>16</sup> +n+0	110	0.020	
	7.28	$\frac{1}{2}^+$	O <sup>16</sup> +n+2	210	0.075	
	7.72	$\frac{1}{2}^-$	O <sup>16</sup> +n+1	750	0.120	
	8.25	$\frac{3}{2}^-$	O <sup>16</sup> +n+1	260	0.037	
F <sup>17</sup>	3.10	$(\frac{1}{2}^-)$ <sup>a</sup>	O <sup>16</sup> +p+1	18.7	0.010	
	3.86	$(\frac{3}{2}^-)$	O <sup>16</sup> +p+3	<3.3	<0.018	
	4.5	$(\frac{1}{2}^-)$	O <sup>16</sup> +p+1	~400	~0.08	
	4.6	$(\frac{3}{2}^+)$	O <sup>16</sup> +p+2	~350	~0.16	
O <sup>18</sup>	8.22	2+	O <sup>17</sup> +n+0	0.014	9×10 <sup>-6</sup>	We58
	8.29	3-	O <sup>17</sup> +n+1	0.83	0.0024	
F <sup>20</sup>	6.626	2-	F <sup>19</sup> +n+1	0.3	0.015	Ne55
	6.647	1-	F <sup>19</sup> +n+1	1.42	0.033	Bl56
	6.70	(1-)	F <sup>19</sup> +n+(1)	(10)	(0.085)	
Ne <sup>20</sup>	13.19	1+	F <sup>19</sup> +p+0	0.045	0.057	Ba55a
			F <sub>1</sub> <sup>19</sup> +p+1	<0.0005	<0.21	Ba55c
			F <sub>2</sub> <sup>19</sup> +p+2	<0.0001	<10 <sup>8</sup>	We55
	13.43	(2-)	F <sup>19</sup> +p+1	0.043	0.0057	
			F <sub>1</sub> <sup>19</sup> +p+2	<0.5	<0.45	
			F <sub>2</sub> <sup>19</sup> +p+1	<0.5	<2.2	
	13.51	1+	(as 13.19)	7.3	0.14	
				0.046	0.009	
				0.0005	0.006	
	13.68	0+	F <sup>19</sup> +p+0	23	0.16	
			F <sub>1</sub> <sup>19</sup> +p+1	~0.05	~0.0021	
			F <sub>2</sub> <sup>19</sup> +p+2	<0.01	<0.014	
	13.70	2-	(as 13.43)	1.1	0.022	
				<0.002	<0.001	
				0.57	0.040	
13.76	1+	(as 13.19)	1.4	0.0066		
			3.0	0.075		
			<0.020	<0.01		
14.15	2-	(as 13.43)	0.3	0.001		
			0.3	0.014		
			0.6	0.0037		
14.17	2-	(as 13.43)	2.5	0.0079		
			0.7	0.029		
			1.4	0.0084		
14.22	1+	(as 13.19)	12.4	0.014		
			2.2	0.0084		
			<0.035	<0.0017		
Ne <sup>21</sup>	7.62	$\frac{3}{2}^-$	Ne <sup>20</sup> +n+1	14	0.009	Co59
	7.98	$\frac{1}{2}^-$	Ne <sup>20</sup> +n+1	6	0.003	Si58
	8.00	$\frac{1}{2}^-$	Ne <sup>20</sup> +n+1	32	0.016	
	8.06	$(\frac{3}{2}^+)$	Ne <sup>20</sup> +n+2	(9)	0.015	
	8.30	$\frac{3}{2}^-$	Ne <sup>20</sup> +n+1	27	0.012	
	8.36	$\frac{1}{2}^+$	Ne <sup>20</sup> +n+2	10	0.012	
	8.60	$\frac{1}{2}^+$	Ne <sup>20</sup> +n+2	32	0.03	
	8.66	$\frac{3}{2}^-$	Ne <sup>20</sup> +n+1	48	0.02	
Na <sup>21</sup>	4.18	$\frac{3}{2}^-$	Ne <sup>20</sup> +p+1	169	0.32	
	4.31	$\frac{1}{2}^+$	Ne <sup>20</sup> +p+2	6	0.048	Ha55a
	4.49	$\frac{1}{2}^+$	Ne <sup>20</sup> +p+2	16	0.095	Ha55b
	5.48	$\frac{3}{2}^+$	Ne <sup>20</sup> +p+0	84	0.026	
			Ne <sup>20</sup> +p+2	21	0.72	
	5.85	$\frac{3}{2}^-$	Ne <sup>20</sup> +p+1	20	0.0083	
			Ne <sup>20</sup> +p+1(3)	4	0.0072(0.48)	
	6.10	$(\frac{5}{2}, \frac{7}{2})^-$	Ne <sup>20</sup> +p+3	0.23	0.0012	
			Ne <sup>20</sup> +p+1(3)	6	0.0072(0.36)	
	6.53	$(\frac{3}{2}, \frac{5}{2})^+$	Ne <sup>20</sup> +p+2	~140	~0.0835	
Ne <sup>20</sup> +p+0			8	0.0036		

<sup>a</sup> All uncertain entries are bracketed ( ).  
<sup>b</sup> In extracting the dimensionless reduced widths, a radius of  $1.45(A^{1/3}+1) \times 10^{-13}$  cm was used throughout.  
<sup>c</sup> For a given nucleus the references usually apply to several levels. As a rule, references are given only when they are not mentioned in the published compilations (En54, En57).  
<sup>d</sup> Sixty-six levels are reported in the excitation energy range 7.7 to 8.2 Mev [C. T. Hibdon, Phys. Rev. 114, 179 (1959)].



TABLE XIII.—Continued.

Compound nucleus	Excitation in Mev	Spin and parity	Channel: residual nucleus + nucleon + l	Obs channel width (kev in center of mass)	Obs value of $g^2 b$	Reference <sup>a</sup>
Na <sup>24</sup>	6.96	(2-)	Na <sup>23</sup> +n+(0)	0.40	0.0024	Ly58
	7.01	3-	Na <sup>23</sup> +n+1	0.78	0.015	
	7.15	1(-)	Na <sup>23</sup> +n+(1)	5	0.016	Ne55
					0.040	B156
	7.16	0(-)	Na <sup>23</sup> +n+(1)	14	0.017	
	7.19	1, 2(-)	Na <sup>23</sup> +n+(1)	7		
	7.24	1+	Na <sup>23</sup> +n+0	4	0.0022	
	7.33	1(-)	Na <sup>23</sup> +n+(1)	22	0.030	
	7.39	1	Na <sup>23</sup> +n+(1,2)	0	(0.011, 0.11)	
	7.47	(1+)	Na <sup>23</sup> +n+(0)	37	0.015	
Mg <sup>24</sup>	11.983	2-	Na <sup>23</sup> +p+1	≤ 0.8	≤ 250	Ne54
	12.177	1+	Na <sup>23</sup> +p+0	≤ 0.8	≤ 0.4	St54a
	12.256	3-(2-)	Na <sup>23</sup> +p+1	~2	~2	St54b
	12.334	3+	Na <sup>23</sup> +p+2	≤ 1	≤ 4	Se53
	12.382	0-	Na <sup>23</sup> +p+1	~7	~1.2	Ba56b
	12.451	1-	Na <sup>23</sup> +p+1	~4	~0.4	Pr56
	12.468	2+	Na <sup>23</sup> +p+0	~3	~0.06	En57
	12.501	4+	Na <sup>23</sup> +p+2	≤ 1	≤ 0.7	
	12.527	1+(2+)	Na <sup>23</sup> +p+0	~8	~0.12	
	12.571	2+	Na <sup>23</sup> +p+0	~3	~0.04	
	12.657	3+(2+)	{Na <sup>23</sup> +p+1	<0.8	<0.02	
			{Na <sup>23</sup> +p+1	0.02	0.026	
	12.666	2-	Na <sup>23</sup> +p+1	6	0.24	
	12.734	2+	{Na <sup>23</sup> +p+0	<7.9	<0.05	
			{Na <sup>23</sup> +p+0	0.012	0.002	
	12.804	1-(2+)	{Na <sup>23</sup> +p+0	<1.2	<0.015	
			{Na <sup>23</sup> +p+0	0.06	0.009	
	12.814	1+	Na <sup>23</sup> +p+0	1.6	0.007	
	12.844	(2-)	Na <sup>23</sup> +p+1	<0.3	<0.004	
	12.849	(3+)	Na <sup>23</sup> +p+2	0.3	0.03	
	12.893	1+	{Na <sup>23</sup> +p+0	0.3	0.001	
			{Na <sup>23</sup> +p+0	0.03	0.018	
	12.921	1-	Na <sup>23</sup> +p+1	7	0.05	
	12.953	3+	Na <sup>23</sup> +p+2	<2.1	<0.1	
	12.996	0-	Na <sup>23</sup> +p+1	<1.2	<0.007	
	13.028	3+	{Na <sup>23</sup> +p+2	0.35	0.01	
			{Na <sup>23</sup> +p+0	0.021	0.0003	
	13.048	4+	Na <sup>23</sup> +p+2	<0.3	<0.01	
	13.087	3-	{Na <sup>23</sup> +p+1	9	0.04	
			{Na <sup>23</sup> +p+1	0.43	0.014	
Mg <sup>25</sup>	7.40	( $\frac{3}{2}$ -)	Mg <sup>24</sup> +n+1	8	0.080	Ne55
	7.58	$\frac{3}{2}$ -	Mg <sup>24</sup> +n+1	~80	~0.17	B156
	7.73	$\frac{3}{2}$ -	Mg <sup>24</sup> +n+1	~30	~0.038	Ta56
Al <sup>25</sup>	3.08	$\frac{3}{2}$ -	Mg <sup>24</sup> +p+1	1.5	0.19	
	3.72	-	Mg <sup>24</sup> +p+3	0.3	0.23	
	3.85	-	Mg <sup>24</sup> +p+1	36	0.16	Cr56b
	3.88	+	Mg <sup>24</sup> +p+2	0.1	0.004	Ag56,
	4.22	$\frac{3}{2}$ +	{Mg <sup>24</sup> +p+2	~0.17	~0.002	Li56
			{Mg <sup>24</sup> +p+0	~0.04	~0.016	
	4.60	$\frac{5}{2}$ +	{Mg <sup>24</sup> +p+2	~0.21	~0.002	
			{Mg <sup>24</sup> +p+0	~0.27	~0.004	
5.31	$\frac{3}{2}$ -	Mg <sup>24</sup> +p+1	<200	<0.12		
5.80	( $\frac{3}{2}$ , $\frac{5}{2}$ +) )	Mg <sup>24</sup> +p+(2)	≤ 10	≤ 0.011		
Al <sup>26</sup> d			Al <sup>27</sup> +n+(1)			
			Al <sup>27</sup> +n+0			
			Al <sup>27</sup> +n+(0)			
Si <sup>29</sup>	8.66	$\frac{1}{2}$ +	Si <sup>28</sup> +n+0	~80	0.058	Ne55
	8.92	$\frac{3}{2}$ -	Si <sup>28</sup> +n+1	~15	0.014	
P <sup>29</sup>	4.33	$\frac{3}{2}$ -	Si <sup>28</sup> +p+1	50	0.45	Ne56
S <sup>32</sup>	10.688	1-	P <sup>31</sup> +p+1	≤ 24	≤ 0.16	Go54
	10.820	1-	P <sup>31</sup> +p+1	≤ 24	≤ 0.12	Pa55b
	10.910	1-	P <sup>31</sup> +p+1	≤ 5	≤ 0.02	
S <sup>33</sup>	8.753	$\frac{1}{2}$ +	S <sup>32</sup> +n+0	18	0.018	
	8.841	( $\frac{3}{2}$ , $\frac{5}{2}$ )-	S <sup>32</sup> +n+(1)	(2)	(0.006)	
	8.910	( $\frac{1}{2}$ , $\frac{3}{2}$ )-	S <sup>32</sup> +n+(1)	(3)	(0.006)	
	8.926	( $\frac{3}{2}$ , $\frac{5}{2}$ )-	S <sup>32</sup> +n+(1)	(3)	(0.006)	

TABLE XIII.—Continued.

Compound nucleus	Excitation in Mev	Spin and parity	Channel: residual nucleus + nucleon + $l$	Obs channel width (kev in center of mass)	Obs value of $\theta^2$ <sup>b</sup>	Reference <sup>c</sup>
S <sup>33</sup>	9.009	$\frac{1}{2}+$	S <sup>32</sup> +n+0	12	0.006	La56
	9.312	$(\frac{5}{2})$	S <sup>32</sup> +n+ (2)	(1)	(0.011)	
	9.320	$\frac{1}{2}+$	S <sup>32</sup> +n+0	12	0.005	
	9.348	$\frac{1}{2}(\frac{3}{2})-$	S <sup>32</sup> +n+1	5	0.004	
	9.365	$\frac{1}{2}(\frac{3}{2})-$	S <sup>32</sup> +n+1	5	0.004	
Cl <sup>33</sup>	4.13	$\frac{3}{2}-$	S <sub>0</sub> <sup>32</sup> +p+1	8	0.064	Go55a
	4.52	$\frac{1}{2}-$	S <sub>0</sub> <sup>32</sup> +p+1	55	0.18	
	4.78	$\frac{3}{2}(\frac{7}{2})-$	S <sub>0</sub> <sup>32</sup> +p+3	0.25	0.014	En57
	5.01	$\frac{3}{2}-$	S <sub>0</sub> <sup>32</sup> +p+1	6	0.009	
			S <sub>1</sub> <sup>32</sup> +p+1	~0.0015	~0.7	
	5.09	$\frac{1}{2}-$	S <sub>0</sub> <sup>32</sup> +p+1	360	0.51	Ol58
	5.10	$(\frac{3}{2}, \frac{7}{2})-$	S <sub>0</sub> <sup>32</sup> +p+3	<0.5	<0.014	
			S <sub>1</sub> <sup>32</sup> +p+1	~0.001	~0.014	
	5.11	$\frac{3}{2}+$	S <sub>0</sub> <sup>32</sup> +p+2	1.5	0.006	
			S <sub>1</sub> <sup>32</sup> +p+0	~0.0018	~0.0024	
	5.28	$\frac{5}{2}-$	S <sub>0</sub> <sup>32</sup> +p+3	0.29	0.006	
			S <sub>1</sub> <sup>32</sup> +p+1	0.05	0.15	
	5.38	$\frac{5}{2}+$	S <sub>0</sub> <sup>32</sup> +p+2	0.43	0.0012	
			S <sub>0</sub> <sup>32</sup> +p+0	0.01	0.0035	
	5.46	$\frac{1}{2}+$	S <sub>0</sub> <sup>32</sup> +p+0	32	0.020	
			S <sub>1</sub> <sup>32</sup> +p+2	<0.01	<0.015	
	5.56	$\frac{7}{2}-$	S <sub>0</sub> <sup>32</sup> +p+3	0.40	0.0045	
			S <sub>1</sub> <sup>32</sup> +p+1	0.60	0.15	
5.66	$\frac{3}{2}-$	S <sub>0</sub> <sup>32</sup> +p+1	100	0.082		
		S <sub>1</sub> <sup>32</sup> +p+1	<0.08	<0.012		
5.75	$\frac{1}{2}+$	S <sub>0</sub> <sup>32</sup> +p+0	40	0.020		
		S <sub>1</sub> <sup>32</sup> +p+2	<0.01	<0.0015		
5.89	$\frac{5}{2}-$	S <sub>0</sub> <sup>32</sup> +p+3	0.84	0.0063		
		S <sub>1</sub> <sup>32</sup> +p+1	0.66	0.028		

In Na<sup>21</sup>, Al<sup>25</sup>, P<sup>29</sup>, and Cl<sup>33</sup>, there is a  $\frac{3}{2}-$  state with large width; this is interpreted on the shell model as the single-particle  $2p_{3/2}$  state which is predicted to have  $\theta^2 = \theta_p^2$ . On the strong-coupling model, the state is a member of a  $K = \frac{1}{2}-$  band from the  $(2p, 1f)$  states and  $\theta^2 = \langle \omega | j \rangle^2 \frac{1}{2} \theta_p^2$ . The factor  $\langle \omega | j \rangle^2$  depends on the extent of the deformation and the type (oblate or prolate) of deformation. From consideration of level spectra, the deformation in the case of Al<sup>25</sup> has been estimated as  $\beta = 0.25$ . This predicts that  $\theta^2 \sim 0.13 \theta_p^2$ , which compares favorably with the observed value  $\theta^2 = 0.19$  (Li56, Li58). In the case of Al<sup>25</sup>, the  $\frac{3}{2}-$  state (at 3.08 Mev) is a member of a  $K = \frac{1}{2}$  rotational band with other members at 3.73 Mev ( $\frac{7}{2}-$ ) and 3.85 Mev ( $\frac{1}{2}-$ ). The observed widths of these are  $\theta^2 = 0.23, 0.16$ , respectively, and the predicted values are  $\theta^2 = 0.17 \theta_p^2, 0.04 \theta_p^2$ .

Also in Al<sup>25</sup>, there are states at 3.88 ( $\frac{5}{2}+$ ), 4.22 ( $\frac{3}{2}+$ ), and 4.60 ( $\frac{5}{2}+$ ). The first has been assigned to a  $K = \frac{1}{2}+$  particle band and the second and third to a  $K = \frac{3}{2}+$  particle band. Theoretical widths for these levels are:  $\theta^2 = 0.05, 0.5$ , and  $0.02$ , respectively. These are much larger than the observed values. This suggests that the intrinsic nature of the last two states is not simply a closed shell (Mg<sup>24</sup>) plus a  $\omega = \frac{3}{2}+$  particle, but rather it involves excitation of the closed shells. For example, the least tightly bound state in Mg<sup>24</sup> is  $\omega = \frac{3}{2}+$ ; a nucleon may be raised from this state to the  $\omega = \frac{1}{2}+$  state making a pair of  $\omega = \frac{1}{2}+$  particles and leaving a  $\omega = \frac{3}{2}+$  hole. Rotational states based on such an intrinsic state have zero reduced width. This agrees well with the very small

observed values and also with various branching ratios (Li58). The strong coupling model gives good agreement with the reduced widths of bound levels of Mg<sup>25</sup> (Li58) and Si<sup>29</sup> (Br57) as obtained from stripping yields. Litherland also has found agreement with the widths of the bound states of the odd-odd nucleus Al<sup>28</sup> (Sh56b).

#### (d) Alpha-Particle Channels

At present, the only alpha-particle widths reported in nuclei of the mass range  $16 < A \leq 40$  are of states in the nuclei O<sup>18</sup>, F<sup>18</sup>, Ne<sup>20</sup>, Mg<sup>24</sup>. These values, given in Table XIV, are characterized by their extreme spread from the largest value  $\theta^2, 0.7$ , down to the smallest value some  $10^4$  less. As we have seen in the earlier discussion of the theoretical prediction of alpha widths, there is plenty of scope for such large variations arising from the various factors that enter the theoretical expression for  $\theta^2$ .

#### (e) Photon Channels

In Table XV we list the radiation widths that are known at present. In estimating the dimensionless ratios  $\Lambda^2$ , we have calculated the single-particle widths from the formulas of Table III assuming  $2p \rightarrow 1d$  for E1 transitions,  $1d \rightarrow 1d$  for E2 transitions, and  $b = 1.90 \times 10^{-13}$  cm (El55a). In several cases where both M1 and E2 radiation is possible between the two given states, we assume that M1 radiation dominates. For certain transitions in Al<sup>25</sup>, the ratio between the two types of

TABLE XIV. Alpha-particle widths of states of nuclei in the mass range  $16 < A \leq 40$ .

Compound nucleus	Excitation in Mev	Spin and parity	Channel: residual nucleus $+I_\alpha$	Obs channel width (kev in center of mass)	Obs value of $\theta_\alpha^2$ <sup>b</sup>	Reference <sup>c</sup>
O <sup>18</sup>	8.05	1-	C <sup>14</sup> +1	<5	<0.04	We58
	8.22	2+	C <sup>14</sup> +2	1.2	0.014	
	8.29	3-	C <sup>14</sup> +3	6.9	0.30	
F <sup>18</sup>	6.26	(2, 3, 4-) <sup>a</sup>	N <sup>14</sup> + (3)	<1.9	<1	He58a
	6.27	(1+)	N <sup>14</sup> + (0)	<3	<0.05	
	6.58	(3, 4, 5+)	N <sup>14</sup> + (4)	<0.8	<1	
	6.66	1-	N <sup>14</sup> +1	93	1.08	
	6.83	2-	N <sup>14</sup> +1	85	0.75	
Ne <sup>20</sup>	6.738	0+	O <sup>16</sup> +0	24	0.33	Ba55a
	7.182	3-	O <sup>16</sup> +3	10	0.54	
	7.218	0+	O <sup>16</sup> +0	5	0.16	We55
	7.450	2+	O <sup>16</sup> +2	10	0.71	
	7.854	2+	O <sup>16</sup> +2	3	0.009	
	13.18	1+	O <sub>2</sub> <sup>16</sup> +3	2.8	0.28	
			O <sub>3</sub> <sup>16</sup> +2	0.016	0.016	
			O <sub>4</sub> <sup>16</sup> +1	0.075	0.11	
	13.43	(2-)	O <sub>2</sub> <sup>16</sup> +2	37	0.46	
			O <sub>3</sub> <sup>16</sup> +1	<0.1	<0.008	
			O <sub>4</sub> <sup>16</sup> +2	<0.1	<0.08	
	13.51	1+	O <sub>2</sub> <sup>16</sup> +3	0.11	0.0038	
			O <sub>3</sub> <sup>16</sup> +2	0.0004	7×10 <sup>-6</sup>	
			O <sub>4</sub> <sup>16</sup> +1	0.025	0.0041	
	13.68	0+	O <sup>16</sup> +0	0.033	8.5×10 <sup>-4</sup>	
	13.70	2-	O <sub>1</sub> <sup>16</sup> +0	0.005	1.1×10 <sup>-3</sup>	
			O <sub>2</sub> <sup>16</sup> +2	2.4	0.016	
			O <sub>3</sub> <sup>16</sup> +1	0.85	0.022	
			O <sub>4</sub> <sup>16</sup> +2	0.30	0.051	
	13.76	1+	O <sub>2</sub> <sup>16</sup> +3	2.8	0.049	
			O <sub>3</sub> <sup>16</sup> +2	0.100	0.0051	
			O <sub>4</sub> <sup>16</sup> +1	0.78	0.036	
	14.148	2-	O <sub>2</sub> <sup>16</sup> +2	1.8	0.0054	
			O <sub>3</sub> <sup>16</sup> +1	0.45	0.003	
			O <sub>4</sub> <sup>16</sup> +2	1.05	0.031	
	14.173	2-	O <sub>2</sub> <sup>16</sup> +2	9.1	0.022	
			O <sub>3</sub> <sup>16</sup> +1	0.84	0.0044	
			O <sub>4</sub> <sup>16</sup> +2	0.52	0.011	
14.221	1+	O <sub>2</sub> <sup>16</sup> +3				
		O <sub>3</sub> <sup>16</sup> +2				
		O <sub>4</sub> <sup>16</sup> +1				
			≤0.04	≤0.2		
Mg <sup>24</sup>	12.256	3-(2-)	Ne <sup>20</sup> +3	~0.2	~0.0063	Ne54 St54a St54b Ba56d Pr56
	12.451	1-	Ne <sup>20</sup> +1	~1	~0.0049	
	12.468	2+	Ne <sup>20</sup> +2	~2	~0.018	
	12.571	2+	Ne <sup>20</sup> +2	2	0.015	
	12.657	3-(2+)	Ne <sub>1</sub> <sup>20</sup> +1	0.011	0.033	
	12.734	2+	Ne <sub>1</sub> <sup>20</sup> +0	0.006	0.0056	
	12.777	0+	Ne <sup>21</sup> +0	30		
	12.804	1-(2+)	Ne <sub>1</sub> <sup>20</sup> +1	0.053	0.055	
	12.893	1+	Ne <sub>1</sub> <sup>20</sup> +2	0.027	0.036	
	12.921	(1-)	Ne <sub>1</sub> <sup>20</sup> +1	0.021	0.0009	
	13.028	3+	Ne <sub>1</sub> <sup>20</sup> +2	<0.0006	<0.0002	
	13.087	3-	Ne <sub>1</sub> <sup>20</sup> +1	0.007	0.009	

<sup>a</sup> All uncertain entries are bracketed ( ).

<sup>b</sup> In extracting the dimensionless reduced widths, a radius of  $1.45(A^{1/3}+1) \times 10^{-13}$  cm was used throughout.

<sup>c</sup> For a given nucleus the references usually apply to several levels. As a rule, references are given only when they are not mentioned in the published compilations (En54, En57).

radiation has been measured. In general,  $E2$  radiation is much less than  $M1$  but, on occasion, it may compete favorably with it. For each of the three types of radiation  $E1$ ,  $M1$ , and  $E2$ , the values of  $\Lambda^2$  for the various transitions in Al<sup>25</sup> vary by at least a factor of 100.

We have already discussed the  $E2$  transitions in O<sup>17</sup> and F<sup>19</sup> in Sec. III. 3(a). The smallness of the  $E1$  radiation width in F<sup>19</sup> is somewhat surprising because the

interpretation of  $\frac{1}{2}-$  state as a  $1p_{3/2}-$  holes (Ch54) would, in general, allow the transition. Since the structure of the ground states of Ne<sup>20</sup> and F<sup>19</sup> involve both  $2s$  and  $1d$  particles, one explanation could be a cancellation between the two contributions  $2s \rightarrow 1p$ ,  $1d \rightarrow 1p$ .

One curious feature of the  $M1$  radiation observed in Ne<sup>20</sup> is that it prefers to go to the first excited state rather than the ground state. The shell model could

TABLE XV. Radiation widths of states of nuclei in the mass range  $16 < A \leq 40$ .

Nucleus	Initial state	Spin and parity	Final state	Spin and parity	Type of radiation <sup>b</sup>	Obs width in ev	$\Lambda^2 \times 10^4$ <sup>c</sup>	Reference <sup>d</sup>
O <sup>17</sup>	0.872	$\frac{1}{2}+$	0	$\frac{5}{2}+$	E2	$2.6 \times 10^{-6}$	3000	
F <sup>19</sup>	0.110	$\frac{1}{2}-$	0	$\frac{1}{2}+$	E1	$\sim 7 \times 10^{-7}$	$\sim 30$	El55a
	0.197	$\frac{5}{2}+$	0	$\frac{1}{2}+$	E2	$\sim 8 \times 10^{-9}$	$\sim 15$ 000	Ba55a
Ne <sup>20</sup>	1.63	2+	0	0+	E2	$0.87 \times 10^{-3}$	45 000	De56
	13.19	1+	1.64	2+	(M1)	<1.6	<160	Ba55a
	13.43	(2-) <sup>a</sup>	1.64	2+	E1	<15	<1000	Ba55c
	13.50	1+	0	0+	(M1)	2.2	200	
			1.64	2+	(M1)	<0.02	<1	
	13.70	2-	1.64	2+	E1	$\sim 1$	$\sim 50$	
	13.76	1+	1.64	2+	(M1)	$\sim 1$	$\sim 90$	
	14.15	2-	1.64	2+	E1	<2	<70	
	14.17	2-	1.64	2+	E1	$\sim 3$	$\sim 100$	
	14.23	1+	1.64	2+	(M1)	4.5	350	
Na <sup>23</sup>	0.44	$(\frac{5}{2}+)$	0	$\frac{3}{2}+$	E2	$5.2 \times 10^{-6}$	19 000	He54
					M1	$\begin{cases} < 7 \times 10^{-3} \\ > 7 \times 10^{-4} \end{cases}$	$\begin{cases} < 12\ 000 \\ > 1200 \end{cases}$	Kr56
Mg <sup>24</sup>	1.37	2+	0	0+	E2	$1.8 \times 10^{-4}$	22 000	Co55
	12.000	2-	1.37	2+	E1	0.044	2.4	Ne54
			4.23	2+	E1	0.066	9.3	Ba56b
			5.23	2(-)	(M1)	0.015	4.9	Pr56
	12.197	1+	1.37	2+	(M1)	0.089	11	
			4.23	2+	(M1)	0.022	6.7	
	12.271	3-	1.37	2+	E1	0.027	1.4	
			4.23	2+	E1	0.051	6.5	
			5.23	3(-)	(M1)	0.016	7.1	
	12.354	3+	1.37	2+	(M1)	0.033	3.8	
			4.23	2+	(M1)	0.13	37	
			5.23	3(-)	(E1)	0.063	15	
	12.829	1-(2+)	0	0+	E1	0.5	16	
			1.37	2+	E1	0.4	17	
	12.935	(3-)	1.37	2+	(E1)	0.14	6	
			4.23	2+	(E1)	0.43	43	
			5.23	3(-)	(M1)	0.57	1900	
	13.043	3+	1.37	2+	(M1)	0.7	70	
			4.23	2+	(M1)	0.14	31	
			5.23	3(-)	(E1)	2.0	270	
13.102	(3-)	1.37	2+	(E1)				
		4.23	2+	(E1)				
		5.23	3(-)	(M1)				
Al <sup>26</sup>	2.51	$\frac{1}{2}+$	0	$\frac{5}{2}+$	E2	$\leq 0.0002$	$\leq 1200$	
			0.45	$\frac{1}{2}+$	M1	$\sim 0.012$	$\sim 210$	
			0.95	$\frac{3}{2}+$	(M1)	$\sim 0.0017$	$\sim 71$	
	2.70	$\frac{3}{2}+$	0	$\frac{5}{2}+$	(M1)	$\sim 0.0037$	$\sim 29$	Cr56b
					E2	$\sim 8 \times 10^{-5}$	$\sim 350$	Ag56
			0.45	$\frac{1}{2}+$	(M1)	$\sim 0.004$	$\sim 54$	Li56
			0.95	1-	(M1)	$\leq 0.0002$	$\leq 6$	
			1.81	$\frac{1}{2}+$	(M1)	0.0056	1220	
	3.09	$\frac{3}{2}-$	0	$\frac{1}{2}+$	E1	0.014	34	
			0.45	$\frac{3}{2}+$	E1	0.084	330	
			0.95	$\frac{5}{2}+$	E1	0.010	73	
	3.44	9/2+	0	$\frac{1}{2}+$	E2	0.00045	550	
			1.61	$\frac{3}{2}+$	(M1)	0.0045	110	
					E2	0.00013	3700	
	3.72	$\frac{7}{2}-$	0	$\frac{5}{2}+$	E1	0.0036	5	
			1.61	$\frac{3}{2}+$	E1	$\leq 0.0001$	$\leq 0.8$	
	3.85	$\frac{1}{2}-$	1.81	$\frac{5}{2}+$	E1	0.0084	87	
			0.45	$\frac{3}{2}+$	E1	0.15	270	
0.95			$\frac{5}{2}+$	E1	0.30	890		
2.51			$\frac{7}{2}+$	E1	0.075	2200		

<sup>a</sup> All uncertain entries are bracketed ( ).

<sup>b</sup> When both M1 and E2 radiation are possible and no measurement of the relative contributions has been made, we assume that M1 radiation predominates and enter M1 in brackets in column 6.

<sup>c</sup> In extracting the dimensionless quantities  $\Lambda^2 (= \Gamma/\Gamma_p)$  of column 8, the single-particle widths  $\Gamma_p$  were estimated as described in the text.

<sup>d</sup> For a given nucleus the references usually apply to several levels. As a rule, references are only given when they are not mentioned in the published compilations (En54, En57).

TABLE XV—(Continued)

Nucleus	Initial state	Spin and parity	Final state	Spin and parity	Type of radiation <sup>b</sup>	Obs width in ev	$\Lambda^2 \times 10^4$ °	Referenced	
Al <sup>25</sup>	3.88	$\frac{5}{2}+$	0	$\frac{5}{2}+$	$\left\{ \begin{array}{l} M1 \\ E2 \end{array} \right.$	0.0040	11		
			0.45	$\frac{1}{2}+$	$\left\{ \begin{array}{l} E2 \\ E2 \end{array} \right.$	0.0013	900		
			0.95	$\frac{3}{2}+$	$\left\{ \begin{array}{l} M1 \\ E2 \end{array} \right.$	0.0033	3700		
				$\frac{3}{2}+$	$\left\{ \begin{array}{l} M1 \\ E2 \end{array} \right.$	0.037	230		
				$\frac{3}{2}+$	$\left\{ \begin{array}{l} E2 \\ (M1) \end{array} \right.$	$5.2 \times 10^{-5}$	140		
	4.22	$\frac{3}{2}+$	2.70	$\frac{3}{2}+$	$\left\{ \begin{array}{l} (M1) \\ (M1) \end{array} \right.$	0.0058	60		
			0	$\frac{3}{2}+$	$\left\{ \begin{array}{l} (M1) \\ M1 \end{array} \right.$	$\leq 0.01$	$\leq 20$		
			0.45	$\frac{3}{2}+$	$\left\{ \begin{array}{l} M1 \\ E2 \end{array} \right.$	0.18	520		
				$\frac{3}{2}+$	$\left\{ \begin{array}{l} E2 \\ M1 \end{array} \right.$	0.0026	1700		
			0.95	$\frac{3}{2}+$	$\left\{ \begin{array}{l} M1 \\ E2 \end{array} \right.$	0.16	710		
	4.60	$\frac{5}{2}+$	0	$\frac{5}{2}+$	$\left\{ \begin{array}{l} (M1) \\ E2 \end{array} \right.$	0.0004	750		
			0.45	$\frac{3}{2}+$	$\left\{ \begin{array}{l} (M1) \\ E2 \end{array} \right.$	0.001	$\leq 1$		
			0.95	$\frac{3}{2}+$	$\left\{ \begin{array}{l} (M1) \\ (M1) \end{array} \right.$	0.02	$\leq 10\ 000$		
				$\frac{3}{2}+$	$\left\{ \begin{array}{l} E1 \\ E1 \end{array} \right.$	$\sim 0.063$	$\sim 200$		
				$\frac{3}{2}+$	$\left\{ \begin{array}{l} E1 \\ E1 \end{array} \right.$	0.16	40		
Al <sup>26</sup>	6.96	3-	1.76	2+	$\left\{ \begin{array}{l} E1 \\ E1 \end{array} \right.$	0.22	100	Gr56b	
			0.42	3+	$\left\{ \begin{array}{l} E1 \\ E1 \end{array} \right.$	0.02	3	En57	
			2.08	2+	$\left\{ \begin{array}{l} E1 \\ E1 \end{array} \right.$	0.2	100		
	7.00	3-	3.16	2, 3+	$\left\{ \begin{array}{l} E1 \\ E1 \end{array} \right.$	$< 0.02$	$< 10$		
			4.55	2+	$\left\{ \begin{array}{l} E1 \\ E1 \end{array} \right.$	0.14	700		
			0.42	3+	$\left\{ \begin{array}{l} E1 \\ E1 \end{array} \right.$	0.012	3		
	7.06	2, 3-	2.08	2+	$\left\{ \begin{array}{l} E1 \\ E1 \end{array} \right.$	0.15	70		
			3.16	2, 3+	$\left\{ \begin{array}{l} E1 \\ E1 \end{array} \right.$	0.24	200		
			0.23	0+	$\left\{ \begin{array}{l} E1 \\ E1 \end{array} \right.$	0.35	50		
	7.21	1-	2.08	2+	$\left\{ \begin{array}{l} E1 \\ E1 \end{array} \right.$	0.17	80		
2.08			2+	$\left\{ \begin{array}{l} E1 \\ E1 \end{array} \right.$	0.48	200			
Al <sup>28</sup> Si <sup>28</sup>	2, 3-	0	3+	$\left\{ \begin{array}{l} M1 \\ E2 \end{array} \right.$	$0.2 \times 10^{-6}$	1200			
		0	0+	$\left\{ \begin{array}{l} E2 \\ E2 \end{array} \right.$	$< 7.3 \times 10^{-4}$	$< 2.5 \times 10^4$	De56		
P <sup>29</sup> P <sup>30</sup>	4.30	$\frac{3}{2}-$	0	$\frac{1}{2}+$	$\left\{ \begin{array}{l} E1 \\ E1 \end{array} \right.$	$> 2.2 \times 10^{-2}$	$> 7.5 \times 10^5$		
			0	1+	$\left\{ \begin{array}{l} E1 \\ E1 \end{array} \right.$	1.73	1640	Se56	
			0.71	1+	$\left\{ \begin{array}{l} E1 \\ E1 \end{array} \right.$	$\sim 0.012$	4	Va58	
	5.96	1-	1.45	2+	$\left\{ \begin{array}{l} E1 \\ E1 \end{array} \right.$	$\sim 0.0014$	0.7		
			0	1+	$\left\{ \begin{array}{l} E1 \\ E1 \end{array} \right.$	$\sim 0.0007$	0.5		
			0.68	0+	$\left\{ \begin{array}{l} E1 \\ E1 \end{array} \right.$	0.0047	1.5		
	6.23	1-	1.45	2+	$\left\{ \begin{array}{l} E1 \\ E1 \end{array} \right.$	0.070	30		
			2.94	2+	$\left\{ \begin{array}{l} E1 \\ E1 \end{array} \right.$	0.0008	0.6		
			0	1+	$\left\{ \begin{array}{l} E1 \\ E1 \end{array} \right.$	0.0024	6		
			0.71	1+	$\left\{ \begin{array}{l} E1 \\ E1 \end{array} \right.$	0.0012	0.3		
			1.45	2+	$\left\{ \begin{array}{l} E1 \\ E1 \end{array} \right.$	0.0012	0.5		
			1.97	1+	$\left\{ \begin{array}{l} E1 \\ E1 \end{array} \right.$	0.021	20		
			2.54	1+	$\left\{ \begin{array}{l} E1 \\ E1 \end{array} \right.$	0.012	16		
	6.27	3-	2.72	2+	$\left\{ \begin{array}{l} E1 \\ E1 \end{array} \right.$	0.019	30		
			2.84	2+	$\left\{ \begin{array}{l} E1 \\ E1 \end{array} \right.$	0.0054	9		
2.94			2+	$\left\{ \begin{array}{l} E1 \\ E1 \end{array} \right.$	0.014	27			
4.18			2+	$\left\{ \begin{array}{l} E1 \\ E1 \end{array} \right.$	0.007	50			
0			$\frac{1}{2}+$	$\left\{ \begin{array}{l} M1, E2 \\ M1, E2 \end{array} \right.$	0.015		En57		
P <sup>31</sup>	7.78	$\frac{3}{2}+$	1.26	$\frac{1}{2}+$	$\left\{ \begin{array}{l} M1, E2 \\ M1, E2 \end{array} \right.$	0.010			
			2.23	$\frac{1}{2}+$	$\left\{ \begin{array}{l} M1, E2 \\ M1, E2 \end{array} \right.$	0.0015			
			0	$\frac{1}{2}+$	$\left\{ \begin{array}{l} M1 \text{ or } E1 \\ M1, E2 \text{ or } E1 \end{array} \right.$	0.9			
	7.90	$\frac{1}{2}$	1.26	$\frac{1}{2}+$	$\left\{ \begin{array}{l} M1, E2 \\ M1, E2 \end{array} \right.$	0.015			
			0	$\frac{1}{2}+$	$\left\{ \begin{array}{l} M1, E2 \\ M1, E2 \end{array} \right.$	0.004			
			1.26	$\frac{1}{2}+$	$\left\{ \begin{array}{l} M1, E2 \\ M1, E2 \end{array} \right.$	0.004			
	8.03	$\frac{3}{2}+$	0	$\frac{1}{2}+$	$\left\{ \begin{array}{l} M1, E2 \\ M1, E2 \end{array} \right.$	0.0012			
			1.26	$\frac{1}{2}+$	$\left\{ \begin{array}{l} M1, E2 \\ M1, E2 \end{array} \right.$	0.0066			
			2.23	$\frac{1}{2}+$	$\left\{ \begin{array}{l} M1, E2 \\ M1, E2 \end{array} \right.$	0.0012			
	8.04	$\frac{3}{2}+$	0	$\frac{1}{2}+$	$\left\{ \begin{array}{l} M1, E2 \\ M1, E2 \end{array} \right.$	0.03			
1.26			$\frac{1}{2}+$	$\left\{ \begin{array}{l} M1, E2 \\ M1, E2 \end{array} \right.$	0.001				
2.23			$\frac{1}{2}+$	$\left\{ \begin{array}{l} M1, E2 \\ M1, E2 \end{array} \right.$	0.0005				
0			$\frac{1}{2}+$	$\left\{ \begin{array}{l} M1, E2 \\ E1, M1 \end{array} \right.$	0.03				
S <sup>32</sup>	8.10	$(\frac{3}{2}, \frac{5}{2}+)$	1.26	$\frac{3}{2}+$	$\left\{ \begin{array}{l} M1, E2 \\ M1, E2 \end{array} \right.$	0.03			
			0	0+	$\left\{ \begin{array}{l} E1, M1 \\ E1, M1 \end{array} \right.$	0.12			
	9.65	1	0	0+	$\left\{ \begin{array}{l} E1, M1 \\ E2 \end{array} \right.$	0.63			
			0	0+	$\left\{ \begin{array}{l} E2 \\ E2, M1 \end{array} \right.$	0.048	320		
		10.06	2(+)	$\left\{ \begin{array}{l} 2.25 \\ 2.25 \end{array} \right.$	2+	$\left\{ \begin{array}{l} E2, M1 \\ E1 \end{array} \right.$	0.92		
		10.69	1-	0	0+	$\left\{ \begin{array}{l} E1 \\ E1, M1 \end{array} \right.$	12.0	780	
		10.78	1	0	0+	$\left\{ \begin{array}{l} E1, M1 \\ E1 \end{array} \right.$	4.4		
		10.82	1-	0	0+	$\left\{ \begin{array}{l} E1 \\ E1 \end{array} \right.$	8.7	560	
		10.91	1-	0	0+	$\left\{ \begin{array}{l} E1 \\ E1, M1 \end{array} \right.$	1.3	84	
		11.10	1	0	0+	$\left\{ \begin{array}{l} E1, M1 \\ E1, M1 \end{array} \right.$	6.7		
11.12		1	0	0+	$\left\{ \begin{array}{l} E1, M1 \\ E1, M1 \end{array} \right.$	21.0			

provide a ready explanation for this, namely, that the ground state of  $\text{Ne}^{20}$  is a closed  $(2s_3)^4$  shell so that, from the nature of the  $M1$  operator, all  $M1$  transitions to this state are forbidden because a change in orbit must be involved. The observed  $E1$  radiations in  $\text{Ne}^{20}$  are weak and this might be ascribed to operation of the isotopic spin selection rule (Wi53b), assuming the emitting states to be fairly pure  $T=0$  states. Such purity would be surprising considering that states of the same  $J, \pi$  have spacings of the order of only hundreds of kev near the emitting states.

Several radiation widths are implicitly contained in measurements of thermal-neutron cross sections in the present mass region. These have been discussed exhaustively in the literature (Ki54).

The values of  $\Lambda^2$  for  $E2$  transitions between low-lying states may be analyzed in terms of the strong-coupling model. The observed transitions are:

$$\begin{aligned} \text{F}^{19}: & 0.197 \left(\frac{5}{2}^+\right) \rightarrow 0\left(\frac{1}{2}^+\right), \Gamma = 8.5 \times 10^{-9} \text{ ev}, \Lambda^2 = 2.0, \\ \text{Ne}^{20}: & 1.63 (2^+) \rightarrow 0(0^+), \Gamma = 0.87 \times 10^{-8} \text{ ev}, \Lambda^2 = 5.1, \\ \text{Na}^{23}: & 0.44 \left(\frac{5}{2}^+\right) \rightarrow 0\left(\frac{3}{2}^+\right), \Gamma = 2.1 \times 10^{-6} \text{ ev}, \Lambda^2 = 8.8, \\ \text{Mg}^{24}: & 1.37 (2^+) \rightarrow 0(0^+), \Gamma \sim 1.8 \times 10^{-4} \text{ ev}, \Lambda^2 \sim 2.6, \\ \text{Si}^{28}: & 1.78 (2^+) \rightarrow 0(0^+), \Gamma \lesssim 7.3 \times 10^{-4} \text{ ev}, \Lambda^2 \lesssim 2.8. \end{aligned}$$

The experimental values are all derived from lifetime measurements or Coulomb excitation. It is significant that all the values of  $\Lambda^2$  (except possibly  $\text{Si}^{28}$ ) are  $>1$  and therefore suggest the applicability of the strong-coupling model. This is especially true of  $\text{Na}^{23}$  where  $\Lambda^2$  has the very large value of 8.8. (The values quoted for  $\Lambda^2$  depend somewhat upon our conventional choice of single-particle transition, *viz.*, that for a  $1d \rightarrow 1d$  proton transition. If  $2s \rightarrow 1d$  or  $1d \rightarrow 2s$  had been used, the values of  $\Lambda^2$  would be smaller by a factor 7/20 or greater by a factor 7/4.) From the formula of Sec. II. 3(b), we may extract values of  $Q_0^2$  for the above transitions. In (barns)<sup>2</sup>, they are  $Q_0^2 = 0.17, 0.45, 0.48, \sim 0.23, \lesssim 0.26$ , respectively. By taking the mean nuclear radius  $a$  as  $1.3 A^{1/3} \times 10^{-13}$  cm, the corresponding values of  $\beta$  are  $-0.5, 0.7, 0.6, \sim 0.4$ , and  $\lesssim 0.3$ .

#### ACKNOWLEDGMENT

The writer's grateful thanks are due to those numerous experimenters who have advised him during the preparation of this compilation, especially to Dr. F. Ajzenberg-Solove, Dr. A. E. Litherland, and Dr. D. H. Wilkinson.

#### BIBLIOGRAPHY

- Ad52 R. K. Adair, Phys. Rev. **86**, 155 (1952).  
 Ad53 R. K. Adair, Phys. Rev. **92**, 1491 (1953).  
 Ad54 R. K. Adair, Phys. Rev. **96**, 709 (1954).  
 Ag56 H. Ager-Hanssen, D. M. Lonsjo, and R. Nordhagen, Phys. Rev. **101**, 1779 (1956).  
 Aj52 F. Ajzenberg and T. Lauritsen, Revs. Modern Phys. **24**, 321 (1952).  
 Aj55 F. Ajzenberg and T. Lauritsen, Revs. Modern Phys. **27**, 77 (1955).  
 Aj59 F. Ajzenberg and T. Lauritsen (unpublished).  
 Al59 Alburger, Gallmann, and Wilkinson, Phys. Rev. (to be published).  
 Am57 R. D. Amado, Proc. Phys. Soc. (London) **A70**, 532 (1957).  
 Au55 T. Auerbach and J. B. French, Phys. Rev. **98**, 1276 (1955).  
 Ba51 S. Bashkin and H. T. Richards, Phys. Rev. **84**, 1124 (1951).  
 Ba54 G. A. Bartholomew, F. Brown, H. E. Gove, A. E. Litherland, and E. B. Paul, Phys. Rev. **96**, 1114 (1954).  
 Ba55a C. A. Barnes, Phys. Rev. **97**, 1226 (1955).  
 Ba55b G. A. Bartholomew, F. Brown, H. E. Gove, A. E. Litherland, and E. B. Paul, Can. J. Phys. **33**, 441 (1955).  
 Ba55c E. Baranger, Phys. Rev. **99**, 145 (1955).  
 Ba56a F. C. Barker, Phil. Mag. **1**, 329 (1956).  
 Ba56b N. P. Baumann, F. W. Prosser, W. G. Read, and R. W. Krone, Phys. Rev. **104**, 376 (1956).  
 Ba57 G. A. Bartholomew and P. J. Champion, Can. J. Phys. **35**, 1347 (1957).  
 Bi54 J. W. Bittner and R. D. Moffat, Phys. Rev. **96**, 374 (1954).  
 Bl56 R. C. Block and H. Newson, Bull. Am. Phys. Soc. **1**, 55 (1956).  
 Bl57 S. D. Bloom, C. M. Turner, and D. H. Wilkinson, Phys. Rev. **105**, 232 (1957).  
 Bo53 A. Bohr and B. R. Mottleson, Kgl. Danske Videnskab. Selskab. Mat. fys. Medd. **27**, No. 16 (1953).  
 Bo55 J. M. Bowcock, Proc. Phys. Soc. (London) **A68**, 512 (1955).  
 Bo56 C. K. Bockelman, A. Leveque, and W. W. Buechner, Phys. Rev. **104**, 456 (1956).  
 Bo57 T. W. Bonner, F. W. Prosser, and J. H. Slattery, Bull. Am. Phys. Soc. **2**, 180 (1957).  
 Br57 Broude, Green, Singh, and Willmott, Phil. Mag. **2**, 1006 (1957).  
 Bu55 R. Budde and P. Huber, Helv. Phys. Acta **28**, 49 (1955).  
 Bu56 Bunbury, Devons, Manning, and Towle, Proc. Phys. Soc. (London) **A69**, 165 (1956).  
 Ca54a R. R. Carlson and E. B. Nelson, Phys. Rev. **95**, 641 (1954).  
 Ca54b B. C. Carlson and I. Talmi, Phys. Rev. **96**, 436 (1954).  
 Ca55 R. R. Carlson and E. B. Nelson, Phys. Rev. **98**, 1310 (1955).  
 Ch53 R. F. Christy, Phys. Rev. **89**, 839 (1953).  
 Ch54 R. F. Christy and W. A. Fowler, Phys. Rev. **96**, 851(L) (1954).  
 Ch56 R. F. Christy (private communication).  
 Cl56 A. B. Clegg, Phil. Mag. **1**, 1116 (1956).  
 Co53 A. V. Cohen and A. P. French, Phil. Mag. **44**, 1259 (1953).  
 Co55 C. F. Coleman, Phil. Mag. **46**, 1135 (1955).  
 Co56 Cohn, Bair, and Willard, Bull. Am. Phys. Soc. **1**, 346 (1956).  
 Co59 H. Cohn and J. L. Fowler (to be published).  
 Cr56a J. W. Cronin, Phys. Rev. **101**, 298 (1956).  
 Cr56b D. S. Craig, Phys. Rev. **101**, 1479 (1956).  
 De49 S. Devons and H. N. G. Hine, Proc. Roy. Soc. (London) **A199**, 73 (1949).  
 De54a S. Devons and G. Goldring, Proc. Phys. Soc. (London) **A67**, 413 (1954).  
 De54b D. M. Dennison, Phys. Rev. **96**, 378 (1954).  
 De55 Devons, Manning, and Bunbury, Proc. Phys. Soc. (London) **A68**, 18 (1955).  
 De56 Devons, Manning, and Towle, Proc. Phys. Soc. (London) **A69**, 173 (1956).  
 De57 G. Dearnaley, Phil. Mag. **1**, 821 (1957); and to be published.  
 Do52 D. C. Dodder and J. L. Gammel, Phys. Rev. **88**, 520 (1952).  
 Ed52 A. R. Edmonds and B. H. Flowers, Proc. Roy. Soc. (London) **A214**, 515 (1952).  
 El53 Elliott, Hope, and Jahn, Proc. Roy. Soc. (London) **A246**, 912 (1953).  
 El55a J. P. Elliott and B. H. Flowers, Proc. Roy. Soc. (London) **A229**, 536 (1955).  
 El55b J. P. Elliott and T. H. R. Skyrme, Proc. Roy. Soc. (London) **A232**, 561 (1955).  
 El56a F. A. El-Bedewi, Proc. Phys. Soc. **A69**, 221 (1956).  
 El56b J. P. Elliott, Phil. Mag. **1**, 503 (1956).  
 El56c J. P. Elliott, Phys. Rev. **101**, 1212 (1956).

- El57a J. P. Elliott and A. M. Lane, *Encyclopaedia of Physics* (Springer-Verlag, Berlin, Germany, 1957), Vol. 39.
- El58 J. P. Elliott, Proc. Roy. Soc. (London) **A245**, 128, 562 (1958).
- En54 P. M. Endt and J. C. Kluyver, Revs. Modern Phys. **26**, 95 (1954).
- En57 P. M. Endt and C. M. Braams, Revs. Modern Phys. **29**, 683 (1957).
- Fe59a A. J. Ferguson and H. E. Gove, Can. J. Phys. **37**, 660 (1959).
- Fe59b Ferguson, Clark, and Gove, Phys. Rev. (to be published).
- Fo55 J. L. Fowler and C. M. Johnson, Phys. Rev. **98**, 728 (1955).
- Fo58 J. L. Fowler and H. Cohn, Phys. Rev. **109**, 89 (1958).
- Fr55 Freeman, Lane, and Rose, Phil. Mag. **46**, 17 (1955).
- Fr56 J. B. French, Phys. Rev. **103**, 1391 (1956).
- Fr57 J. B. French and A. Fujii, Phys. Rev. **105**, 653 (1957).
- Ga55 A. I. Galonsky and M. T. McEllistrem, Phys. Rev. **98**, 590 (1955).
- Ga56 A. Galonsky and C. H. Johnson, Phys. Rev. **104**, 421 (1956).
- Go54 H. Gove and E. B. Paul, Phys. Rev. **95**, 650 (A) (1954).
- Go55a H. Gove (private communication).
- Go55b C. R. Gossett, G. C. Phillips, J. P. Schiffer, and P. M. Windham, Phys. Rev. **100**, 203 (1955).
- Gr56a T. S. Green and R. Middleton, Proc. Phys. Soc. (London) **A69**, 28 (1956).
- Gr56b Green, Singh, and Willmott, Proc. Phys. Soc. (London) **A69**, 335 (1956).
- Gu59 E. Guth and C. J. Mullin, Phys. Rev. **76**, 234 (1949).
- Ha55a W. Habaerli, Phys. Rev. **99**, 640(A) (1955).
- Ha55b W. Habaerli (private communication).
- Ha56 F. B. Hagedorn, F. S. Mozer, T. S. Webb, W. A. Fowler, and C. C. Lauritsen, Phys. Rev. **104**, 1402 (1956).
- Ha57a F. B. Hagedorn, Phys. Rev. **108**, 735 (1957); F. E. Hagedorn and J. B. Marion, Phys. Rev. **108**, 1015 (1957).
- Ha57b E. C. Halbert and J. B. French, Phys. Rev. **105**, 1563 (1957).
- He54 N. P. Heydenberg and G. M. Temmer, Phys. Rev. **96**, 426 (1954).
- He56 N. P. Heydenberg and G. M. Temmer, Phys. Rev. **104**, 123 (1956).
- He58a D. F. Herring, Phys. Rev. **112**, 1217 (1958).
- He58b D. F. Hebbard, Bull. Am. Phys. Soc. Ser. II, **3**, 406 (1958).
- Ho53 J. R. Holt and T. N. Marsham, Proc. Phys. Soc. (London) **A66**, 1932 (1953).
- Ho55 W. F. Hornyak and R. Sherr, Phys. Rev. **100**, 1409 (1955).
- Hu52 P. Huber and E. Baldinger, Helv. Phys. Acta **25**, 435 (1952).
- Hu58 D. J. Hughes and J. A. Harvey, "Neutron Cross Sections" Brookhaven Rept. BNL325 (1958), second edition.
- In53 D. R. Inglis, Revs. Modern Phys. **25**, 390 (1953); *ibid.* **27**, 76 (1955).
- In55 D. R. Inglis (private communication).
- Ja51 H. A. Jahn and H. Van Wieringen, Proc. Roy. Soc. (London) **A209**, 502 (1951).
- Ja53 H. L. Jackson and A. I. Galonsky, Phys. Rev. **89**, 370 (1953).
- Ja54 B. G. Jancovici, Phys. Rev. **95**, 389 (1954).
- Jo54a G. A. Jones and D. H. Wilkinson, Phil. Mag. **45**, 703 (1954).
- Jo54b C. H. Johnson, H. B. Willard, and J. K. Bair, Phys. Rev. **96**, 985 (1954).
- Ke56 A. K. Kerman, Kgl. Danske Videnskab. Selskab. Mat. fys. Medd. **30**, No. 15 (1956).
- Ke59 L. Keszthelyi and I. Fodor, Nuclear Phys. **10**, 564 (1959).
- Ki54 B. B. Kinsey and G. A. Bartholomew, Phys. Rev. **93**, 1260 (1954).
- Ko52 L. J. Koester, Phys. Rev. **85**, 643 (1952).
- Ko58 D. Kohler and H. Hilton, Phys. Rev. **110**, 1094 (1958).
- Kr56 Krone, Everett, and Hanna, Bull. Am. Phys. Soc. **1**, 329 (1956).
- Ku56 D. Kurath, Phys. Rev. **101**, 216 (1956).
- Ku57 D. Kurath, Phys. Rev. **106**, 975 (1957).
- Ku59 D. Kurath and L. Picman, Nuclear Phys. **10**, 313 (1959).
- La51 R. A. Laubenstein and M. J. W. Laubenstein, Phys. Rev. **84**, 18 (1951).
- La52 A. M. Lane (unpublished).
- La53 A. M. Lane, Proc. Phys. Soc. (London) **A66**, 977 (1953).
- La54 A. M. Lane and L. A. Radicati, Proc. Phys. Soc. (London) **A67**, 167 (1954).
- La55a A. M. Lane, Proc. Phys. Soc. (London) **A68**, 189 (1955).
- La55b A. M. Lane, R. G. Thomas, and E. P. Wigner, Phys. Rev. **98**, 693 (1955).
- La56 R. O. Lane and J. E. Monahan, Bull. Am. Phys. Soc. **1**, 346 (1956).
- La57 A. M. Lane and R. G. Thomas, Revs. Modern Phys. **30**, 257 (1958).
- Le55 S. H. Levine, R. S. Bender, and J. N. McGruer, Phys. Rev. **98**, 1276 (1955).
- Li56 A. E. Litherland, E. B. Paul, G. A. Bartholomew, and H. E. Gove, Phys. Rev. **102**, 208 (1956).
- Li57 Lidofsky, Weil, Bent, and Jones, Bull. Am. Phys. Soc. **2**, 29 (1957).
- Li58 Litherland, McManus, Paul, Bromley, and Gove, Can. J. Phys. **36**, 378 (1958).
- Lo55 Lonsjo, Os, and Tangen, Phys. Rev. **98**, 727 (1955).
- Ly58 Lynn, Firk, and Moxon, Nuclear Phys. **5**, 603 (1958).
- Ma54 R. J. Mackin, Phys. Rev. **94**, 648 (1958).
- Ma55 Marion, Bonner, and Cook, Phys. Rev. **100**, 91 (1955).
- Ma56a P. R. Malmberg, Phys. Rev. **101**, 114 (1956).
- Ma56b C. B. Mast and C. J. Mullin, Bull. Am. Phys. Soc. **1**, 180 (1956).
- Ma56c J. B. Marion, Bull. Am. Phys. Soc. **1**, 196 (1956).
- Ma56d J. B. Marion and F. B. Hagedorn, Phys. Rev. **104**, 1028 (1956).
- Ma56e J. B. Marion, G. Weber, and F. S. Mozer, Phys. Rev. **104**, 1402 (1956).
- Ma57a J. B. Marion, Nuclear Phys. **4**, 282 (1957).
- Ma57b Maxson and Bennett, Bull. Am. Phys. Soc. **2**, 180 (1957).
- McD55 W. M. McDonald, Phys. Rev. **98**, 60 (1955).
- McD56 W. M. McDonald, Phys. Rev. **101**, 271 (1956).
- McG55 J. N. McGruer, E. K. Warburton, and R. S. Bender, Phys. Rev. **100**, 235 (1955).
- Me56 S. Meshkov and C. W. Ufford, Phys. Rev. **101**, 734 (1956).
- Me59 Meyerhof, Tanner, and Hudson, Phys. Rev. (to be published).
- Mi56 D. W. Miller, R. M. Carmichael, U. C. Gupta, V. K. Rasmussen, and M. B. Sampson, Phys. Rev. **101**, 740 (1956).
- Mi58a D. W. Miller, Phys. Rev. **109**, 1669 (1958).
- Mi58b P. D. Miller and G. C. Phillips, Phys. Rev. **112**, 2048 (1958).
- Mi58c P. D. Miller and G. C. Phillips, Phys. Rev. **112**, 2043 (1958).
- Mo51 Mooring, Koester, Goldberg, Saxon, and Kaufmann, Phys. Rev. **84**, 703 (1951).
- Mo56 F. S. Mozer, Phys. Rev. **104**, 1386 (1956).
- Ne54 J. O. Newton, Phys. Rev. **96**, 242 (1954).
- Ne55 H. Newton (private communication).
- Ni55 S. G. Nilsson, Kgl. Danske Mat. Videnskab. Selskab. fys. Medd. **29**, No. 16 (1955).
- Ne56 J. O. Newton (private communication).
- Ne57 H. W. Newson, R. M. Williamson, K. W. Jones, J. H. Gibbons, and H. Marshak, Phys. Rev. **108**, 1294 (1957).
- Ol58 J. W. Olness, W. Habaerli, and H. W. Lewis, Phys. Rev. **112**, 1702 (1958).
- Pa55a W. C. Parkinson (private communication).
- Pa55b E. B. Paul, H. E. Gove, A. E. Litherland, and G. A. Bartholomew, Phys. Rev. **99**, 1339 (1955).
- Pa57 E. B. Paul, Phil. Mag. **2**, 311 (1957).
- Pe56 J. Perring and T. H. R. Skyrme, Proc. Phys. Soc. (London) **A69**, 600 (1956).
- Pr56 F. W. Prosser, N. P. Baymann, D. K. Brice, W. G. Read, and R. W. Krone, Phys. Rev. **104**, 369 (1956).
- Ra43 G. Racah, Phys. Rev. **63**, 367 (1943).
- Ra53 L. A. Radicati, Proc. Phys. Soc. (London) **A66**, 139 (1953); *ibid.* **A67**, 39 (1954).
- Ra55a V. K. Rasmussen, D. W. Miller, M. B. Sampson, and U. C. Gupta, Phys. Rev. **100**, 851 (1955).
- Ra57 G. Rakavy, Nuclear Phys. **4**, 375 (1957).
- Re55 M. Redlich, Phys. Rev. **99**, 1427 (1955).
- Re56a J. B. Reynolds and K. G. Standing, Phys. Rev. **101**, 158 (1956).

- Re56b C. W. Reich, G. C. Phillips, and J. L. Russell, Phys. Rev. **104**, 143 (1956).
- Ri54 F. L. Ribe and J. D. Seagrave, Phys. Rev. **94**, 934 (1954).
- Ro48 L. Rosenfeld, *Nuclear Forces* (North-Holland Publishing Company, Amsterdam, 1948).
- Ro54 R. H. Rohrer, H. W. Newsom, J. H. Gibbons, and P. Cap, Phys. Rev. **95**, 302(A) (1954).
- Ru56 J. L. Russell, G. C. Phillips, and C. W. Reich, Phys. Rev. **104**, 135 (1956).
- Sa54 S. Sack, L. C. Biedenharn, and G. Breit, Phys. Rev. **93**, 321 (1954).
- Sa58 G. R. Satchler, Ann. Phys. **3**, 275 (1958).
- Sc55 L. I. Schiff, Phys. Rev. **98**, 1281 (1955).
- Sc56 H. Schneider, Helv. Phys. Acta **29**, 55 (1956).
- Se47 R. Serber, Phys. Rev. **72**, 1114 (1947).
- Se51 J. D. Seagrave, Phys. Rev. **84**, 1219 (1951).
- Se53 J. Seed, Phil. Mag. **44**, 921 (1953).
- Se56 J. C. Severiens and S. S. Hanna, Phys. Rev. **104**, 1612 (1956).
- Sh51 C. G. Shull and E. O. Wolland, Phys. Rev. **81**, 527 (1951).
- Sh53 Shire, Wormald, Lindsay-Jones, Lunden, and Stanley, Phil. Mag. **44**, 1197 (1953).
- Sh55a E. S. Shire and R. Edge, Phil. Mag. **46**, 640 (1955).
- Sh55b R. D. Sharp, A. Sperduto, and W. W. Buechner, Phys. Rev. **99**, 632(A) (1955).
- Sh56a B. Sherman and D. G. Ravenhall, Phys. Rev. **103**, 949 (1956).
- Sh56b R. K. Sheline, Nuclear Phys. **2**, 382 (1956).
- Si58 C. P. Sikkema, *Proceedings of International Conference on Nuclear Physics, Paris, July, 1958* (Dunod, Paris, 1959).
- So57 J. M. Soper, Phil. Mag. **2**, 1219 (1957).
- St54a P. H. Stelson and W. M. Preston, Phys. Rev. **95**, 974 (1954).
- St54b P. H. Stelson, Phys. Rev. **96**, 1584 (1954).
- St56 K. G. Standing, Phys. Rev. **101**, 152 (1956).
- Su58 R. G. Summers-Gill, Phys. Rev. **109**, 1591 (1958).
- Sw57 C. P. Swann, F. R. Metzger, and V. K. Rasmussen, Bull. Am. Phys. Soc. **2**, 29 (1957).
- Ta51 I. Talmi, Helv. Phys. Acta **20**, 185 (1951).
- Ta56 A. Taylor, H. Marshak, and H. W. Newson, Bull. Am. Phys. Soc. **1**, 62 (1956).
- Th51 R. G. Thomas, Phys. Rev. **84**, 1061 (1951).
- Th52 R. G. Thomas, Phys. Rev. **88**, 1109 (1952).
- Th53 J. Thirion and V. L. Telegdi, Phys. Rev. **92**, 1253 (1953).
- Th54 R. G. Thomas (unpublished).
- Th56 R. G. Thomas, M. Walt, R. B. Walton, and R. C. Allen, Phys. Rev. **101**, 759 (1956).
- Tr55 P. B. Treacy, Proc. Phys. Soc. (London) **A64**, 204 (1955).
- Va58 C. van der Leun and P. M. Endt, Phys. Rev. **110**, 96 (1958).
- We55 T. S. Webb, F. B. Hagedorn, W. A. Fowler, and C. C. Lauritsen, Phys. Rev. **99**, 138 (1955).
- We56 Weber, Davis, and Marion, Phys. Rev. **104**, 1307 (1956).
- We58 J. A. Weinman and E. A. Silverstein, Phys. Rev. **111**, 277 (1958).
- Wi53a D. H. Wilkinson, Nature **172**, 576 (1955).
- Wi53b D. H. Wilkinson and A. B. Clegg, Phil. Mag. **44**, 1322 (1953).
- Wi54 D. H. Wilkinson, Phil. Mag. **45**, 259 (1954).
- Wi55a H. B. Willard, J. K. Bair, and J. D. Kington, Phys. Rev. **98**, 669 (1955).
- Wi55b H. B. Willard, J. D. Kington, and J. K. Bair, Phys. Rev. **98**, 1184 (A) (1955).
- Wi56a H. B. Willard, J. D. Kington, J. K. Bair, and H. O. Cohn, Phys. Rev. **101**, 765 (1956).
- Wi56b D. H. Wilkinson, Phil. Mag. **1**, 127 (1956).
- Wi56c J. E. Wills, Bull. Am. Phys. Soc. **1**, 175 (1956).
- Wi56d D. H. Wilkinson and A. B. Clegg, Phil. Mag. **1**, 291 (1956).
- Wi57 H. B. Willard, J. K. Bair, H. D. Cohn, and J. D. Kington, Phys. Rev. **105**, 202 (1957).
- Wo54 H. H. Woodbury, A. V. Tollestrup, and R. B. Day, Phys. Rev. **93**, 1311 (1954).
- Yo54 S. Yoshida, Progr. Theoret. (Kyoto) **12**, 141 (1954).
- Zi57 D. Zipoy, G. Freier, and K. Famularo, Phys. Rev. **106**, 93 (1957).
- Zi58 D. M. Zipoy, Phys. Rev. **110**, 995 (1958).